IMMUNOPATHOGENESIS OF CORTICAL DEMYELINATION IN MULTIPLE SCLEROSIS

DOCTORAL THESIS

In partial fulfillment of the requirements for the degree

"Doctor rerum naturalium (Dr. rer. nat.)"

In the Molecular Medicine Study Program

at the Georg-August University Göttingen

Submitted by

NIELSEN LAGUMERSINDEZ DENIS

born in

Havana, Cuba

Göttingen, August 2015

Members of the Thesis Committee

Supervisor (Reviewer)

Prof. Dr. Wolfgang Brück

Department of Neuropathology

University Medical Center Göttingen

Second Member of the Thesis Committee (Reviewer)

Prof. Dr. Holger Reichardt

Department of Cellular and Molecular Immunology

University Medical Center Göttingen

Third Member of the Thesis Committee

Prof. Dr. Thomas Bayer

Division of Molecular Psychiatry

University Medical Center Göttingen

Assistant supervisor

Dr. Stefan Nessler

Department of Neuropathology

University Medical Center Göttingen

Date of Disputation:

A MIS PADRES

Affidavit

I hereby declare that my doctoral thesis entitled “Immunopathogenesis of cortical demyelination in multiple sclerosis” has been written independently with no other sources and aids than quoted.

_____

Göttingen, August 2015

List of Publications

Original Articles

C-Phycocyanin is neuroprotective against global cerebral ischemia/reperfusion injury in gerbils.

Pentón-Rol G, Marín-Prida J, Pardo-Andreu G, Martínez-Sánchez G, Acosta-Medina EF, Valdivia-Acosta A, Lagumersindez-Denis N, Rodríguez-Jiménez E, Llópiz-Arzuaga A, López-Saura PA, Guillén-Nieto G, Pentón-Arias E.

Brain Res Bull 2011; 86(1-2):42-52

C-Phycocyanin ameliorates experimental autoimmune encephalomyelitis and induces regulatory T cells.

Pentón-Rol G, Martínez-Sánchez G, Cervantes-Llanos M, Lagumersindez-Denis N, Acosta-Medina EF, Falcón-Cama V, Alonso-Ramírez R, Valenzuela-Silva C, Rodríguez-Jiménez E, Llópiz-Arzuaga A, Marín-Prida J, López-Saura PA, Guillén-Nieto GE, Pentón-Arias E.

Int Immunopharmacol 2011; 11(1):29-38

Protective effects of C-Phycocyanin against lipid peroxidation of serum lipoproteins and hepatic microsomes.

Livan Delgado Roche, Nielsen Lagumersindez Denis, Alexey Llopiz-Arzuaga, Eduardo Pentón-Arias, Giselle Pentón-Rol.

Pharmacologyonline 2011; 3:668-676

Reviews

Biochemical changes in mitochondria and its role in cell death during myocardial ischemia-reperfusion injury.

Livan Delgado Roche, Nielsen Lagumersindez Denis, Gregorio Martínez Sánchez

Pharmacologyonline 2009; 2:850-872

Esclerosis múltiple: aspectos generales y abordaje farmacológico.

Nielsen Lagumersindez Denis

Rev Cubana Farm 2009; v.43 n.2

Abstracts

A new mouse model of inflammatory cortical demyelination.

Nielsen Lagumersindez Denis, Claudia Wrzos, Wolfgang Brück, Christine Stadelmann, Stefan Nessler

J Neuroimmunol 2014; 275(1-2):119 (Poster) 12th International Congress of Neuroimmunology, Mainz 9-13 November, 2014.

TABLE OF CONTENTS

Acknowledgements

First, I would like to thank my supervisor **Dr. Stefan Nessler**, for giving me the opportunity to be part of this great project, for his scientific advices and for making out of me definitively a stronger person.

I would also like to express my gratitude to **Prof. Dr. Wolfgang Brück**, for giving me the opportunity to come to his lab four years ago and accept me as a PhD student in the Neuropathology Department. Thanks for the supervision of the project and for the scientific discussions during the Thesis Committee meetings.

I want to thank **Prof. Dr. Christine Stadelmann-Nessler** for the fruitful discussions and comments, for the many hours behind the microscope showing me the beauty of the Neuropathology and for always having an open door to me…THANKS!

Furthermore, I am thankful to **Prof. Dr. Holger Reichardt** and **Prof. Dr. Thomas Bayer** for being part of my Thesis Committee and for the scientific discussions and suggestions made during our meetings.

I want to thank **Prof. Dr. Christopher Linington** (University of Glasgow, UK) for providing the 8-18C5 and the Z2 hybridomas used in this thesis. Thanks to **Prof. Dr. Mathias Mack** (University Hospital Regensburg, Germany) for providing the DOC-2 Fr2 and the AMBA antibodies for the marmoset study. Additional thanks to **PD. Dr. Christina Schlumbohm** (Neu Encepharm) for conducting the depletion experiments in marmosets. Thanks also to **Dr. Benoit Barrette** (Max Planck Institute for Experimental Medicine, Göttingen, Germany) for providing the primers for the genotyping of the CD59a$^{-/-}$, CCR2$^{-/-}$ and Rag1$^{-/-}$ mice. Thanks to **Prof. Dr. George Trendelenburg** (Neurology Department, University Medical Center, Göttingen) for providing the CD59a$^{-/-}$ mice and to **Prof. Michael Schön** (Department of Dermatology, University Medical Center, Göttingen) for providing us the OT-II mice.

I would like to thank specially **Dr. Claudia Wrzos** for performing most of the intracerebral injections of this study, but also for the emotional support during all these years working together. Thanks a lot Claudi!! Thanks to **Dr. Franziska Paap** for her collaboration with the qRT-PCR analysis and for introducing me into this technique. Franzi, I want to say thanks also for your support during these last months.

My special thanks to our “top team” of technicians for the excellent assistance and for always having the willingness to help: **Katja, Briggite, Olga, Heidi**, **Mareike** and **Utah**. My gratitude goes also to **Cynthia** and **Heidi** for their support. My endless gratitude to one of the most lovely persons I have met: **Chris** thanks a lot for being like my adoptive mother when I arrived to Germany, and for all your support.

In addition, I want to express my gratitude to my working colleagues **Silke**, **Erika**, **Nadine**, **Lena**, **Patrick**, **Linda**, **Alonso**, **Nasrin**, **Martina**, **Angie**, **Darius**, **Sarah**, **Wiebke**, **Insa**, **Shailender and Christin**. Guys, thanks a lot for the discussions, for the funny times together and for the support during these years. I want to thank also **Sandra**, muchas gracias guapa por tu apoyo y por prestarme tu “rincón oscuro” para escribir mi tesis. Funcionó!!

Next I want to thank my friend **Anne(a)** for being one of the nicest persons I know, for your support, for helping me to fight against Microsoft Word, for listening, for sharing so many good times together, but most importantly for being always there for me and let me be your friend. A mis queridos salseros y bachateros: **Susana**, **Vicente**, **Daria** y **David**. Chicos gracias por tantos momentos lindos q hemos vivido juntos y por todo el apoyo emocional y las buenas “vibras”. A mi hermano **Ney**, gracias por estar ahí siempre a pesar de la distancia mi herma, apoyándome y dándome mucho ánimo, te adoro.

A mis padres, **Eva** y **Juan**: esta tesis se las dedico a ustedes, por todo lo que representa para mí, por tantos años de sacrificio que me han regalado, por apoyarme en todo momento en mis decisiones, por creer en mí siempre y por mover cielo y tierra con tal de procurar lo mejor para mí. Esta tesis es el resultado de todo ello…GRACIAS!

Finally, I would like to thank someone who has became a fundamental part in my life: **Bernhard**, thanks a lot for your support, for reading my thesis, for holding me up and giving me the strength to move forward and for being there until everything was over. Wir haben es geschafft!!

Abstract

Cortical demyelination is a key pathological feature of multiple sclerosis (MS) and clinically linked to cognitive deficits and disability progression. Extensive band-like subpial demyelination is even a specific feature of the disease. However, the immunological mechanisms driving cortical demyelination have not yet been defined due to a lack of cortical pathology in the classical experimental models of MS.

To elucidate the immunopathogenesis of cortical demyelination, we developed a novel mouse model with subpial and perivascular cortical MS-like lesions. We demonstrate that in addition to a pathogenic anti-myelin antibody response, perivascular cortical demyelination is primarily dependent on activated encephalitogenic T cells, natural killer (NK) cells and CCR2+ inflammatory monocytes. In contrast, subpial cortical demyelination occurs independently of activated T cells, but requires specific antibodies and a fully functional complement cascade.

To translate the results obtained into a treatment option for MS, we evaluated the therapeutic efficacy of a humanized mouse anti-human CCR2 antibody, which efficiently depletes CCR2+ monocytes in marmosets with experimental autoimmune encephalomyelitis (EAE). Depleting inflammatory monocytes was well tolerated and significantly reduced cortical demyelination in marmoset monkeys with EAE.

Our findings thus delineate a differential involvement of immunological effector mechanisms in perivascular and subpial cortical lesion formation, shed light on the exquisite vulnerability of subpial cortical tissue in multiple sclerosis and translate into a preclinical treatment approach for cortical demyelination.

List of Figures

List of Tables

Abbreviations

2D2 mice	MOG-specific T cell receptor transgenic mice
ADCC	Antibody dependent cellular cytotoxicity
ANOVA	Analysis of variance
APC	Antigen-presenting cell
APP	Amyloid precursor protein
BCR	B cell receptor
C5	C5 convertase
CAE	Chloracetate esterase
CCL2	Chemokine (CC motif) ligand 2
CCR2	Chemokine (CC motif) receptor 2
CD	Cluster of differentiation
cDNA	Complementary DNA
CFA	Complete Freund´s adjuvant
CMC	Carboxymethyl cellulose
CNS	Central nervous system
CSF	Cerebrospinal fluid
Cy7	Cyanine 7
DAB	3,3'-Diaminobenzidine
DAPI	4',6-diamidino-2-phenylindole
DMEM	Dulbecco's modified Eagle medium
DMSO	Dimethyl sulfoxide
dNTP	Deoxynucleotide triphosphate
EAE	Experimental autoimmune encephalomyelitis
EDTA	Ethylenediaminetetraacetic acid
FACS	Fluorescence-activated cell sorting
FCS	Fetal calf serum
FITC	Fluorescein isothiocyanate
FoxP3	Forkhead box P3
GAPDH	Glyceraldehyde 3-phosphate dehydrogenase
GrB	Granzyme B
HCl	Hydrochloric acid
HEPES	4-(2-hydroxyethyl)-1-piperazineethanesulfonic acid
HLA	Human leukocyte antigen
i.p.	Intraperitoneally

i.v.	Intravenous(ly)
IFNγ	Interferon gamma
IgG	Immunoglobulin , isotype G (analogous for other isotypes)
IHC	Immunohistochemistry
IL	Interleukin
iNOS	Inducible-nitric oxide synthase
KLH	Keyhole limpet hemocyanin
LFB	Luxol fast blue
Ly6C	Lymphocyte antigen 6 complex, locus C
m/h	Mouse/human
mAb	Monoclonal antibody
Mac-3	Macrophage 3 antigen
MBP	Myelin basic protein
MCP-1	Monocyte chemoattractant protein-1
MEM	Minimum essential medium
$MgCl_2$	Magnesium chloride
MHC	Major histocompatibility complex
MOG, MOG_{35-55}	Myelin oligodendrocyte glycoprotein, (MOG consisting of amino acids 35-55)
MS	Multiple sclerosis
n/a	Not applicable
NaCl	Sodium chloride
NAGM	Normal appearing grey matter
NeuN	Neuronal Marker NeuN
NK	Natural killer
NKp46	Natural killer cell p46-related protein
NOS2	Nitric oxide synthase 2
OCB	Oligoclonal band (s)
Olig2	Oligodendrocyte transcription factor 2
OSE mice	Optico-spinal-EAE mice
OVA, $OVA_{323-329}$	Ovalbumin, (consisting of amino acids 323-329)
PBS	Phosphate buffered saline
PCR	Polymerase chain reaction
PE	Phycoerythrin
PerCP	Peridinin chlorophyll protein
PFA	Paraformaldehyde
PLP	Proteolipid protein
PMN	Polymorphonuclear neutrophils

PPMS	Primary progressive multiple sclerosis
PTX	Pertussis toxin
qPCR	Quantitative PCR
RAG1	Recombination-activating gene 1
Rag1$^{-/-}$	RAG1-deficient
rMOG, rMOG$_{1-125}$	Recombinant MOG, (consisting of amino acids 1-125)
RRMS	Relapsing remitting multiple sclerosis
s.c.	Subcutaneous
SAS	Subarachnoid space
SDS	Sodium dodecyl sulfate
SPMS	Secondary progressive multiple sclerosis
TBE	Tris/Borate/EDTA
TBS	Tris-buffered saline
TCR	T cell receptor
Th/+ mice	Heterozygous MOG-specific B cell receptor transgenic mice
TNFα	Tumor necrosis factor alpha
TPPP/p25	Tubulin polymerization promoting protein TPPP/p25
Treg	Regulatory T cell(s)
Tris	Tris(hydroxymethyl)aminomethane
VCAM-1	Vascular cell adhesion molecule 1
VLA-4	Very late antigen 4
WM	White matter
Wt	Wild type
γc	Common gamma chain
γc$^{-/-}$	γc-deficient

1 INTRODUCTION

1.1 Multiple Sclerosis

Multiple sclerosis (MS) is a chronic inflammatory demyelinating disease of the central nervous system (CNS), affecting mostly young adults. The clinical symptomatology of the disease is quite heterogeneous and the etiology is not fully understood yet, but likely involves a genetic predisposition in close interaction with environmental factors.

1.1.1 Clinical subtypes

MS typically starts in adults between 20 and 45 years of age, but it can also occur in children (under 18 years of age). Patients with MS experience a variety of symptoms, and the most common are visual problems, fatigue, spasticity, problems with gait and balance and the presence of the Uhthoff's phenomenon (a transient temperature-dependent numbness, weakness, or loss of vision due to a defective nerve conduction in demyelinated axons) (Davis et al., 2008, Browning et al., 2012).

In 1996, the US National Multiple Sclerosis Society Advisory Committee on Clinical Trials in Multiple Sclerosis defined four standardized clinical subtypes of MS (Lublin and Reingold, 1996) according to the clinical course of the disease: relapsing-remitting (RRMS), secondary progressive (SPMS), primary progressive (PPMS) and progressive relapsing (PRMS). These categories did not include imaging and biological correlates as well as clinical aspects of the disease recently identified; therefore, they were re-examined in 2012 by the International Advisory Committee on Clinical Trials of MS (Lublin et al., 2014). As a result, two major consensual changes in the classification system were suggested: the clinically isolated syndrome (CIS) was officially included as an MS descriptor and the PRMS category was eliminated. The core descriptions of relapsing and progressive disease were maintained, but two modifiers of these core phenotypes were settled: disease activity (defined by clinical assessment or CNS imaging) and disease progression (assessment of whether progression of disability has occurred over a given time period) (Lublin et al., 2014).

The different MS subtypes are defined as follows:

Clinically isolated syndrome

CIS is defined as the first clinical presentation of a disease showing characteristics of inflammatory demyelination that could be MS, but still does not fulfill the criteria of dissemination in time (Miller et al., 2005). Disease activity in CIS patients should be followed up and in case of subsequent clinical relapses, or new magnetic resonance imaging (MRI) lesions, the clinical course should be classified as RRMS (Lublin et al., 2014).

Relapsing-remitting MS

Around 85-90 % of the MS patients are diagnosed with RRMS at the onset of the disease. The patients experience episodes of neurological deficits (relapses), followed by periods of complete or partial recovery of the symptoms (remission) that can last months to years (Compston and Coles, 2002). Typically, women have a higher risk than men of developing this form of MS. A relapse can be defined as an episode of neurological symptoms, which lasts at least 24 h in the absence of fever and infection and is consistent with a demyelinating event in the CNS (Polman et al., 2011). According to the disease modifiers recently established, RRMS patients can be sub-classified in RR-active [e.g., presence of new gadolinium-enhancing (GdE) lesions in MRI] or RR-not active (patient with a relapsing course but not presenting clinical relapses, new GdE lesions or enlarging T2 lesions during the assessment period) (Lublin et al., 2014).

Secondary progressive MS

50 % of the RRMS patients transition into a secondary progressive phase within 2 decades (Duffy et al., 2014, Scalfari et al., 2014). Men often experience a more rapid progression than women (Koch et al., 2010). SPMS patients present with a slow decline of neurological functions and often the ability to walk decreases (Browning et al., 2012). To date there are no clear criteria to define the transition point when RRMS converts to SPMS (Lublin et al., 2014).

Primary progressive MS

PPMS accounts for 10-15 % of the MS cases. In the diagnosed patients, the disease continuously evolves from the onset, without phases of remission. Contrary to RRMS, men

have a higher risk than women of being affected by PPMS and usually the onset is later in life (40 years on average) (Noseworthy et al., 2000, Holland et al., 2011).

According to the International Advisory Committee on Clinical Trials of MS, PPMS and SPMS can also be sub-classified based on activity (active versus non-active) and progression (with progression versus without progression) (Lublin et al., 2014).

1.1.2 Diagnosis

The diagnosis of MS is based on clinical symptoms, MRI findings and analysis of cerebrospinal fluid (CSF). Traditionally, MS was diagnosed following the Poser's criteria (Poser et al., 1983), defined as the occurrence of two or more demyelinating attacks involving two or more parts of the CNS. Along with the introduction of modern MRI techniques, these criteria were substituted by the McDonald criteria implemented in 2000 (McDonald et al., 2001), and subsequently revised in 2005 (Polman et al., 2005) and 2010 (Polman et al., 2011). Accordingly, the presence of hyperintense T2-weighted lesions by MRI, disseminated in space (DIS) and time (DIT) are predictive for MS. T2 lesions are typically located juxtacortically, periventricularly, in the posterior fossa and in the spinal cord. The presence of at least one T2 lesion in at least two of the regions mentioned fulfills the DIS criterion. The DIT criterion is satisfied when asymptomatic GdE and non-enhancing lesions are simultaneously present in one single MRI scan, or when a new T2 or GdE lesion is detected on a follow-up MRI (Polman et al., 2011). Acute lesions show enhancement after gadolinium administration on T1-weighted images, indicative of inflammatory infiltration and a recent breakdown of the blood brain barrier (BBB) (Filippi et al., 2002). Furthermore, the presence of oligoclonal bands (OCBs) in the CSF (found in about 90-95 % of the patients) and an intrathecal immunoglobulin G (IgG) synthesis both support the MS diagnosis (Compston and Coles, 2002).

1.1.3 Epidemiology and etiology

MS affects about 2.5 million people around the world, and its incidence is continuously increasing (Milo and Kahana, 2010, Browning et al., 2012, Hemmer et al., 2015). MS usually starts in early adulthood with a female: male ratio of 3:1 in Caucasians (Constantinescu et al., 2011, Wallin et al., 2012). Studies have shown that the incidence of MS is rising with

increasing distance to the equator (Koch-Henriksen and Sorensen, 2010), and people with Nordic origin are more often affected (Hauser and Goodwin, 2008). Regions of high risk comprise Northern Europe, Israel, Northern USA, Canada, New Zealand, San Marino and Cyprus (Kurtzke, 2000, Healthline, 2015). In Germany the actual prevalence of the disease is 149 patients per 100 000 inhabitants (Healthline, 2015). Regions with low prevalence can be found in Asia and South America (Kurtzke, 2000).

The knowledge collected from epidemiological and family studies in patients with MS support a role of genetic risk factors in the disease. Studies revealed that first-degree relatives of MS patients have seven times higher chances of developing MS compared with others (Compston and Coles, 2002). In this respect, an MS concordance rate of 15-25 % in monozygotic twins and of 3-5 % in dizygotic twins has been identified (Mumford et al., 1994, Hansen et al., 2005, Ramagopalan et al., 2008).

Since already three decades, genetic variations in the human leukocyte antigen (HLA) alleles have been strongly associated with the MS risk (Jersild et al., 1973). For example, the HLA class II alleles *DRB1*1501*, *DRB1*0301*, and *DRB1*1303* expressed on cells of the innate immune system, have been linked to an increased risk of developing MS, whereas the HLA class I allele A2 is associated with a lower risk to develop MS (Sawcer et al., 2011). Peptides are presented to the T cell receptor of Cluster-of-differentiation 4 positive (CD4+) and Cluster-of-differentiation 8 positive (CD8+) T cells in the context of HLA class II and I molecules by antigen presenting cells (APC), emphasizing the role of the immune system in MS. In addition, genetic variations in interleukin-2 (IL-2) and interleukin-7 (IL-7) receptor α chains, have been related to an increased susceptibility for the disease (Compston and Coles, 2008). Furthermore, genome-wide association studies have identified over 100 single nucleotide polymorphisms (SNPs) connected to MS (Sawcer et al., 2011, Beecham et al., 2013, Farh et al., 2015). Interestingly, most of the SNPs identified occurred in gene loci related to T cell differentiation, as well as in genes related to modulation and reprogramming of T cell effector functions like secretion of cytokines (Sawcer et al., 2011).

Despite of the solid evidence supporting the role of a genetic component in the etiology of the disease, non-genetic factors, namely viral infections and other environmental factors, have been also associated with MS. For example, Epstein-Barr virus (EBV) infection

was strongly associated with MS (Haahr and Hollsberg, 2006, Ascherio and Munger, 2007, Almohmeed et al., 2013) and it has been proposed that molecular mimicry between viral and myelin components may play a role in disease pathogenesis (Lang et al., 2002). However, defining a conclusive role of the Eppstein-Barr Virus in MS has been undermined by the fact that more than 95 % of the adult population is seropositive for the virus (Ascherio and Munger, 2007).

Studies of migration patterns have shown that a child migrating from a high- to a low-risk region (or the other way around) takes on the risk level of the new location. However, if the migration takes place after puberty, the risk from the region of origin is retained (Compston and Coles, 2008). Additionally, smoking might increase the risk for MS 1.5-fold and might accelerate the transition from RRMS to SPMS (Hernan et al., 2001, Healy et al., 2009). A recent study addressing the immunological effects of high-dose vitamin D in healthy volunteers, reported that a high serum concentration of vitamin D results in increased IL-10 production by peripheral blood mononuclear cells and a reduced frequency of Th17 cells (Allen et al., 2012), which might explain the benefits reported on reducing the risk of MS (Ascherio and Munger, 2007).

1.1.4 Immunopathogenesis

It is widely accepted that MS pathogenesis has an important immunological component. This view is based on findings from immunological, genetic and histopathological studies as well as experiences acquired from clinical trials where different immunomodulatory and immunosuppressive treatments have been successfully applied. Two main hypotheses on the initiation of MS have been postulated. The most widely accepted one claims that the activation of a CNS antigen-specific response takes place in the periphery and as a result, an adaptive immune response targeting the CNS is orchestrated. The second hypothesis proposes that CNS homeostasis is intrinsically disturbed and that this initial event will trigger a subsequent adaptive immune response resulting in inflammatory demyelination (Hemmer et al., 2015).

The sequence of events proposed in the first theory is described as follows: autoreactive T cells are primed in peripheral lymphoid organs by dendritic cells (DCs) through mechanisms of molecular mimicry, bystander activation or direct cross-reactivity

(Wucherpfennig and Strominger, 1995, Sospedra and Martin, 2005). In the draining lymph nodes, B cells can also capture soluble antigens and act as APC for the T cells. B cells proliferate and mature into antibody-secreting plasma cells, which can migrate to the bone marrow or to inflamed tissues. Under specific conditions, a few of these primed T cells, together with some B cells invade the CNS compartment (Henderson et al., 2009, Graber and Dhib-Jalbut, 2011). T cell migration is mediated by the upregulation of adhesion molecules like the very late antigen-4 (VLA-4) in T helper 1 (Th1) cells, which interacts with its ligand, the vascular cell adhesion molecule- 1 (VCAM- 1) on endothelial cells. On the other hand the migration of T helper 17 (Th17) cells is thought to be mediated by the interaction between the chemokine (CC motif) receptor 6 (CCR6) and the chemokine (CC motif) ligand 20 (Engelhardt and Ransohoff, 2012). Furthermore, activated T cells secrete metalloproteinase like the matrix metalloproteinases-2 and -9 (MMP-2, MMP-9) contributing to the breakdown of the BBB (Graber and Dhib-Jalbut, 2011). T cells are re-activated by local APC within the CNS, preferentially in the perivascular space, and start to secrete pro-inflammatory cytokines like interferon-gamma (IFNγ) and interleukin-17 (IL-17) (Axtell et al., 2010), creating an inflammatory environment that alters the homeostasis of oligodendrocytes, astrocytes and microglial cells. This results in an increased permeability of the BBB and additional inflammatory cells are recruited, including monocytes and plasma cells contributing to the perpetuation of the lesions (Vogel et al., 2013). In this regard, several studies report the presence of monocytes degrading myelin products (Breij et al., 2008, Lucchinetti et al., 2011), and plasma cells in the lesions, which potentially could produce antibodies targeting myelin sheaths and glial cells (Buc, 2013, Hemmer et al., 2015).

Regarding the second, alternative hypothesis, resident CNS microglia are activated in response to an initiating event, leading to the subsequent amplification of an immune response involving a secondary recruitment of innate and adaptive immune cells (Henderson et al., 2009). This hypothesis is based on observations made in some lesions or in the normal appearing white matter, where oligodendrocyte loss and microglia activation can be observed in the absence of lymphocyte infiltrations. It has been proposed that the oligodendrocyte loss may be caused by a genetic mutation, a metabolic disturbance or an increased vulnerability of these cells, leading to their spontaneous death (Barnett and Prineas, 2004). Then, antigens will drain out of the CNS via the CSF, as studies have

suggested in mice (Xie et al., 2013), toward deep cervical lymph nodes to induce a secondary immune response in the periphery. In most non-CNS tissues, antigens released by local tissue damage will be processed and presented by APC in the corresponding draining lymph nodes and there, T cells will be primed and subsequently migrate to the target tissue to exert their effector functions. Several studies argue against the existence of such an efferent route for DCs to leave the CNS (Hatterer et al., 2006, Galea et al., 2007, Ransohoff and Engelhardt, 2012). Nevertheless, immune cells bearing DC surface markers have been identified in the juxtavascular CNS parenchyma in mice (Prodinger et al., 2011) and their migration along the rostral migratory stream (a specialized migratory route reaching the main olfactory bulb) to the cervical lymph nodes has been recently described (Mohammad et al., 2014). In the cervical lymph nodes, B cells are also capable of recognizing soluble antigens and present them to T cells (Yuseff et al., 2013). Finally the activation of antigen-specific T cells in the draining lymph nodes results in the orchestration of an adaptive immune response to target myelin and oligodendrocytes, similar to the one described in the previous hypothesis (Hemmer et al., 2015).

This hypothesis has various detractors, since primary neurodegenerative diseases or traumatic insults affecting oligodendrocytes or the myelin sheaths do not regularly lead to a destructive activation of the adaptive immune system (Eichler and Van Haren, 2007, Locatelli et al., 2012). Furthermore, primary damage to oligodendrocytes is not supported by the genetic studies done in patients. Alternatively, the possibility that a persistent infectious agent in oligodendrocytes would damage the cells seems unlikely, because in this case, it should be expected that most of the damage would be induced by immune infiltrating cells trying to clear the pathogen (Hemmer et al., 2015).

MS has been historically considered a CD4+ T cell driven autoimmune disease, mainly based on data derived from experimental autoimmune encephalomyelitis (EAE). However CD8+ T cells are observed in active demyelinating lesions, even outnumbering the amount of CD4+ T cells (Buc, 2013). Expanded clones of CD8+ T cells are found in the CSF and blood of MS patients, persisting even for years (Babbe et al., 2000, Skulina et al., 2004).

Also, increased numbers of CD8+ T cells can be observed infiltrating the cortex in MS patients at early stages (Lucchinetti et al., 2011) and near demyelinated axons in the CNS (Babbe et al., 2000). In addition, acute axonal damage in early MS lesions has been correlated with increased numbers of CD8+ T cells within the lesions (Bitsch et al., 2000).

Regulatory T (Treg) cells seem to be implicated in the pathogenesis of MS as well, since a loss of their immunosuppressive functions has been observed in MS patients (Viglietta et al., 2004, Haas et al., 2005), possibly contributing to the activation of pathogenic Th1 and Th17 cells. In addition, remission phases in RRMS patients are associated with increased numbers of Forkhead box P3 (FoxP3)+ Treg cells in the blood (Dalla Libera et al., 2011, Peelen et al., 2011). However, few of these cells are found in MS lesions independent of the disease activity (Fritzsching et al., 2011), making it difficult to establish their exact contribution to lesion formation in the CNS.

As mentioned above, B cells can contribute to the pathogenesis of MS (Yuseff et al., 2013), among others by presenting antigens to autoreactive T cells and, upon differentiation into plasma cells, by secreting antibodies against myelin structures. In support of this hypothesis, deposition of IgG and immunoglobulin M (IgM) on myelin and oligodendroglial cells, co-localizing with complement deposition in demyelinated areas, has been shown (Storch et al., 1998, Sadaba et al., 2012). Moreover, the presence of OCBs and intrathecal IgG synthesis is important for the diagnosis of MS (Sharief and Thompson, 1991). Furthermore, the B cell depleting antibody Rituximab significantly reduces the relapse rate and disease activity in RRMS patients (Hauser et al., 2008).

1.1.5 Pathology

The main pathological characteristics of MS are the presence of multifocal areas in the CNS featuring myelin loss, defined as plaques or lesions, accompanied by variable gliosis and inflammation and relative axonal preservation (Bruck and Stadelmann, 2005). Lesions disseminate through the CNS, but optic nerves, spinal cord, brainstem, cerebellum and juxtacortical and periventricular white matter (WM) regions constitute predilection sites (Popescu and Lucchinetti, 2012, Popescu et al., 2013).

Recent pathological findings highlight the presence of demyelinated lesions also in the cortical grey matter (GM) of MS patients (Kidd et al., 1999, Peterson et al., 2001, Bo et al., 2003a, Bo et al., 2003b, Pirko et al., 2007, Geurts and Barkhof, 2008) already early in the disease (Lucchinetti et al., 2011). Cortical grey matter pathology is described in detail in section 1.2.

1.1.5.1 Acute active demyelinating lesions

Acute active demyelinating lesions are the most frequent lesion type in WM regions in RRMS patients underlying the occurrence of clinical attacks in this group (Filippi et al., 2012, Popescu and Lucchinetti, 2012, Metz et al., 2014). These plaques contain numerous macrophages containing myelin debris, which is considered the pathological signature for defining active demyelinating plaques (Bruck et al., 1995). Myelin oligodendrocyte protein (MOG), 2´,3´-cyclic nucleotide 3´-phosphodiesterase (CNPase) and myelin associated glycoprotein (MAG) are considered “minor”, less abundant, myelin proteins, that can be degraded within 1-3 days; therefore, when found in macrophages designate early active demyelination. In contrast, if degradation products from “major”, extremely abundant, myelin proteins like proteolipid protein (PLP) or myelin basic protein (MBP), which are digested more slowly, are identified within macrophages, lesions are classified as late active (Popescu et al., 2013). Inactive lesions may still display macrophages but these are not immunopositive for any of the myelin proteins mentioned above (Bruck et al., 1995). In addition to macrophages/microglia, T cells (CD4+ and CD8+), B-lymphocytes, as well as plasma cells invade the CNS parenchyma and perivascular areas (Frischer et al., 2009), reinforcing the inflammatory nature of these lesions. Astrocytes proliferate and adopt a plump shape, with homogeneous eosinophilic cytoplasm and numerous fibrillary processes (Popescu and Lucchinetti, 2012), while oligodendrocyte loss is quite variable (Bruck et al., 1995).

1.1.5.2 Remyelinated lesions

Remyelinated lesions are characterized by the presence of newly formed, thinner myelin sheaths that can be identified as “pale”, mostly sharply delineated areas in LFB-PAS histochemistry (Popescu et al., 2013). Frequently, signs of extensive remyelination, such as abundant mature oligodendrocytes and MBP- and MOG-positive myelin sheaths, are observed within early MS lesions, but remyelination capacity apparently decreases during the chronic phase of the disease (Goldschmidt et al., 2009). However, remyelinated plaque regions can be observed in almost half of chronic lesions in MS, mostly at the periphery of the lesion (Barkhof et al., 2003, Patrikios et al., 2006).

1.1.5.3 Axonal and neuronal damage

Persisting disability in MS is associated with neuronal and axonal degeneration. Axonal damage already takes place early in the disease and is most pronounced during active demyelination (Trapp et al., 1998, Bitsch et al., 2000, De Stefano et al., 2001, Kuhlmann et al., 2002). Axonal damage is evidenced by the presence of axonal swellings and accumulation of amyloid-β precursor protein (APP) (Bjartmar et al., 2003). Axonal pathology contributes to the disability observed during the relapses of the patients and correlates with the extent of inflammatory infiltration in active lesions (Bitsch et al., 2000, Filippi et al., 2012, Popescu and Lucchinetti, 2012). Neuronal loss in MS has been reported in neocortical areas, hippocampus and in demyelinated as well as non-demyelinated cortex (Wegner et al., 2006, Papadopoulos et al., 2009, Magliozzi et al., 2010, Lucchinetti et al., 2011). It has been proposed that neuronal and axonal damage is caused by the secretion of toxic inflammatory mediators like reactive oxygen species (ROS), nitric oxide (NO), proteases and cytokines from the inflammatory cells, causing mitochondrial dysfunction, oxidative stress and energy deficiency (Dutta and Trapp, 2007, Stirling and Stys, 2010, Dutta and Trapp, 2011, Fischer et al., 2012). Furthermore, excitotoxic mechanisms might also lead to axonal damage (Pitt et al., 2003, Srinivasan et al., 2005).

1.1.5.4 Chronic lesions

Chronic lesion are the most frequent lesion type found in brain autopsies from patients with long-standing MS (Stadelmann et al., 2011) and can be classified as chronic active lesions (smoldering lesions) or chronic inactive plaques (Popescu et al., 2013). Chronic active lesions are well-demarcated areas of demyelination with a hypocellular center surrounded by a slowly expanding rim of activated microglia. Few myelin-laden phagocytes can also be present at the lesion edge. Additionally, T cells are often found perivascularly located in these lesions (Stadelmann et al., 2011). Several studies proposed that smoldering lesions might contribute to disease progression in MS (Prineas et al., 2001, Filippi et al., 2012, Popescu and Lucchinetti, 2012). On the other hand, chronic inactive lesions are completely demyelinated and hypocellular (few macrophages/microglia and lymphocytes), featuring a substantial loss of axons (up to 80 %) (Frischer et al., 2009) and oligodendrocytes, as well as a dense astrogliosis (Kuhlmann et al., 2008, Popescu and Lucchinetti, 2012).

1.1.6 Therapies for MS

So far, there is no cure for MS and the therapies available reduce the relapse rate and MRI disease activity (disease-modifying therapies, DMT) or aim at improving symptoms. For managing acute relapses in MS, the intravenous (i.v.) administration of high dose methylprednisolone is recommended. If this fails, plasma exchange (plasmapheresis) or i.v. infusion of Ig (IVIG) should be used (Cortese et al., 2011). DMTs are unfortunately not effective in progressive MS (Wingerchuk and Carter, 2014). Up-to-date, several DMT have been approved for the long-term treatment of RRMS comprising: interferon-β (IFNβ) (six available formulations), glatiramer acetate (GA), teriflunomide, dimethyl fumarate, alemtuzumab, natalizumab, fingolimod and mitoxantrone (Gajofatto and Benedetti, 2015). Currently, additional studies are carried on to address the potential therapeutic effects of new substances like laquinimod, daclizumab and rituximab for MS.

1.1.7 Experimental autoimmune encephalomyelitis model

Several animal models of MS have been developed so far, but the most commonly used and also the best understood is the rodent EAE model. EAE can be induced by either active immunization with myelin-derived proteins or peptides emulsified in adjuvants (Stromnes and Goverman, 2006) or by adoptive transfer of activated myelin-specific CD4+ T cells into recipient animals (Ben-Nun et al., 1981, Stromnes and Goverman, 2006). The immunization induces the activation of T cells in the periphery (lymph nodes and spleen). Subsequently, autoreactive T cells migrate across the BBB into the CNS, where they are reactivated by local APC, starting an inflammatory cascade that contributes to the recruitment of additional immune cells and leads to tissue injury (Constantinescu et al., 2011). EAE is most frequently induced in mice, but also rats, marmoset monkeys and other species can be used. The disease course is characterized by an ascending paralysis manifesting about seven to fourteen days after active EAE immunization or earlier, if induced by adoptive transfer protocols.

EAE targets mostly the spinal cord and sometimes the cerebellum, generating inflammation, demyelination and axonal damage, but the pathological features vary depending on the animal species, strain, induction method and auto-antigen used. The same factors influence the disease course as well (Baxter, 2007, Miller and Karpus, 2007). Thus, C57BL/6 mice display a monophasic disease course upon immunization with a variable degree of remission, in contrast to SJL/J mice for example, which develop a relapsing-remitting form of EAE after immunization with $PLP_{139-151}$ (Gold et al., 2006).

The generation of the OSE (optico-spinal-EAE) mice that spontaneously develop EAE (Krishnamoorthy et al., 2006) has set an important milestone in EAE and MS research. These mice were generated by crossbreeding 2D2 mice bearing a T cell receptor (TCR) specifically recognizing the MOG_{35-55} myelin peptide (Bettelli et al., 2003) with Th mice, whose B cell receptor (BCR) is also specific for MOG (Litzenburger et al., 1998). OSE mice develop EAE spontaneously with an incidence of around 50 % and demyelinating lesions can be found in spinal cord as well as optic nerves (Krishnamoorthy et al., 2006).

1.2 Grey matter pathology in multiple sclerosis

For many decades, MS was considered a predominant WM nosological entity, since disseminated focal demyelinated lesions constitute a classical hallmark of the disease. Nevertheless, early studies already reported grey matter (GM) demyelinated lesions (Sander, 1898, Dawson, 1916, Lumsden, 1970). It was not until 1962, that post-mortem tissue research started to pay more attention to GM pathology in MS. In this early date, a pioneer study of post-mortem material from 22 MS patients, reported the occurrence of macroscopically visible demyelinated lesions in the cortical GM in 26 % of the cases (Brownell and Hughes, 1962). Yet, the lack of specific immunohistochemical techniques at that time suggested that this number represented an underestimation of the real prevalence of GM lesions (Engelhardt and Ransohoff, 2012, Calabrese et al., 2015). In the beginning of the 21st century, the improvement of histopathological methods for staining myelin (Kidd et al., 1999, Peterson et al., 2001, Bo et al., 2003b) facilitated the detection of GM abnormalities in MS.

Nowadays, the cortex is recognized as one of the preferential locations of demyelination in MS (Kidd et al., 1999, Peterson et al., 2001, Bo et al., 2003b, Kutzelnigg et al., 2005, Vercellino et al., 2005, Gilmore et al., 2009). Cortical lesions are predominantly located in the insular cortex, the frontobasal cortex, the temporobasal cortex and the gyrus cinguli (Kutzelnigg and Lassmann, 2006), although hippocampus and cerebellum can be also affected (Geurts et al., 2007). In addition, it has been demonstrated that cortical lesions occur independently of WM or deep GM pathology (Bo et al., 2003b, Kutzelnigg et al., 2005, Vercellino et al., 2005, Bo et al., 2007). Moreover, cortical demyelination has been associated with cognitive impairment of the patients (Calabrese et al., 2009, Roosendaal et al., 2009, Rodriguez et al., 2014) and has been related to the occurrence of epileptic seizures in MS (Calabrese et al., 2008).

Cortical demyelination has been reported to be a restricted feature of late-stage MS (Bo et al., 2003b, Kutzelnigg et al., 2005). Cortical demyelination was found in almost 95 % of post-mortem brains from chronic MS patients (Bo et al., 2003b, Kutzelnigg et al., 2005, Albert et al., 2007). Around 40 % of the patients in the progressive phase of the disease also displayed large areas of cerebellar demyelinated cortex, which may be a correlate of

cerebellar dysfunction in MS (Gilmore et al., 2009). Interestingly, a recent study in biopsy material from 138 early MS patients described the presence of extensive cortical lesions in 38 % of the samples analyzed (Lucchinetti et al., 2011).

1.2.1 Classification of cortical lesions in multiple sclerosis

Cortical lesions are classified into three types depending on their localization within the cortex. Type 1 lesions (leukocortical), involve both GM and WM and the GM-WM junction, while the superficial cortical layers are spared. Type 2 lesions are purely intracortical, usually small-sized and located mostly perivascularly around inflamed vessels, sparing superficial cortex and adjacent WM. Type 3 lesions (subpial), extend from the pial surface of the brain into the deeper cortical layers, sometimes involving several gyri (Peterson et al., 2001, Bo et al., 2003a, Calabrese et al., 2010). Subpial lesions are the most common type of lesions found in MS autopsies of chronic patients, sometimes covering up to 70 % of the cortical area (Kidd et al., 1999, Bo et al., 2003b, Kutzelnigg et al., 2005) and are considered a specific feature of the disease (Kidd et al., 1999).

Cortical demyelinated lesions in early MS

Early cortical lesions display myelin-laden macrophages, a typical hallmark of active demyelination (Lucchinetti et al., 2011, Popescu et al., 2011, Fischer et al., 2013). Inflammatory infiltrates located around vessels and also in the parenchyma have been observed in these early lesions, composed mostly of macrophages, T cells and few B cells and plasma cells (Lucchinetti et al., 2011, Popescu et al., 2011) conferring inflammatory features to the lesions. Furthermore, a wealth of inflammatory (adaptive) genes have been found upregulated in early cortical lesions in MS, suggesting that the neuronal loss, as well as the damage to oligodendrocytes and axons observed in early MS, is not due to a primary neurodegenerative process, but rather a result of the inflammation (Fischer et al., 2013).

The presence of diffuse meningeal inflammation in early MS has been correlated to the occurrence of cortical demyelination (Lucchinetti et al., 2011). This observation has led to the hypothesis that the secretion of pro-inflammatory cytokines in the subarachnoid space (SAS) may be an important driver of cortical pathology not only at this early stage, but also in the progressive phase of the disease (Magliozzi et al., 2007, Choi et al., 2012).

Cortical demyelinated lesions in chronic MS

Chronic cortical lesions in MS are characterized by well-demarcated areas of demyelination, accompanied by some axonal reduction and decrease of oligodendrocytes (Peterson et al., 2001, Albert et al., 2007, Rodriguez et al., 2014). Cortical lesions in progressive MS do not exhibit breakdown of the BBB, in contrast to early cortical lesions (Popescu et al., 2013). Furthermore, less inflammatory infiltrates and complement deposition compared to early WM lesions was observed in such lesions (Peterson et al., 2001). The presence of meningeal infiltrates formed by T cells, B cells and macrophages associated to subpial demyelinated areas has been documented in cortical chronic lesions as well (Magliozzi et al., 2007, Howell et al., 2011, Choi et al., 2012), correlating with the activation of microglia and the extent of demyelination and neurodegeneration in those regions. In addition, meningeal infiltrates consisting of B cell accumulations have been described in SPMS, located in the deep cortical sulci and topographically associated to subpial lesions (Howell et al., 2011).

1.2.2 Neuronal damage in cortical lesions

So far, the relationship of local GM demyelination to neurodegeneration is not clear. Some studies reported the presence of neuronal damage and neuronal loss in cortical demyelinated lesions, but no differences when comparing NAGM and control cortex (Peterson et al., 2001, Wegner et al., 2006). Thus, substantial glial (-36 %) and neuronal loss (-10 %), as well as loss of synapses (47 %) was detected in leukocortical lesions, while in NAGM the only sign of neuronal damage was the presence of neurons with rounded shapes, indicative of axonal and/or dendrite loss (Wegner et al., 2006). In contrast to these findings, another study reported a significant loss of neurons (up to 65 % in upper subpial demyelinated layers) in both cortical demyelinated lesions and NAGM from SPMS patients, when compared with controls (Magliozzi et al., 2010). More recently, another group informed the presence of significant neuronal loss (-25 %), neuronal atrophy and axonal loss (-31 %) in subpial lesions and NAGM when compared with control samples, but no differences were seen if the comparison was done within MS samples (Klaver et al., 2015), suggesting that neuronal damage might be largely independent of the demyelination in the cortex.

1.2.3 MR-imaging of cortical demyelination and clinical correlates

One of the reasons why cortical demyelination has not been in the focus for several decades has to do with the very limited sensitivity of conventional MRI techniques to detect these lesions (Geurts et al., 2005a). This also impedes the establishment of good clinical correlates of cortical lesions. T1-weighted and T2-weighted standard MRI can detect predominantly juxtacortical lesions located at the interface between cortex and WM, but subpial lesions, which are the most abundant in cortical demyelination, are the most difficult to visualize (Stadelmann et al., 2008). These difficulties partially arise from the intrinsic characteristics of cortical demyelinated lesions: low inflammatory load, less BBB damage and low myelin density in upper cortical layers. Partial volume effects due to the proximity of cortical lesions to the CSF contributes as well (Stadelmann et al., 2008). Imaging methods have further evolved, improving the detection of cortical lesions (Boggild et al., 1996, Filippi et al., 1996), ranging from the 2-D fast fluid-attenuated inversion recovery (FLAIR) MRI, to the 3-D double inversion recovery (DIR) sequences (Geurts et al., 2005b, Pouwels et al., 2006). However, DIR still misses 80 % of pathologically confirmed, mostly subpial, cortical lesions (Seewann et al., 2011, Seewann et al., 2012).

GM lesion load has been correlated with clinical disability in all MS phenotypes (Calabrese et al., 2007, Calabrese et al., 2009, Nelson et al., 2011, Calabrese et al., 2012). For example, the size of the cortical lesions, but not the specific location in the cortex, may better explain the correlation found with cognitive impairment (Nelson et al., 2011). Furthermore, higher lesion loads correlate with higher EDSS, and patients with clinical progression have the highest rate of cortical lesion accumulation (Calabrese et al., 2012). Nevertheless, the imaging methods available need to be improved to achieve more reliability and a better understanding of how cortical demyelination relates to the disease process and to clinical disability in MS.

1.3 Experimental models of cortical demyelination

Along with the growing interest in MS cortical pathology, several experimental models of cortical demyelination have been reported in rodents and non-human primates during the last decade, but still the pathological mechanism leading to the formation of the lesions are only poorly understood.

It has been shown that common marmoset monkeys immunized with recombinant MOG protein (rMOG) develop - in addition to WM lesions - cortical demyelinated lesions reflecting all the subtypes described in MS (subpial, perivascular and leukocortical lesions) (Pomeroy et al., 2005, Merkler et al., 2006c, Kramann et al., 2015). Inflammatory infiltrates composed of numerous activated macrophages/microglia and T cells in a lesser extent, as well as few perivascular B cells (Merkler et al., 2006c) have been identified in the lesions. A more recent study, reported the presence of higher numbers of T cells and plasma cells in the meninges overlying subpial cortical demyelinated regions in the marmoset-EAE model when compared to normal appearing cortex (Kramann et al., 2015). These findings suggest that local meningeal infiltrates might relate to subpial pathology. Furthermore, cortical lesions in the marmoset revealed Ig leakage and complement C9 deposition restricted to perivascular vessels located intracortically (Merkler et al., 2006a, Merkler et al., 2006c), suggesting a possible contribution of pathogenic antibodies and complement to the lesion pathogenesis.

Cortical demyelination has been also observed in congenic Lewis rats sharing certain major histocompatibility complex (MHC) I and II alleles and immunized with rMOG (Storch et al., 2006), demonstrating that the presence of cortical lesions is controlled by MHC genes. The most frequent type of lesions observed in this model corresponded to the subpial classification. In addition, deposition of Ig and complement on myelin sheaths was observed in subpial-demyelinated areas, accompanied by macrophage infiltration during the early stage of lesion formation (Storch et al., 2006). Moreover, cortical demyelination have been induced in sub-clinically MOG-immunized rats following a cortical targeted lesion approach for the local application of pro-inflammatory cytokines in the cortex (Merkler et al., 2006b, Rodriguez et al., 2014). Furthermore, a recent study reported the generation of cortical demyelinated lesions in rats by administration of inflammatory cytokines in the SAS, at the

sagittal sulcus (Gardner et al., 2013). In these models, inflammation resolves quickly, followed by a successful remyelination of the lesions. This was true even when the animals were subjected to repeated episodes of inflammatory demyelination (Rodriguez et al., 2014). Similar to observations made in the marmoset-EAE model (Kramann et al., 2015), Gardner and colleagues reported the presence of T and B cells accumulating in the meninges of rats displaying extensive subpial demyelinated areas (Gardner et al., 2013).

Only few studies have reported the presence of cortical demyelination in murine models. For example, C57BL/6 mice fed with cuprizone exhibited prominent cortical demyelination (Skripuletz et al., 2008) in addition to the demyelination of the corpus callosum typically observed in this model (Matsushima and Morell, 2001, Torkildsen et al., 2008). These mice showed cortical demyelination after 6 weeks of cuprizone feeding, followed by a time-dependent remyelination after cuprizone was removed from the diet (Skripuletz et al., 2008). Furthermore, the authors demonstrated that cuprizone-induced cortical demyelination in the mice is strain-dependent, since BALB/cJ mice, exhibited significantly less cortical demyelination when fed with cuprizone. However, it is difficult to made inferences regarding the pathogenic mechanisms leading to cortical demyelination in MS out of this model, because there is neither an involvement of the adaptive immune system nor a disruption of the BBB (McMahon et al., 2001, Praet et al., 2014), like it is the case in MS. Furthermore, in situ analysis of myelin in the classic chronic EAE model in C57BL/6 mice immunized with MOG_{35-55} revealed a mild loss of myelin in the cerebral cortex (Girolamo et al., 2011), making it hard to establish any resemblance to cortical demyelinated lesions in MS.

In general, these experimental models of cortical demyelination rely on the presence of demyelinating antibodies against MOG and the local opening of the cortical BBB, supporting the hypothesis of a role for meningeal inflammation and complement mediated damage in cortical demyelination in MS. However, a more detailed description of the mechanisms regulating the formation of the different types of cortical lesions is still missing. Therefore, the establishment of a new mouse model of cortical demyelination in transgenic animals allowing the realization of functional studies is required.

1.4 Aims of the study

Cortical demyelination is a pathological hallmark of MS. So far, animal models with cortical demyelination have been established in marmosets and rats.

The aims of the present study are listed below:

1. To establish a mouse model of cortical demyelination on a C57BL/6 background.
2. To characterize the immunological mechanisms of cortical lesion formation.
3. To evaluate, if the identified pathomechanisms can serve as a target for a novel treatment approach against cortical demyelination.

2 MATERIALS AND METHODS

2.1 Materials

2.1.1 Reagents

Table 1: Reagents

Reagent	Supplier
3,3´-diaminobenzidine (DAB)	Sigma Aldrich, St. Louis, MO, USA
Acetic acid	Sigma Aldrich, St. Louis, MO, USA
Agarose	StarLab GmbH, Hamburg, Germany
Albumin, fluorescein isothiocyanate conjugate	Sigma Aldrich, St. Louis, MO, USA
Aquatex medium	Merck Millipore, Darmstadt, Germany
BD FACS™ Lysing solution, 10x	BD Biosciences, Franklin Lakes, NJ, USA
BD Pharm Lyse™, 10x	BD Biosciences, Franklin Lakes, NJ, USA
Betaine Q	Sigma Aldrich, St. Louis, MO, USA
Boric acid	Merck Millipore, Darmstadt, Germany
DePex medium	VWR International, Darmstadt, Germany
(DAPI) Diamidino-2-phenylindole, 1 mg/ml	Thermo Scientific, Waltham, MA, USA
dimethyl sulfoxide	Sigma Aldrich, St. Louis, MO, USA
dNTP (desoxynucleoside triphosphate) mix	Thermo Scientific, Waltham, MA, USA
EDTA (ethylenediamine tetraacetic acid disodium salt dihydrate)	Carl Roth, Karlsruhe, Germany
Ethanol, 100 %	Merck Millipore, Darmstadt, Germany
Ethidium bromide	Sigma Aldrich, St. Louis, MO, USA
ExtrAvidin-Peroxidase, buffered aqueous solution	Sigma Aldrich, St. Louis, MO, USA
Fast Blue BB Salt hemi (zinc chloride) salt	Sigma Aldrich, St. Louis, MO, USA
FCS (fetal calf serum)	Sigma Aldrich, St. Louis, MO, USA
Fluorescence mounting medium	Dako, Deutschland GmbH, Hamburg
FoxP3 Fixation/Permeabilization Concentrate	eBioscience, San Diego, CA, USA
FoxP3 Fixation/Permeabilization Diluent	eBioscience, San Diego, CA, USA
FoxP3 Permeabilization buffer, 10X	eBioscience, San Diego, CA, USA
GeneRuler™, 100 bp DNA ladder Plus	Thermo Scientific, Waltham, MA, USA
Go-Taq® DNA polymerase buffer, 10x	Promega, Madison, WI, USA
Go-Taq® DNA polymerase buffer, 5x	Promega, Madison, WI, USA
HCl (hydrochloric acid)	Merck Millipore, Darmstadt, Germany
HEPES (4-(2-hydroxyethyl)-1-	Sigma Aldrich, St. Louis, MO, USA

Reagent	Supplier
piperazineethanesulfonic acid) buffer, 1 M	
Isopentane	Sigma-Aldrich, St. Louis, MO, USA
Isopropyl alcohol	Merck Millipore, Darmstadt, Germany
Ketamine, 10 %	Medistar®, Ascheberg, Germany
L-glutamine, 200 mM	Sigma Aldrich, St. Louis, MO, USA
Lithium carbonate	Sigma Aldrich, St. Louis, MO, USA
Luxol fast blue (LFB)	VWR International LLC, Radnor, PA, USA
Mannide monooleate	Sigma Aldrich, St. Louis, MO, USA
Mayer´s hemalaum solution	Merck Millipore, Darmstadt, Germany
MEM (minimum essential medium) non-essential amino-acids, 100x	Sigma Aldrich, St. Louis, MO, USA
$MgCl_2$ (magnesium chloride)	Promega, Wisconsin, USA
N,N-Dimethylformamide	Sigma Aldrich, St. Louis, MO, USA
NaCl (sodium chloride)	Carl Roth, Karlsruhe, Germany
NaCl (sodium Chloride), 0.9 % solution, sterile	B. Braun Melsungen AG, Germany
Naphtol-AS-MX phosphate, disodium salt	Sigma Aldrich, St. Louis, MO, USA
OCT medium	Tissue-Tek, Sakura Finetek, USA
Paraffin oil	Carl Roth, Karlsruhe, Germany
Paraformaldehyde (PFA)	Merck Millipore, Darmstadt, Germany
PBS (phosphate buffered salt solution), sterile	Sigma Aldrich, St. Louis, MO, USA
Penicillin, 10 000 units/streptomycin, 10 mg/ml	Sigma Aldrich, St. Louis, MO, USA
Percoll	GE Healthcare Life Science, Germany
Periodic acid	Sigma Aldrich, St. Louis, MO, USA
Perm/Wash™ buffer, 10x	BD Biosciences, Franklin Lakes, NJ, USA
QIAzol Lysis Reagent	Qiagen, Maryland, MD, USA
RPMI-1640 (Roswell Park Memorial Institute-1640)	Sigma Aldrich, St. Louis, MO, USA
Schiff´s reagent	Sigma Aldrich, St. Louis, MO, USA
SDS (sodium dodecyl sulfate)	Sigma Aldrich, St. Louis, MO, USA
Sodium carboxymethyl cellulose (CMC)	Sigma-Aldrich, St. Louis, MO, USA
Sodium pyruvate, 100 mM	Sigma Aldrich, St. Louis, MO, USA
Tris (tris(hydroxymethyl)aminomethane)	Carl Roth, Karlsruhe, Germany
Trypan blue	Sigma Aldrich, St. Louis, MO, USA
Xylazine solution, 20 mg/ml	Ecuphar, Oostkamp, Belgium
Xylene	Chemsolute, Th. Geyer GmbH & Co. KG, Renningen, Germany
β-mercaptoethanol	Sigma Aldrich, St. Louis, MO, USA

2.1.2 Composition of solutions, buffers and cell culture media

Table 2: Solutions, buffers and cell culture media composition

Solution	Composition
3,3' DAB solution	Stock Solution: 1 g DAB, 40 ml PBS Working solution: 1 ml stock solution, 49 ml PBS, 20 µl 30 % H_2O_2
CFA (Complete Freund´s Adjuvant)	85 % Paraffin oil, 15 % Mannide monooleate, 6.7 mg/ml Mycobacterium tuberculosis H37RA
Chloral hydrate 14 % anesthesia	100 ml bidistilled water, 14 g Chloral hydrate
DMEM (High Glucose (4.5 g/l), w/ L-Glutamine, sodium pyruvate	Gibco, Life Technologies GmbH, Darmstadt, Germany
FACS (fluorescence-activated cell sorting) buffer	PBS, sterile, 2 % FCS
Fast Blue Solution	Bidistilled water, Tris-HCl buffer pH 8.2, Naphtol-AS-MX phosphate, N,N-Dimethylformamide, Levamisol, Fast Blue BB salt
HCl buffer	1 ml 2M HCl, 500 ml bidistilled water, pH 2.5
IFA (Incomplete Freund´s Adjuvant)	85 % Paraffin oil, 15 % mannide monooleate
Ketamine/Xylazine anesthesia	NaCl, 0.9 %, sterile, 12 % Ketamine, 10 % Xylazine
Luxol Fast Blue (LFB) solution	1 g LFB, 1000 ml 96 % Ethanol, 5 ml 10 % Acetic acid
Paraformaldehyde (PFA), 4 %	4 g PFA, 100 ml PBS, pH 7.4
$RPMI_{complete}$	RPMI-1640, 10 % FCS, 1 mM sodium pyruvate, 1x non-essential amino acids, 13 mM HEPES buffer, 50 µM β-mercaptoethanol, 100 units penicillin, 0.1 mg/ml streptomycin, 2 mM L-glutamine
Tail Lysis Buffer	Bidistilled water, 0.1 M Tris-HCl pH 8.5, 5 mM EDTA, 200 mM NaCl, 0.2 % SDS, pH 8.5
TBE (Tris/Borate/EDTA) buffer	Bidistilled water, 90 mM Tris, 90 mM Boric acid, 2 mM EDTA
Tris-buffered saline (TBS) 1X	50 mM Tris-Cl pH 7.5, 150 mM NaCl
Tris-EDTA buffer	Bidistilled water, 10 mM Tris Base, 1mM EDTA, pH 9.0

2.1.3 Antibodies for intracerebral injection and bacteria derived products

Table 3: Antibodies for intracerebral and intravenous injection and bacteria-derived products

Organism	Supplier
8-18C5 hybridoma	Prof. Dr. Christopher Linington, University of Glasgow, UK
Z2 hybridoma	Prof. Dr. Christopher Linington, University of Glasgow, UK
Mycobacterium butyricum desiccated, non-viable	DIFCO, Detroit, MI, USA
Mycobacterium tuberculosis H37RA, non-viable	DIFCO, Detroit, MI, USA

2.1.4 Proteins, cytokines and dyes

Table 4: Proteins and enzymes

Proteins and enzymes	Supplier
Collagenase D	Roche, Basel, Switzerland
DNAse I	Roche, Basel, Switzerland
Go-Taq® DNA polymerase	Promega, Madison, WI, USA
MOG_{35-55}	Institute of Medical Immunology, University Medical Center Charité, Berlin, Germany
$OVA_{323-339}$, chicken	InvivoGen, San Diego, CA, USA
Proteinase K	Sigma Aldrich, St. Louis, MO, USA
PTX (pertussis toxin)	List Biological Laboratories, Campbell, CA, USA
RedTaq® DNA polymerase	Sigma Aldrich, St. Louis, MO, USA
$rMOG_{1-125}$	His-tag purified at the Institute of Neuropathology, University Medical Center, Göttingen, Germany

Table 5: Cytokines and dyes

Cytokines and dyes	Supplier
FITC-Albumin	Sigma Aldrich, St. Louis, MO, USA
IFNγ, mouse, recombinant	R&D Systems, Minneapolis, MN, USA
IL-12, mouse, recombinant	R&D Systems, Minneapolis, MN, USA
IL-2, mouse, recombinant	R&D Systems, Minneapolis, MN, USA
Monastral blue	Sigma Aldrich, St. Louis, MO, USA
TNFα, mouse, recombinant	R&D Systems, Minneapolis, MN, USA

Table 6: Monoclonal antibodies for flow cytometry

Specificity	Clone	Fluorochrome	Dilution	Supplier
Anti-B220	RA3-6B2	PerCP	1:200	BD Biosciences, Franklin Lakes NJ, USA
Anti-CCR2	475301	APC	1:10	R&D Systems, Minneapolis, MN, USA
Anti-CD11b	M1/70	PE-Cy7	1:200	BioLegend, San Diego, CA, USA
Anti-CD11c	N418	PE	1:200	BioLegend, San Diego, CA, USA
Anti-CD16/32	93	-	1:100	BioLegend, San Diego, CA, USA
Anti-CD19	eBio1D3	FITC	1:200	eBioscience, San Diego, CA, USA
Anti-CD25	PC61.5	APC	1:200	eBioscience, San Diego, CA, USA
Anti-CD3	145-2C11	FITC	1:200	BioLegend, San Diego, CA, USA
Anti-CD4	RM4-5	PerCP	1:200	BioLegend, San Diego, CA, USA
Anti-CD45	30-F11	APC-Cy	1:200	BioLegend, San Diego, CA, USA
Anti-CD8	53-6.7	PE-Cy7	1:200	BioLegend, San Diego, CA, USA
Anti-FoxP3	FJK-16S	PE	1:100	eBioscience, San Diego, CA, USA
Anti-Ly6C	HK1.4	PE-Cy7	1:200	BioLegend, San Diego, CA, USA
Anti-Ly6G	1A8	PE	1:500	BioLegend, San Diego, CA, USA
Anti-NK1.1	PK-136	PE-Cy7	1:500	BioLegend, San Diego, CA, USA
Anti-Nkp46	29A1.4	PerCP	1:200	BioLegend, San Diego, CA, USA
Anti-γδ TCR	eBioGL3	APC	1:200	eBioscience, San Diego, CA, USA

2.1.5 Antibodies and inhibitors for depletion and blocking experiments

Table 7: Antibodies and inhibitors for depletion and blocking experiments

Name/Specificity	Clone	Species/Isotype	Application	Supplier
AMBA	n/a	Mouse/IgG	Isotype control antibody	Prof. Dr. Matthias Mack, University Hospital Regensburg, Germany
Anti-KLH	LTF-2	Rat/IgG2b	Isotype control antibody	Bio X Cell, West Lebanon, NH, USA
Anti-Ly6G	1A8	Rat/IgG2a	PMN depletion	Bio X Cell, West Lebanon, NH, USA
Anti-m/h VLA4 (Cd49d)	PS/2	Rat/IgG2b	Inhibition of leukocyte transmigration into the CNS	Bio X Cell, West Lebanon, NH, USA
Anti-NK1.1	PK136	Mouse/IgG2a	NK cell depletion	Bio X Cell, West Lebanon, NH, USA
BB5.1	BB5.1	Mouse/IgG1	C5 convertase inhibitor	Hycult Biotech, Plymouth, USA
DOC-2 Fr-2	DOC-2	Mouse/IgG 1	Depletion of CCR2+ monocytes in marmosets	Prof. Dr. Matthias Mack, University Hospital Regensburg, Germany
Mouse Isotype Control	MOPC-21	Mouse/IgG1	Isotype control antibody	BioLegend, San Diego, CA, USA
RS 504393	n/a	n/a	Selective CCR2 antagonist	R&D Systems, Minneapolis, MN, USA
Unknown	2A3	Rat/IgG2a	Isotype control antibody	Bio X Cell, West Lebanon, NH, USA
Unknown	C1.18.4	Mouse/IgG2a	Isotype control antibody	Bio X Cell, West Lebanon, NH, USA
Unknown	R35-95	Rat/IgG2a	Isotype control antibody	BD Biosciences, NJ, USA

Table 8: Antibodies for antigen-independent activation of T-cell proliferation *in vitro*

Specificity	Clone	Supplier
Anti-CD28	PV-1	Bio X Cell, West Lebanon, NH, USA
Anti-CD3	145-2C11	Bio X Cell, West Lebanon, NH, USA

2.1.6 Antibodies for histology and immunohistochemistry

Table 9: Primary antibodies used in paraffin-embedded and frozen tissue

Antigen	Species	Dilution	Antigen retrieval/Buffer	Catalog No.	Supplier
APP	Mouse	1:2000	Microwave/Citrate buffer 10 mM, pH 6	MAB348	Chemicon, Temecula, CA, USA
CCR2	Rabbit	1:100	Microwave/Tris-EDTA Buffer, 10 mM, pH 9	ab32144	Abcam, Cambridge, UK
CD107b (Mac-3)	Rat	1:200	Microwave/Citrate buffer 10 mM, pH 6	553322	BD Bioscience, Franklin Lakes NJ, USA
CD14	Mouse	1:10	Microwave/Tris-EDTA Buffer, 10 mM, pH 9	NCL-CD14-223	Leica Biosystems Newcastle Ltd., UK
CD3	Rabbit	1:150	Microwave/Citrate buffer 10 mM, pH 6	C1597C01	DCS, Hamburg, Germany
CD3	Rabbit	1:50	Microwave/HCl 2 mM, pH 2.5	A0452	Dako, Hamburg, Germany
FITC	Rabbit	1:50	Microwave/Citrate buffer 10 mM, pH 6	P5100	Dako, Hamburg, Germany
GrB	Mouse	1:50	Microwave/HCl 2 mM, pH 2.5	M7235	Dako, Hamburg, Germany
KiM1P	Mouse	1:5000	Microwave/Citrate buffer 10 mM, pH 6	n/a	Provided by the Institute of Pathology, University of Kiel, Germany
MBP	Rabbit	1:1000	n/a	A0623	Dako, Hamburg, Germany
NeuN	Mouse	1:200	Microwave/Citrate buffer 10 mM, pH 6	MAB377	Merck Millipore, Darmstadt, Germany
NKp46/NCR1	Goat	1:50	Ethanol fixation 1 h, Cryosections	AF225	R&D Systems, Minneapolis, MN, USA
Olig2	Rabbit	1:150	Microwave/Citrate buffer 10 mM, pH 6 Tris-EDTA Buffer, 10 mM, pH 9	18953	IBL, Hamburg, Germany
rMOG	Rat	1:1000	Microwave/Citrate buffer 10 mM, pH 6	n/a	Purified at the Institute of Neuropathology, UMG, Germany
TPPP/p25	Rabbit	1:500	Microwave/Tris-EDTA Buffer, 10 mM, pH 9	92305	Abcam, Cambridge, UK

Table 10: Secondary biotinylated antibodies for IHC

Species/Specificity	Dilution	Blocking buffer	Catalog No.	Supplier
Anti-mouse, biotinylated	1:200	10 % FCS/PBS	RPN1001	GE Healthcare Ltd, UK
Donkey-anti-goat, biotinylated	1:200	10 % FCS/PBS	RPN1025	GE Healthcare Ltd, UK
Donkey-anti-rabbit, biotinylated	1:100	10 % FCS/PBS	RPN 1001	GE Healthcare Ltd, UK
Goat-anti-rabbit-AP	1:50	10 % FCS/TBS	D 0487	Dako, Hamburg, Germany
Goat-anti-rabbit-AP	1:50	10 % FCS/Tris-EDTA Buffer, 10 mM, pH 9	D 0487	Dako, Hamburg, Germany
Goat-anti-rat	1:500	10 % FCS/PBS	AS-2100-16	DCS, Hamburg, Germany
Rabbit-anti-rat, biotinylated	1:100	10 % FCS/PBS	E0468	Dako, Hamburg, Germany

Table 11: Secondary antibodies fluorochrome-conjugated for fluorescent IHC

Specie/Specificity	Dilution	Blocking buffer	Catalog No.	Supplier
Cy™3-conjugated Streptavidin	1:100	10 % FCS/PBS	016-160-184	Jackson ImmunoResearch Lab, PA, USA
goat-anti-mouse Cy™3-conjugated	1:200	10 % FCS/PBS	115-165-146	Jackson ImmunoResearch Lab, PA, USA
Goat-anti-rabbit AlexaFluor® 488	1:200	10 % FCS/PBS	A11034	Molecular Probes, OR, USA

2.1.7 Kits

Table 12: Kits used

Kit	Supplier
High Capacity RNA-to-cDNA™ Kit	Life Technologies, Applied Biosystems, USA
Naphtol AS-D Chloroacetate (Specific esterase) kit	Sigma-Aldrich, St. Louis, MO, USA
qPCR Core Kit	Eurogentec, Germany
RNeasy Micro Kit	Qiagen, Germany
Tyramide Signal Amplification kit (TSA™ Kit 21)	Invitrogen, Life Technologies, USA

2.1.8 Oligonucleotide primers and FAM labeled primers/probes

Table 13: Oligonucleotide primers for genotyping of transgenic mice

Name	Sequence (5´-> 3´) (bp)	Gene	Mouse Line
8.18C5-antisense	GGA GAC TGT GAG AGT GGT GCC T (22)	anti-MOG IgH (8.18C5)	Th
8.18C5-sense	TGA GGA CTC TGC CGT CTA TTA CTG T (25)	anti-MOG IgH (8.18C5)	Th
CD59_exon 3	GCT ACC ACT GTT TCC AAC CGG TG (23)	Cd59a	Th/+ CD59a$^{-/-}$
CD59_neomycin	GAA CCT GCG TGC AAT CCA TCT TG (23)	Cd59a	Th/+ CD59a$^{-/-}$
CD59a_intron 3	GGT GAC CAA CTG GTG TTA ACA AAG GG (26)	Cd59a	Th/+ CD59a$^{-/-}$
Ja18-2D2-M	GCG GCC GCA ATT CCC AGA GAC ATC CCT CC (29)	Valpha 3.2 TCR	2D2
mIgH-antisense	TGG TGC TCC GCT TAG TCA AA (20)	Igh-J	Th
mIgH-sense	ATT GGT CCC TGA CTC AAG AGA TG (23)	Igh-J	Th
oIMR0301	CTT CTT AGT CCT TCA GCT GC (20)	Il2rg ,gamma chain	Rag1$^{-/-}$ γc$^{-/-}$
oIMR0302	AGG CTC AGA ACT GCT ATT CC (20)	Il2rg ,gamma chain	Rag1$^{-/-}$ γc$^{-/-}$
oIMR0303	GTA TGG TAG TGT TCT CAC CG (20)	Il2rg ,gamma chain	Rag1$^{-/-}$ γc$^{-/-}$
RAG com reverse	CCG GAC AAG TTT TTC ACT GT (20)	RAG1	Rag1$^{-/-}$
RAG mutant forward	TGG ATG TGG AAT GTG TGC GAG (21)	RAG1	Rag1$^{-/-}$
RAG wt forward	GAG GTT CCG CTA CGA CTC TG (20)	RAG1	Rag1$^{-/-}$
Va3.2-2D2-M	GGG CAA GGC TCA GCC ATG CTC CTG (24)	Vα 3.2 TCR	2D2
WAK 121	TTC CAT TGC TCA GCG GTG CT (20)	Ccr2	Th/+ CCR2$^{-/-}$
WAK 134	TCA GAG ATG GCC AAG TTG AGC AGA (24)	Ccr2	Th/+ CCR2$^{-/-}$
WAK 32	GTG AGC CTT GTC ATA AAA CCA GTG (24)	Ccr2	Th/+ CCR2$^{-/-}$

Oligonucleotide primers for the genotyping of 2D2, Th and Rag1$^{-/-}$ mice were purchased from Eurofins Genomics, Germany. For the genotyping of Th/+ CD59a$^{-/-}$, Th/+ CCR2$^{-/-}$ and Rag1$^{-/-}$ γc$^{-/-}$ mice, additional primers were kindly provided by Dr. Benoit Barrette, Max Planck Institute for Experimental Medicine, Göttingen, Germany.

Table 14: FAM labeled primers/probes for qRT-PCR

Name	Gene	Supplier
Mm00440502_m1	NOS2/iNOS	TaqMan® Gene Expression Assays, Life Technologies, USA
Mm00441242_m1	CCL2	TaqMan® Gene Expression Assays, Life Technologies, USA
Mm00443258_m1	TNFα	TaqMan® Gene Expression Assays, Life Technologies, USA
Mm99999915_g1	Gapdh	TaqMan® Gene Expression Assays, Life Technologies, USA

2.1.9 Consumables

Table 15: Consumable material

Consumable	Source of supply
Blaubrand® intraMARK micropipettes, 5 µl	Brand GmbH, Wertheim, Germany
Butterfly™ Winged Infusion Set (25G x ¾")	Hospira UK Ltd, UK
Cell culture dish, 60 x 15 mm	Greiner bio-one, Kremsmuenster, Austria
Cell strainer (70 µm)	BD Biosciences, Franklin Lakes, NJ, USA
FACS tube, 5 ml	BD Biosciences, Franklin Lakes, NJ, USA
Feather disposable scalpel (No. 11, No. 21)	PFMmedical AG, Köln, Germany
GEM® Scientific Razor Blades	Alpha Biotech Ltd., Glasgow, UK
Needles (23G, 26G)	BD Biosciences, Franklin Lakes, NJ, USA
Nunc™ MaxiSorp® 96 well ELISA plate	Thermo Scientific, Waltham, MA, USA
Nunc™ Microwell™ Plates, 96 well round bottom	Thermo Scientific, Waltham, MA, USA
Syringes (1 ml, 5ml, 10 ml, 20 ml)	BD Biosciences, Franklin Lakes, NJ, USA
Tubes (0.2 ml, 1,5 ml, 2 ml, 15 ml, 50 ml)	Sarstedt, Nuembrecht, Germany

2.1.10 Technical devices

Table 16: Technical devices

Device	Supplier
Centrifuge 5415 R	Eppendorf, Hamburg, Germany
Centrifuge 5810 R	Eppendorf, Hamburg, Germany
Cryostat Leica CM3050	Leica Instruments GmbH, Germany
FACS Canto™ II	BD Biosciences, Franklin Lakes, NJ, USA
Fluorescence/light microscope, Olympus BX51	Olympus, Germany
Hera cell 150 incubator	Heraeus, Hanau, Germany
iQ5™ Real Time PCR Detection System	Bio-Rad Laboratories, Germany
Keyence Bio REVO BZ-X710 microscope	Keyence, Japan
Microtome Leica SM2000R	Leica Instruments GmbH, Germany
Neubauer chamber	Superior Marienfeld, Lauda-Koenigshofen, Germany
Ocular morphometric grid, 10x10	Olympus, Japan
Power Pac 300	Bio-Rad Laboratories, Germany
Speed vacuum Concentrator 5301	Eppendorf, Hamburg, Germany
Stereotactic device	Stoelting Co., Germany
T3 Thermocycler	Biometra, Germany
Thermo mixer comfort	Eppendorf, Hamburg, Germany
UV transluminator	Vilber Lourmat, Eberhardzell, Germany

2.1.11 Software

Table 17: Software

Software	Application	Supplier
BD FACSDiva 6.1.2	Data acquisition flow cytometry	BD Biosciences, Franklin Lakes, NJ, USA
BZ-II analyzer	Photomerge of high resolution images	Keyence, Japan
CellSens Dimension v.1.7.1 DP71	Image acquisition	Olympus, Germany
FlowJo 7.6.1	Data analysis flow cytometry	Tree Star Inc., Ashland, OR, USA
GraphPad Prism 5.01	Statistical analysis	GraphPad software Inc., La Jolla, CA, USA
Image J v.1.46r	Analysis of digital images	NIH, USA
LabVIEW™-based software	Record of running wheel performance	National Instruments Corp., Germany
PSRemote 1.6.5	Gel documentation	Breeze System Limited, Camberley, UK

2.2 Human tissue samples

In the present study, brain tissue samples including cerebral cortex from eight patients diagnosed with inflammatory demyelination compatible with MS, were available for analysis (see Table 18). Biopsies were performed for diagnostic purposes to exclude the differential diagnoses of lymphoma, tumor or infection. The study was approved by the local ethics committee (Nr. 14/5/03).

Table 18: Clinical findings of MS biopsy cases used in the present study

MS case	Age/Sex	Disease duration (month)	Disease course	Presenting symptom(s)	Brain MRI	Index lesion	OCBs
1	45/F	6	CIS	Slight ataxia, unsteady gait	Multiple intracerebral WM lesions in subcortical, cortical and periventricular areas	Right frontal	N/A
2	48/F	11	RRMS	Blurred vision of right eye	Multiple intracerebral WM lesions, partly cortical and subcortical	Left parietal	+
3	34/F	3	RRMS	Blurred vision of left eye	Multiple intracerebral WM lesions, juxtacortical and brain stem, partly contrast-enhancing	Right temporal	-
4	39/F	0.3	CIS	Minor weakness of left hand	Single lesion frontal right	Right frontal	+
5	26/F	2	CIS	Minor weakness of left hand, symptomatic epilepsy with focal motor seizures	Several intracerebral WM lesions: three subcortical lesions (≤ 3 cm diameter), partly ring-enhancing; two brain stem lesions	Right frontal	+
6	13/F	116	RRMS	Weakness of both legs, pre-existing symptomatic epilepsy, hand tremor, dysarthria	Several supratentorial lesions, partly contrast-enhancing	Left frontal	-
7	42/F	2	CIS	Vision loss, disturbed balance, depression, beginning dementia	Multiple subcortical and periventricular WM lesions, partly contrast-enhancing	Left frontal	N/A
8	64/M	1	CIS	Fatigue, aphasia	Three lesions: precentral left, temporal left, frontal right, partly contrast-enhancing	Left temporal	N/A

Legend

Based on the number of relapses, biopsy cases were either classified as clinically isolated syndrome (CIS) or relapsing-remitting MS (RRMS). CIS patients underwent biopsy after the first relapse. OCBs: oligoclonal bands; F: female; M: male; N/A: not available

2.3 Animals

2.3.1 Mouse strains

The following mouse strains were used for *in vivo* experiments and/or cell isolations. All mice were between 6-10 weeks of age and from both sexes.

C57BL/6J mice

C57BL/6J mice were purchased from Charles River laboratories, Sulzfeld, Germany.

2D2 mice

2D2 mice (also named TCR^{MOG} mice) were generated and characterized in 2003 by Bettelli and colleagues. In 2D2 animals, 90-95 % of the CD4+ T cells express the transgenic TCR Vα 3.2/Vβ 11, which specifically recognizes the MOG_{35-55} peptide. Around 4 % of the mice develop spontaneous EAE and the incidence of developing spontaneous optic neuritis is around 40 % (Bettelli et al., 2003).

Th mice

Th mice were created and characterized by Litzenburger and colleagues in 1998. For the generation of the mice, the VDJ region of the hybridoma 8-18C5 was inserted into the regular location of the rearranged variable (V) gene of the Ig heavy (H) chain. In Th mice (also named IgH^{MOG} mice), 30-40 % of B cells express transgenic IgH chains, resulting in high production of MOG-specific pathogenic antibodies that can be found in the serum. Naïve transgenic animals do not develop spontaneous EAE or any sign of demyelination. However, the presence of the transgene accelerates and exacerbates EAE upon immunization when compared to wild type littermates (Litzenburger et al., 1998). For this thesis only heterozygous animals (Th/+) were used.

OSE mice

OSE mice characterized by Bettelli et al. and Krishnamoorthy et al. were generated by crossbreeding Th/Th mice with 2D2 animals (Bettelli et al., 2006, Krishnamoorthy et al., 2006). OSE mice have MOG-specific T- and B cells and develop spontaneous EAE in 30-50 % of the animals.

Rag1$^{-/-}$ mice

Rag1$^{-/-}$ mice were generated by Mombaerts and colleagues in 1992 and subsequently backcrossed to C57BL/6J mice. In these mice, the recombination activating gene-1 (*RAG1*) was mutated, resulting in reduced lymphoid organs accompanied by a complete absence of mature B and T cells (Mombaerts et al., 1992).

Rag1$^{-/-}$ γc$^{-/-}$mice

Rag1$^{-/-}$ γc$^{-/-}$mice were generated by crossbreeding of γc gene (also known as *Il2rg* gene) deficient mice (Cao et al., 1995) with Rag1 deficient mice (Mombaerts et al., 1992). These mice lack mature B cells, T cells and NK cells.

Th/+ CCR2$^{-/-}$mice

Th/+ and chemokine receptor type 2 (CCR2$^{-/-}$) mice were generated by crossbreeding of Th/Th mice with CCR2$^{-/-}$ mice (see 2.3.2). CCR2 deficient mice showed a severe impairment in leukocyte firm adhesion, extravasation and recruitment of inflammatory monocytes to sites of inflammation *in vivo* (Kuziel et al., 1997).

Th/+ CD59a$^{-/-}$ mice

Th/+ CD59a$^{-/-}$ mice were generated by crossbreeding of Th/Th mice with CD59a$^{-/-}$ mice (Holt et al., 2001) (see 2.3.2). CD59a is the major inhibitor of the membrane attack complex (MAC) formation. CD59a$^{-/-}$ mice are healthy and fertile but exhibited hemoglobinuria and intravascular spontaneous hemolysis, exacerbated upon administration of cobra venom factor (a recognized agent for triggering the depletion of the complement cascade) (Holt et al., 2001). CD59a$^{-/-}$ mice were provided by Prof. Dr. George Trendelenburg (Neurology Department, University Medical Center, Göttingen).

OT-II mice

OT-II [ovalbumin (OVA)-specific, MHC class II-restricted αβ TCR mice] mice were developed and characterized by Barnden and colleagues in 1998. In OT-II transgenic mice CD4+T cells are specific for the $OVA_{323-339}$ peptide (Barnden et al., 1998). OT-II mice used in this thesis were a kindly provided by Prof. Michael Schön (Department of Dermatology, Venereology and Allergology, University Medical Center, Göttingen).

2.3.2 Breeding

All mice used in this study were bred at the animal facility of the University Medical Center Göttingen, under specific pathogen free (SPF) conditions and backcrossed to C57BL/6J for more than 12 generations. Mice were kept in a controlled environment under 12/12 hour light/dark cycles with access to water and food *ad libitum*. Experiments were performed in accordance with the European Communities Council Directive of 24 November 1986 (86/EEC) and were approved by the Government of Lower Saxony, Germany (G 347.11, G 1005.12).

2.3.3 Marmosets

Common marmosets (*Callithrix jacchus*) from both sexes (2-4 years old, n=10) were bred at the German Primate Center (Göttingen, Germany). Depletion experiments of inflammatory monocytes in marmoset-EAE (see 2.4.4.2 for details) were conducted by PD Dr. Christina Schlumbohm (Neu Encepharm) under the guidelines of the European Council Directive of September 2010 (2010/63/EU) and Communities Council Directive 86/609/EEC, and approved by the Lower Saxony Federal State Office for Consumer Protection and Food Safety (LAVES), Germany.

2.4 Methods

2.4.1 Genotyping of genetically modified mice

Genotyping of genetically modified mice and optimization of polymerase chain reaction (PCR) conditions were partially performed by Katja Schulz and Olga Kowatsch (Department of Neuropathology, University Medical Center Göttingen). The genotyping of the OT-II mice used in this thesis was performed at the Dermatology Department, University Medical Center Göttingen (protocol not described here).

2.4.1.1 DNA extraction

Tail biopsies were collected from 2D2, Th/+, Rag1$^{-/-}$, Rag1$^{-/-}$ γc$^{-/-}$, OSE, Th/+ CCR2$^{-/-}$ and Th/+ CD59a$^{-/-}$ mice at 3 weeks of age. For the extraction of genomic DNA, the tails were digested overnight in a mixture of 350 µl tail lysis buffer and 20 µl Proteinase K using a shaker (350 rpm, 56 °C). Samples were centrifuged (5 min, 13200 rpm) and the supernatants

were collected in new eppendorf tubes. For DNA precipitation 350 µl of isopropyl alcohol were added to each sample, thoroughly mixed and centrifuged again. Supernatants were discarded on a tissue and 500 µl of ethanol (70 %) were added followed by a last centrifugation step. The DNA pellet was dried during 10-15 min at 45 °C in a speed vacuum concentrator and resuspended in 100 µl bidistilled water.

2.4.1.2 Polymerase chain reaction

The composition of the PCR reactions for the genotyping of each transgenic mouse is described in Table 19. For additional details regarding the primers used see Table 13. All PCR reactions were run in a T3 thermocycler and the specific cycling conditions are described in Table 20. Ethidium bromide-stained PCR products were separated by electrophoresis on an agarose gel (2 % in TBE buffer) at 120 V for 60-90 min and the product length was evaluated using a 100 bp DNA ladder (Thermo Scientific) under UV light.

For the genotyping of $Rag1^{-/-}\gamma c^{-/-}$ mice, two PCR reactions were performed: one for the *RAG1* gene and one for the gene *Il2rg* (IL-2 receptor, gamma chain). Similarly, for OSE mice, two PCR reactions corresponding to *Vα 3.2 TCR* gene (2D2 mice) and *Igh-J* gene (Th mice) were ran. Finally, for Th/+ $CCR2^{-/-}$ and Th/+ $CD59a^{-/-}$ mice, a PCR reaction to identify the presence of the *Igh-J* gene was performed in addition to the corresponding ones for *Ccr2* and *Cd59a* genes.

Table 19: Composition of PCR reactions for genotyping of transgenic mice

PCR reaction components	Gene					
	Vα 3.2 TCR	***Igh-J***	***RAG1***	***Il2rg***	***Ccr2***	***Cd59a***
Betaine Q	-	-	-	1.1 µl	-	-
DNA template	5 µl	5 µl	1 µl	1.5 µl	2 µl	1 µl
dNTP Mix (10 mM)	0.4 µl	0.4 µl	-	-	1 µl	2 µl
dNTP Mix (2.5 mM)	-	-	0.5 µl	2.2 µl	-	-
Go Taq® DNA pol. Buffer (10X)	-	-	-	2.2 µl	-	-
Go Taq® DNA pol. Buffer (5X)	4 µl	4 µl	2.5 µl	-	5 µl	4 µl
Go Taq® DNA polymerase	0.1 µl	0.1 µl	0.1 µl	-	0.2 µl	0.1 µl
H_2O, bidistilled	9.5 µl	8.5 µl	5.4 µl	9.15 µl	15.3 µl	12.3 µl
$MgCl_2$	-	-	-	1.1 µl	-	-

PCR reaction components	Gene					
	Vα 3.2 TCR	***Igh-J***	***RAG1***	***Il2rg***	***Ccr2***	***Cd59a***
Primers	0.5 µl each	0.5 µl each	1.2 µl (fp) 0.6 µl (rp)	1 µl each	0.5 µl each	0.2 µl each
Red Taq® DNA polymerase	-	-	-	0.75 µl	-	-

Abbreviations

Ccr2: chemokine (C-C motif) receptor 2; Cd59a: CD59a antigen; fp: forward primer; Igh-J: immunoglobulin heavy chain, joining region; Il2rg: IL-2 receptor, gamma chain; RAG1: recombination activating gene 1, rp: reverse primer; Vα 3.2 TCR: alpha chain 3.2 of the T cell receptor, variable region

Table 20: Conditions of PCR reactions and identification of the products

Gene	Step 1 (°C/sec)	Step 2 (°C/sec)	Step 3 (°C/sec)	Step 4 (°C/sec)	Step 5 (°C/sec)	Step 6 (°C/sec)	Product size (bp)
Vα 3.2 TCR	95/120	95/60	58/60	72/60	72/600	4/∞	tg 600-700
Igh-J	95/120	95/60	61/60	72/60	72/600	4/∞	wt 150 ko 100
RAG1	94/120	94/60	58/45	72/45	72/120	4/∞	wt 474 ko 530
Il2rg	94/180	94/30	67/30	72/60	72/120	4/∞	wt 269 ko 349
Ccr2	94/180	94/45	59/45	72/60	72/600	4/∞	wt 180 ko 450
Cd59a	95/120	95/30	59/30	72/30	72/300	4/∞	wt 212 ko 450

Abbreviations: tg: transgene; wt: wild type; ko: knockout; ∞: infinite

Note: Step 1: pre-denaturation; Step 2: denaturation; Step 3: annealing; Step 4: elongation; Step 5: final elongation; Step 6: Hold. Steps 2-4 are repeated for 30-35 cycles

2.4.2 Experimental autoimmune encephalomyelitis

EAE is the most common animal model of MS, used to study mechanisms of autoimmune CNS inflammation and tissue injury (Gran et al., 1999, Engelhardt, 2006, Boretius et al., 2012).

2.4.2.1 Induction and assessment of EAE

EAE induction in mice

EAE was induced in 2D2, C57BL/6J, Th/+, Th/+ CCR2$^{-/-}$, Th/+ CD59a$^{-/-}$ and OSE mice. Therefore, mice were anesthetized by intraperitoneal (i.p.) injection of 100 µl/10 g of body weight of a xylazine/ketamine mixture (xylazine: 20 mg/kg; ketamine: 120 mg/kg). 2D2 mice were subcutaneously (s.c.) immunized with 200 µg/animal of MOG_{35-55} (myelin oligodendrocyte protein, peptide fragment 35-55) emulsified in complete Freund´s adjuvant (CFA) supplemented with 5 mg/ml *Mycobacterium tuberculosis* H37RA. For immunization of the remaining mice strains 100 µg recombinant rat MOG_{1-125}/CFA (myelin oligodendrocyte protein, peptide fragment 1-125) were used. Mice were injected i.p. with 300 ng of pertussis toxin (PTX) dissolved in 200 µl PBS at the day of immunization and again 48 h after. Control animals were immunized with CFA only.

EAE induction in common marmosets

Common marmosets, (see 2.3.3) were immunized s.c. with 50 µg recombinant rat MOG_{1-125} emulsified in Freund´s adjuvant supplemented with 0.25 mg/ml *Mycobacterium butyricum*.

The clinical course of EAE in common marmosets was recorded daily by a trained person using a neurological disability scale first reported by Villoslada and colleagues (Villoslada et al., 2000) and further developed by Boretius and colleagues (Boretius et al., 2006).

In mice, the clinical course of EAE was monitored daily starting on day 7 after immunization following a scoring system ranging from 0 (healthy) to 5 (death) detailed in Table 21.

Table 21: Clinical EAE score in mice

Score	Clinical signs
0	Healthy, no clinical signs
0.5	Partial paralysis of the tail
1	Complete paralysis of the tail
2	Beginning paralysis of the hind limbs; mouse can be turned on its back
2.5	Strong paralysis of the hind limbs
3	Complete paralysis of hind limbs; beginning paralysis of abdominal muscles
3.5	Complete paralysis of abdominal muscles, beginning weakness of fore limbs
4	Pronounced weakness or complete paralysis of fore limbs
5	Dead

For cortical lesion experiments (see 2.4.3), mice were intracortically injected on the second day of EAE.

2.4.3 Generation of cortical lesions in the mouse

For this purpose, a modification of the technique previously developed in our laboratory for the generation of cortical lesions in rats (Merkler et al., 2006b) was used. The method combines EAE immunization of the animals with a focal intracerebral injection of pro-inflammatory cytokines into the cortex. Figure 1 depicts a schematic representation of the experimental setup.

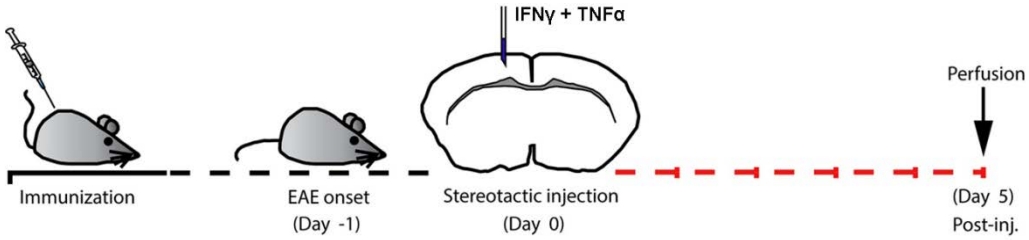

Figure 1: General experimental setup for the generation of cortical demyelinated lesions in the mouse

2.4.3.1 Focal intracerebral injection

Mice were anesthetized by i.p. injections of ketamine/xylazine (10 µl/g of body weight). Once the mice were deeply anesthetized, heads were shaved, the scalp was opened

to expose the skull and the animals were immobilized in a stereotactic device. The exposed periosteum was disrupted with a scalpel and a 2 mm diameter hole was drilled on the right brain hemisphere [0.1 mm caudal to bregma, 0.2 mm lateral to the midline]. A fine, calibrated glass capillary with a diameter between 1-2 µm was inserted into the brain motor cortex (0.7 mm depth) and 2 µl of a mixture of 50 ng tumor necrosis factor-alpha (TNFα) and 60 ng IFNγ were injected over a 3-5 min period. Monastral blue was added to the cytokine mixture to identify the injection site. In all immunized animals, focal intracerebral injections were done on the second day after clinical onset of EAE. Dr. Claudia Wrzos (Department of Neuropathology, University Medical Center Göttingen) performed most of the intracerebral injections.

2.4.4 Depletion and blocking experiments

In mice, all depletion and blocking experiments started at EAE onset unless stated otherwise. The efficiency of the depletion experiments was evaluated by flow cytometry analysis (see 2.4.7.3) immediately before the intracerebral cytokine injection and at the day of sacrifice. Brain and spinal cord tissue was collected for histopathological analysis on day 5 post stereotactic injection.

2.4.4.1 CCR2 inhibition in the mouse

Immunized Th/+ mice received daily 4 mg/kg of the CCR2 inhibitor RS 504393 starting at EAE onset and until day 5 after the intracortical injection of cytokines (Figure 2). Therefore, the dosage was divided into two daily oral gavages of 40 µg from the inhibitor in 200 µl of a mixture of dimethyl sulfoxide (DMSO) and 1 % sodium carboxymethyl cellulose (CMC) solution. A stock solution of the inhibitor (4 µg/µl) in DMSO and a 1 % CMC solution were prepared and mixed as follows: 10 µl stock solution/190 µl of 1 % CMC. Th/+ animals in the control group received only vehicle (DMSO/CMC mixture).

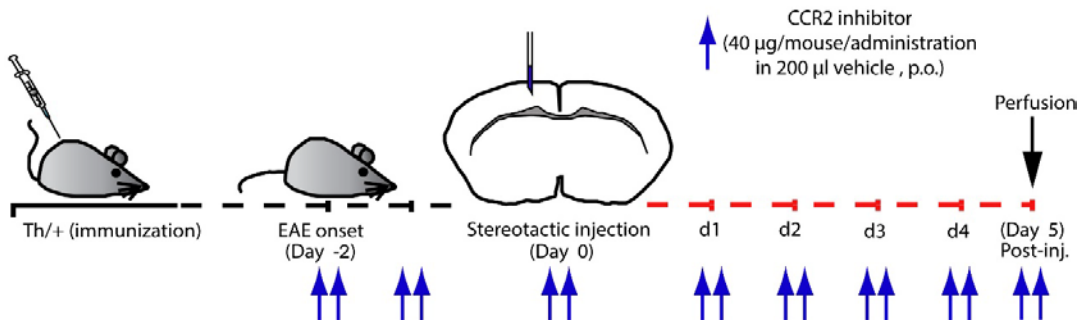

Figure 2: Schematic representation of CCR2 inhibition in Th/+ mice

2.4.4.2 Monocyte depletion in marmosets

For depleting inflammatory monocytes in marmosets with EAE, a humanized monoclonal mouse anti-human CCR2 antibody (named DOC-2 Fr-2) was used. Prof. Matthias Mack (Department of Internal Medicine, University Hospital Regensburg) developed and provided the mouse anti-human CCR2 antibody. This mouse anti-human CCR2 antibody was humanized by Dr. Eilish Cullen (Medical Research Council Technology, Lynton House, London, UK).

For EAE experiments, the DOC-2 Fr-2 antibody was administered twice per week i.v. (5 mg/kg) from day 14-24 after immunization and once weekly thereafter until day 56. Marmosets in the control group received i.v. injections of a control isotype antibody (named AMBA) (see Figure 3).

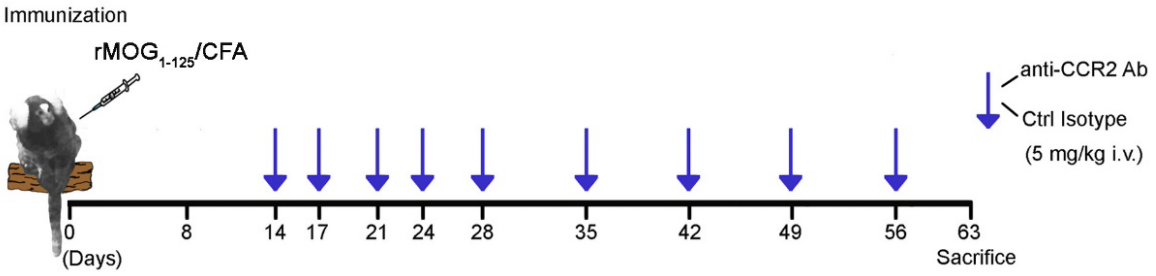

Figure 3: Schematic representation of the treatment protocol for the depletion of inflammatory monocytes in marmoset monkeys

2.4.4.3 Depletion of granulocytes in the mouse

For the depletion of polymorphonuclear leukocytes, Th/+ mice received daily i.p. injections (400 µg/animal) of the depleting antibody anti-Ly6G (clone 1A8) (Daley et al., 2008) or a control isotype (Clone 2A3) (Hermesh et al., 2012) according to Figure 4.

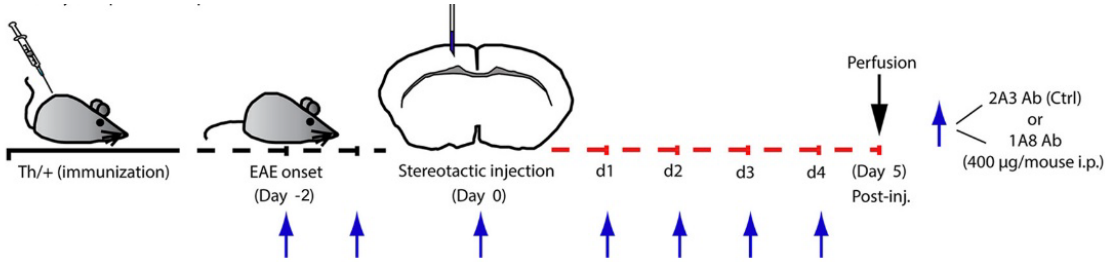

Figure 4: Schematic representation of the granulocyte depletion protocol in Th/+ mice

2.4.4.4 Depletion of natural killer cells in the mouse

Th/+ mice were depleted from NK cells by daily i.p. injections of 300 µg/mouse of the mAb PK136 (anti-NK1.1) (Nierlich et al., 2010). Control Th/+ mice received the same dose of the control isotype antibody C1.18.4 (Lamere et al., 2011). Both antibodies were administered until day 4 post stereotactic injection and the animals were perfused 24 h later (see Figure 5).

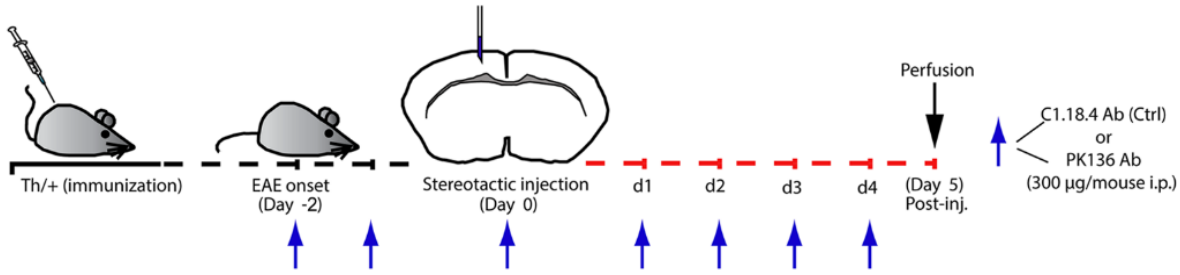

Figure 5: Schematic representation of the protocol for NK cell depletion in Th/+ mice

2.4.4.5 Blockade of the membrane attack complex in the mouse

For blocking the formation of the membrane attack complex (MAC), Th/+ mice received 2 µg of the BB5.1 mAb against the mouse convertase C5 (C5) (Frei et al., 1987, Huugen et al., 2007) or a control IgG1 isotype (clone MOPC-21) (Pohar et al., 2013) as depicted in Figure 6. The antibodies were injected intracortically together with the inflammatory cytokines as described previously and mice were perfused on day 5 post-injection.

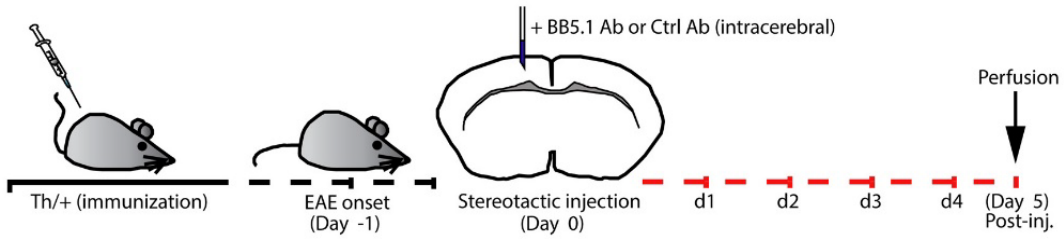

Figure 6: Schematic representation of the protocol to inhibit the formation of the MAC in Th/+ mice

2.4.4.6 Blockade of leukocyte transmigration into the CNS

To study the effect of hampering the transmigration of immune cells into the CNS in the model, the Natalizumab mouse analogue mAb PS/2 (Theien et al., 2001) was used. This rat IgG2b antibody directed against the mouse α4-integrin CD49d (also known as VLA-4), blocks the interaction between the CD49d receptor expressed on leukocytes and its ligand, the vascular cell adhesion molecule-1 (VCAM-1) on endothelial cells. As a result, leukocyte migration into the CNS is inhibited (Yednock et al., 1992, Baron et al., 1993). Therefore, immunized Th/+ mice received daily 200 µg/animal i.p. injections (7 injections in total) of the PS/2 antibody or an anti-key limpet hemocynanine specific rat IgG2b control antibody (Noval Rivas et al., 2009) starting at EAE onset until day 4 after the intracerebral injection.

2.4.5 Adoptive transfer experiments

EAE was induced in Rag1$^{-/-}$ and Rag1$^{-/-}$ γc$^{-/-}$ deficient mice by adoptive transfer of 10 Mio activated MOG-specific T cells from 2D2 donor mice. Recipient mice were immunized s.c. with 10 µg MOG_{35-55}/CFA 12 h after T cell transfer.

10 Mio activated ovalbumin-specific T cells from OT-II mice and activated MOG-specific T cells from 2D2 animals were adoptively transferred into Rag1$^{-/-}$ mice. Recipient mice were immunized s.c. with 10 µg MOG_{35-55} or $OVA_{323-339}$/CFA 12 h after T cell transfer.

2.4.5.1 Isolation, cultivation and transfer of T cells into recipient mice

For the isolation of T cells, donor mice were euthanized by cervical dislocation. The spleens were removed under aseptic conditions and smashed through a sterile cell strainer (70 µm) to obtain single cell suspensions. Splenocytes were collected in 50 ml tubes by flushing 10-15 ml of $RPMI_{complete}$ medium through the cell strainer and tubes were spun down for 10 min at 300 x *g* and 4 °C. Supernatants were discarded and the pellets were resuspended in 2 ml of BD Pharm Lyse™ solution (pre-diluted 1:10 in bidistilled water). Lysis of red blood cells was performed for 3-4 min at room temperature (RT) and the reaction was stopped by adding 20 ml of cold $RPMI_{complete}$. Cells were centrifuged again (same conditions as described above), the supernatants discarded and the cell pellet resuspended in 5 ml of RPMI. Cell viability and cell numbers were assessed in a Neubauer chamber using trypan blue solution (Strober, 2001).

Splenocytes from 2D2 or OT-II mice were first expanded by plate bound anti-CD3 and anti-CD28 stimulation. For this purpose, 96 U-well plates were incubated overnight in a fridge with anti-CD3 antibody (4 µg/ml in PBS, clone 145-2C11). The plates were washed twice with 200 µl RPMI to remove unbound antibody and 2^10^5 splenocytes/well were added in 80 µl RPMI. 20 µl of RPMI containing 0.1 ng rm IL-12 and 0.1 µg anti-CD28 antibody (clone PV-1) were added to each well (final concentrations: 1 ng/ml IL-12; 1 µg/ml anti-CD28 antibody). After 3 days, the splenocytes were transferred to 24 well plates and expanded by rm IL-2 (2 ng/ml). The cells were split every second day and RPMI with 4 ng/ml rm IL-2 was added. 10 days after CD3/CD28 stimulation. 1.5 Mio T cells were re-stimulated with 6 Mio 30 Gy-irradiated splenocytes as APC and 15 µg/ml MOG_{35-55} or $OVA_{323-339}$ peptide for 3 days

at 37°C/5 % CO2 in 24 well plates. The T cells were collected, washed twice with PBS, counted and 10 Mio T cell blasts in 200 µl PBS were injected i.p. into recipient animals. 12 h after the adoptive transfer, recipient mice were s.c. immunized with 10 µg MOG_{35-55} or OVA peptide and received a single i.p. injection of 300 ng PTX.

2.4.6 Motor skill sequence (MOSS) test

Male Th/+ and C57BL/6J mice (20 animals each) were trained during 2 weeks on an activity wheel with regularly spaced crossbars (training wheel) in which animals were allowed to run voluntarily. Next, mice were immunized s.c. with a subclinical dose of 10 µg recombinant rat MOG_{1-125}/CFA. After immunization, animals were put back on the training wheel for 11 more days and then randomized according to their performance on the training wheel into comparable groups, which received stereotactic injections of either 2 µl PBS or inflammatory cytokines:

- 10 Th/+ mice (intracerebral injection of PBS)
- 10 Th/+ mice (intracerebral injection of cytokines)
- 10 C57BL/6J mice (intracerebral injection of PBS)
- 10 C57BL/6J mice (intracerebral injection of cytokines)

One day after surgery, mice were put onto a “complex activity wheel” with irregularly spaced crossbars and the maximum running speed in rpm/min (Vmax) and the accumulative distance in meters reached daily by the animals were continuously recorded using the LabVIEW™-based custom software. The Vmax was expressed in percent, relative to the highest velocity reached at the end of the training in the normal activity wheel. Mice were perfused 8 days after stereotactic injections and brains and spinal cords were collected for histology.

2.4.7 Analysis of immune cells *ex vivo*

To define the immune cell composition of cortical lesions in Th/+ mice and to check depletion efficiency of different cell populations in transgenic mice as well as in the marmosets, blood and cortex were collected and analyzed *ex vivo* by multicolor flow cytometry. The markers defined for the identification of each cell population by flow cytometry are depicted in Table 22.

Table 22: Classification of the cell populations identified by flow cytometry analysis

Cell population	Specific surface and intracellular markers
T cells	$CD45^+$ $CD3^+$
CD4 T cells	$CD45^+$ $CD3^+$ $CD4^+$
Regulatory T cells	$CD45^+$ $CD3^+$ $CD4^+$ $CD25^+$ $FoxP3^+$
CD8 T cells	$CD45^+$ $CD3^+$ $CD8^+$
Inflammatory monocytes	$CD45^+$ $CD11b^+$ $Ly6C^{high}$ $CCR2^+$ $Ly6G^-$
Granulocytes	$CD45^+$ $CD11b^+$ $Ly6G^+$
Microglia	$CD45^{int}$ $CD11b^{int}$ $Ly6C^-$ $Ly6G^-$
NK cells	$CD45^+$ $CD3^-$ $NK1.1^+$ $Nkp46^+$
B cells	$CD45^+$ $CD19^+$

2.4.7.1 Preparation of peripheral blood leukocytes

For preparation of PBMC from mice, 2-3 drops of blood were collected by puncture of the superficial temporal vein (facial vein) into a tube containing 300 µl of 1 mM EDTA, thoroughly mixed and transferred into a FACS tube. 1 ml of FACS buffer was added and tubes were centrifuged at 300 x *g,* 10 min at 4 °C. Cells were resuspended in 1 ml of FACS buffer/EDTA 1 mM.

2.4.7.2 Preparation of CNS mononuclear cells from murine cortex

Immunized Th/+ mice, received stereotactic injections of inflammatory cytokines. Two days later, animals were perfused with ice cold PBS, brains were dissected and cortical tissue was carefully separated from white matter using a scalpel and razor blades. Cortical fragments were isolated from each mouse, put into individual sterile 70 µm cell strainers for mechanical disruption and collected in 50 ml tubes containing DMEM high glucose without supplements.

The cortical tissue collected was subjected to enzymatic digestion for 45 min at 37 °C with 2.5 mg/ml Collagenase D and 1 mg/ml DNAse I in DMEM high glucose without supplements. Digestion was stopped by adding 10 ml DMEM with 2 % FCS and the digested tissue was centrifuged at 1200 rpm/10 min. The pellet was resuspended in 5 ml 37 % Percoll and carefully overlaid on 5 ml 70 % Percoll. The Percoll gradient was centrifuged at

1600 rpm/25 min and the interphase was removed. The cells of the interphase were washed 2 times with FACS buffer and subjected to flow cytometry analysis.

2.4.7.3 Flow cytometry

All flow cytometry data were acquired on a FACS Canto™ II device using the BD FACSDiva Software 6.1.2 and processed with the FlowJo Software 7.61. Unless stated otherwise, staining procedures were performed in 96 well round bottom plates; centrifugation of the plates was performed at 300 x *g* for 5 min at 4 °C and 200 µl FACS buffer were used for each washing step.

2.4.7.3.1 FACS staining procedure of peripheral blood leukocytes

FACS tubes containing PBMC suspensions were centrifuged at 300 x *g*, 8 min at 4 °C. Pellets were resuspended in 50 µl of FACS buffer containing 1 µl anti-CD16/CD32 blocking antibody against Fc receptors and incubated for 15 min at 4 °C. Up to eight fluorochrome-labeled antibodies (0.4 µl of each antibody) were added and incubated for 15 min at 4 °C. Cells were washed with FACS buffer/EDTA 1 mM by centrifugation at 300 x g for 8 min at 4 °C. One further washing step was performed and erythrocytes were subsequently lysed using BD FACS™ lysing solution. For the lysis, the pellet was resuspended in 1 ml of BD FACS™ lysing solution and incubated 4 min at RT. Lysis was stopped by adding 4 ml of FACS buffer, and cells were spun down as described previously, washed with 1 ml FACS buffer and resuspended in 100 µl of FACS buffer for flow cytometry analysis.

2.4.7.3.2 FACS staining procedure of CNS mononuclear cells

Cells were blocked by anti-CD16/CC32 antibodies (1 µl in 50 µl FACS buffer) for 15 min at 4 °C. Up to eight fluorochrome-labeled antibodies were added to each well (0.4 µl of each antibody) and incubated for 15 min. After two washing steps with FACS buffer, cells were resuspended in 100 µl FACS buffer and analyzed by flow cytometry.

Intracellular FoxP3 staining

After staining the cell surface molecules (see 2.4.7.3.2), the cells were fixed for 45 min in 100 µl FoxP3 fixation concentrate diluted 1:4 in FoxP3 dilution buffer. Next, the fixed cells were washed once with permeabilization buffer (10X concentrate diluted 1:10 in bidistilled

water) and then incubated for 35 min with 100 µl of FoxP3 antibody diluted 1:200 in permeabilization buffer. Cells were then washed once with 200 µl Perm/Wash™ buffer and once with FACS buffer and analyzed by flow cytometry.

2.4.8 Blood brain barrier permeability experiments

To study temporary changes in permeability of the BBB in the model, Th/+ mice, healthy or previously immunized with $rMOG_{1-125,}$ were intracortically injected and perfused 6 h and 24 h post-injection. One hour before perfusion, mice received i.v. injections of 100 µg/g of body weight of an albumin-fluorescein isothiocyanate conjugate (FITC-albumine) dissolved in sterile NaCl.

2.4.9 Histology

2.4.9.1 Perfusion, fixation and paraffin embedding of the tissue

After receiving lethal doses of narcosis, mice and marmosets were transcardially perfused with cold PBS followed by 4 % paraformaldehyde (PFA). For mice, perfusion was performed at different time points: 24 h, day 5, day 10, day 20 and day 40 after intracerebral cytokine injection. Post-fixation of the tissue was carried out in PFA 4 % for 48 h. Brains and spinal cords were dissected and later embedded in paraffin. Human biopsies were fixed in buffered formalin and subsequently embedded in paraffin blocks.

2.4.9.2 Cutting and mounting of paraffin-embedded sections

Sections of 1-3 µm thickness were cut from paraffin blocks using a sliding microtome, then mounted on glass slides and dried overnight. The presence of Monastral blue dye (described in 2.4.3.1) in the sections was used for visual identification of the injection site.

2.4.9.3 Deparaffinization and rehydration of paraffin-embedded sections

Before proceeding with any staining protocol, the slides must be deparaffinized and rehydrated. Therefore, paraffin slides were put in an oven for at least 1 h at 56 °C and then gradually deparaffinized by subsequent immersion in xylene followed by immersion in aqueous alcoholic solutions as follows:

1. Xylene: 4 x 5 min
2. Isopropyl alcohol/Xylene: 1 x 2 min
3. Isopropyl alcohol (100 %): 2 x 3 min
4. Isopropyl alcohol (90 %): 1 x 3 min
5. Isopropyl alcohol (70 %): 1 x 3 min
6. Isopropyl alcohol (50 %): 1 x 3 min
7. Distilled water to rinse: 30 sec

After the stainings were performed, slides were dehydrated following a reverse order of the previous steps described above and mounted in DePex medium.

2.4.9.4 Histochemical stainings

2.4.9.4.1 Luxol Fast Blue/periodic acid-Schiff staining

Luxol fast blue (LFB) is a copper phthalocyanine dye that is attracted to the bases found in the lipoproteins of the myelin sheath, allowing myelin visualization (in blue). The periodic acid-Schiff (PAS) staining is a method for detecting polysaccharides and is used as a counterstain in combination with LFB. In this thesis, spinal cord sections from Th/+ $CCR2^{+/+}$ and Th/+ $CCR2^{-/-}$ mice as well as from marmosets treated with the CCR2 depleting antibody (DOC-2 Fr) or control isotype, were stained with LFB/PAS for assessing the extent of demyelination.

Sections were deparaffinized (see 2.4.9.3) until step 4 (90 % isopropyl alcohol), placed in a cuvette with LFB solution and incubated overnight at 60 °C. Sections were transferred to 90 % isopropyl alcohol, then individually differentiated by short dipping in 0.05 % lithium carbonate solution, 70 % isopropyl alcohol, and eventually washed with distilled water. For the PAS counterstaining, the sections were immersed in 1 % acetic acid for 5 min, washed for 5 min in running tap water and rinsed in distilled water afterwards. Next, sections were incubated for 20 min in Schiff´s reagent, washed for 5 min with running tap water, immersed for 2 min in Mayer´s hemalaum solution and rinsed in distilled water. Sections were then counterstained in 1 % HCl-alcoholic solution, blued for 5 min in running tap water, dehydrated and mounted.

2.4.9.4.2 Chloroacetate esterase staining

Esterases are a family of different enzymes found in cells of granulocytic lineage. In the specific esterase Kit used (Sigma), naphthol AS-D chloroacetate is the substrate for the specific esterase enzyme present in granulocytes, which is hydrolyzed, and as a result, a free naphthol compound is released. This compound is then coupled with a diazonium salt, forming colored deposits (bright pink) at sites of enzymatic activity. For identification and quantification of granulocytes in this thesis, chloroacetate esterase (CAE) staining was performed according to the manufacturer´s instructions on paraffin-embedded sections from Th/+ mice treated with the granulocyte depleting antibody 1A8 or the control isotype 2A3 (see 2.4.4.3). The brain samples stained with CAE corresponded to 24 h after the stereotactic injection.

Briefly, the slides were deparaffinized, rinsed in distilled water and preheated in PBS at 37 °C for 30 min-1 h. Sections are incubated for 2 h at 37 °C in a working solution, consisting of 2 % sodium nitrite, 2 % Fast Corinth salt, 10 % Trizmal^{TM} buffer and 2 % naphtol AS-D chloroacetate and washed with distilled water. Nuclei were counterstained briefly in Mayer's hemalum for 30 sec, washed 10 min with tap water for differentiation (blued) and mounted using Aquatex medium.

2.4.10 Immunohistochemistry

Immunohistochemistry (IHC) is a method used to label determined proteins in tissue sections by using specific antibodies. First, tissue sections are deparaffinized and then rehydrated before applying the primary antibody. Then a secondary antibody conjugated to an enzyme (e.g.: avidin, streptavidin, peroxidase) is applied and the antibody-antigen interaction is visualized after adding a substrate specific for the enzyme. Once the cleavage of the substrate occurred, a localized colored precipitate can be observed under light microscopy. Other methods consist in using a secondary antibody conjugated to a fluorophore substance, and the detection in this case is done using fluorescent microscopy.

2.4.10.1 Antigen retrieval of paraffin-embedded tissue

In some cases, antigens in the tissue can be masked due to the fixation with PFA requiring a retrieval step before immunohistochemical staining can proceed. All antibodies used for paraffin-embedded tissue in this thesis required heat-induced epitope retrieval (Shi et al., 2001). For heat-induced antigen retrieval, different buffers were used: sodium citrate buffer 10 mM pH 6, Tris-EDTA buffer 1 mM pH 9 or HCl buffer 4 mM pH 2.5. The sections were heated in a microwave (800 watt) 5 times for 3 min each, refilling the cuvettes between each cycle alternatively with bidistilled water or the corresponding retrieval buffer. Sections were then allowed to cool down for 20 min and rinsed 3 times with bidistilled water. Detailed information on antibodies and the retrieval buffers is listed in Table 9.

2.4.10.2 Processing, cutting and fixation of frozen tissue

Frozen tissue sections (cryosections) from mouse brain were used for NKp46/CD3 double IHC. For this purpose, animals were perfused as described previously (see 2.4.9.1) but only with cold PBS. Brains were dissected, cut in 2-3 mm coronal sections, mounted on OCT medium and frozen in isopentane pre-cooled in liquid nitrogen to form cryo-blocks. If not processed the same day, cryo-blocks were stored at -80 °C until needed. Next, frozen tissues were cut into 6 µm sections using a cryostat at -20 °C, mounted on glass slides and frozen at -80 °C until used. On the day of the histochemical staining, sections were air dried for at least 30 min at RT to prevent the tissue from detaching. Sections were subsequently fixed using an appropriate organic solvent: 100 % ethanol for 1 h at RT, ether for 30 min at RT or acetone for 10 min at -20 °C. Afterwards, slides were air-dried for 10 min, rehydrated for 10 min in PBS and stained with the corresponding primary antibodies.

2.4.10.3 Labeled streptavidin biotin (LSAB) method

For most of the immunohistochemical stainings used in this thesis the LSAB method was used, which relies on the strong affinity of streptavidin for the vitamin biotin. Once the sections (frozen or paraffin-embedded) were deparaffinized/fixated and antigen retrieval was performed where required, the slides were incubated with a 3 % hydrogen peroxide solution in PBS for 20 min at 4 °C or 0.3 % hydrogen peroxide/PBS for 10 min (for frozen tissue sections). This step suppresses endogenous peroxidase activity in the tissue. Slides

were then washed 3 times in PBS and incubated for 20 min at RT in blocking buffer (10 % FCS/PBS) to block unspecific antibody binding before the primary antibody was added onto the sections. For the CD14 staining, 10 % goat serum was used as blocking buffer. Next, the primary antibody, diluted in blocking buffer (see Table 9) was added and sections were incubated over night at 4 °C in a humid chamber.

After overnight incubation slides were rinsed 3 times in PBS and the corresponding biotinylated secondary antibody diluted in blocking buffer was applied onto the slides for 1 h at RT (see Table 10). The excess of non-bound antibody was removed by washing 3 times with PBS. For amplification of the signal, streptavidin conjugated to horseradish peroxidase (HRP) diluted in blocking buffer (1:1000) was added and incubated for 1 h at RT. Slides were washed 3 times with PBS, developed using a 3,3' diaminobenzidine (DAB) solution (Table 2) which yields a dark brown end product and the reaction was controlled under a light microscope. After a washing step with distilled water, slides were counterstained in Mayer's hemalaum for 30 s. Slides were washed again with distilled water, differentiated in 1 % HCl solution, blued in tap water for 7 min, dehydrated and mounted as described above (see 2.4.9.3).

Following this basic procedure double IHC can be performed. In this case, after developing the first reaction with DAB, sections are washed with distilled water or PBS and put in the appropriate blocking buffer in which the primary antibody against the second antigen of interest has to be diluted. From this step on, the same protocol described above is followed but the new product is developed using a different chromogen (e.g.: fast blue for the GrB/CD3 double staining in MS biopsies).

2.4.10.4 Tyramide signal amplification method

For assessment of cortical lesions in the model, brain sections from injected mice were stained for MBP. To achieve an optimal intensity of the staining, the method of tyramide signal amplification was used. In this method, the tyramide portion of tyramine-protein conjugates is covalently attached to the area around the protein of interest through a peroxidase-catalyzed reaction. This process takes place after first applying a primary antibody and a secondary-HRP conjugate. At the end, an amplified signal is obtained by addition of an antibody-enzyme or a –fluorophore conjugate directed against the protein

portion of the tyramine-protein conjugate formed in the previous step. To this end, a Tyramide Signal Amplification kit (see Table 12) was used following the recommendations of the provider.

2.4.10.5 Fluorescent immunohistochemistry

Immunofluorescence was used to simultaneously visualize two antigens of interest in the tissue, for example: CCR2/CD14 in MS biopsies or NKp46/CD3 in Th/+ mice cryosections. Therefore, sections were pretreated as described previously (see 2.4.9.3, 2.4.10.1, 2.4.10.2), washed 3 times with PBS, blocked with 10 % goat serum and incubated with the primary antibodies at 4 °C over night. Subsequently, slides were washed 3 times in PBS and incubated with the corresponding fluorochrome-labeled antibodies (see Table 11) for 30-60 min at RT in darkness. The intensity of the staining was monitored using a fluorescence microscope (Olympus BX51). After three washing steps with PBS, nuclei were counterstained with DAPI (1:10000 in PBS) for 15 min at RT. Slides were washed again 3 times in PBS, rinsed once in distilled water and mounted using fluorescence mounting medium (Dako, Germany).

2.4.10.6 Immunohistochemical stainings in mice, marmosets and human tissue

For detailed information on the antibodies used as well as the corresponding dilutions, etc., please refer to Table 9.

Mice

For evaluating cortical demyelination in mice, brain sections were immunostained for MBP and the signal was enhanced using a Tyramide Signal Amplification kit (Invitrogen) as described previously (see 2.4.10.4).

To characterize inflammatory infiltrates in the lesions, T cells were immunolabelled with a rabbit anti-CD3 antibody, (DCS) and for microglia/macrophages using a rat antibody directed against Mac- 3 (clone M3/84). For the identification of mature oligodendrocytes and oligodendrocyte precursor cells (OPC) in cortical demyelinated areas, double IHC was performed combining a rabbit anti-- Tubulin polymerization promoting protein p25 (TPPP/p25) antibody and a rabbit anti- Oligodendrocyte transcription factor 2 (Olig2) antibody respectively, on sections previously stained with a rat anti-rMOG antibody purified in the Institute of Neuropathology, Göttingen. Additional double IHC on MOG-stained

sections were performed for APP, a recognized marker of axonal damage and NeuN for identifying neurons.

NK cells infiltrating the cortex of stereotactically injected Th/+ mice were immunolabelled in brain cryosections using the primary goat anti-mouse antibody NKp46/NCR1. To distinguish NK from NKT cells, double immunofluorescence labeling was done combining the antibody NKp46 with a rabbit anti-CD3 antibody (Dako) in frozen tissue sections. For visualizing NKp46, a secondary donkey anti-goat biotinylated antibody was added followed by incubation with a Cy™3-conjugated streptavidin antibody. The AlexaFluor® 488 goat anti-rabbit antibody was used to visualize the CD3 IHC, and nuclei were counterstained with DAPI.

Finally, to measure the area of cortical FITC extravasation in Th/+ mice injected with the FITC-albumin conjugate (see 2.4.8), paraffin-embedded brain sections were immunostained with a rabbit anti-FITC antibody conjugated to HRP.

Common Marmosets

For assessing cortical demyelination in marmoset brains, paraffin-embedded tissue sections were immunostained for MBP and enhanced with tyramide as previously described for mice.

Multiple sclerosis tissue

To illustrate the inflammatory cells present in early cortical demyelinated lesions from MS patients, biopsy sections were stained with primary antibodies against MBP, CD3 and KiM1P (pan macrophage marker). To confirm the presence of inflammatory monocytes in these early lesions, double immunofluorescence IHC for CD14 (mouse anti-CD14 antibody) and CCR2 (rabbit anti-CCR2 antibody E68) was performed. Cy™3-conjugated goat anti-mouse antibody and AlexaFluor®488 antibody, respectively, were used for detection and nuclei were counterstained with DAPI.

Furthermore, granzyme B (GrB) and CD3 were co-immunolabelled to identify the presence of NK cells in early cortical demyelinated MS lesions. A biotinylated anti-mouse antibody for GrB and a goat anti-rabbit-AP antibody for CD3 were used for the detection. The GrB staining was developed using DAB as a chromogen and for CD3 Fast Blue was used (Boorsma, 1984).

2.4.11 Morphometric analysis

All measurements of tissue areas were carried out using the Image J software v. 1.46 in previously captured TIFF images. MBP-immunostained sections from mice and marmosets were used to evaluate the extent of cortical demyelination comprising subpial and intracortical perivascular demyelinated areas. In mice, images were acquired using a 40x magnification objective in a light microscope (Olympus BX51) equipped with a digital camera. Coronal sections of marmoset brains were scanned using a Keyence BIO REVO BZ-X710 microscope and compound images were generated (BZ-II analyzer software) from single pictures. In mice, subpial demyelinated areas were measured only in the ipsilateral (injected) brain hemisphere, while perivascular cortical demyelination was assessed in both ipsi- and contralateral cortex. Perivascular demyelinated areas were reported in mm^2 and subpial demyelination in percentage (%). The latter was calculated as follows:

$$subpial\ demyelination\ (\%) = \frac{subpial\ demyelinated\ area}{area\ of\ ipsilateral\ cortex} \times 100$$

Quantitative analyses were performed on day 5 after intracerebral injection unless stated otherwise. All cell quantifications were done at a 400x magnification and cell densities (cells/mm^2) were determined using a 10x10 ocular morphometric grid. In C57BL6/J mice, the densities of p25+, Olig2+ and NeuN+ cells were assessed in the ipsilateral cortical layers extending from cortical layer I to II/III, whereas for Th/+ mice the counts were restricted to subpial demyelinated areas present across the same layers. Axonal damage (APP+ axons) was assessed in both hemispheres around perivascular demyelinated areas. Polymorphonuclear neutrophil (PMN) cell densities were quantified on CAE stained sections from Th/+ mice, treated with the granulocyte depleting antibody 1A8 or the control isotype 2A3, at 24 h after the intracerebral injection. Granulocytes were quantified in the cortical parenchyma and along the meninges. For assessment of BBB permeability in our model,

cortical areas positively-immunostained for FITC were measured with Image J using an incorporated color deconvolution plugin (Ruifrok and Johnston, 2001). The threshold for quantifying the intensity of the brown (DAB) channel was set at (0; 150). For analysis of macrophages/activated microglia in mouse brain, the number of intracortical Mac3 + perivascular cuffings was counted in both hemispheres. For quantification of demyelinated areas in spinal cord sections of mice and marmosets stained with LFB-PAS (see 2.4.9.4.1), images were acquired from at least eight transversal spinal sections of each animal, demyelination within the white matter was measured and reported as percent of total white matter demyelinated.

Human quantitative data comprised the assessment of Ki1MP+ macrophages/activated microglia and T cell (CD3) densities in early MS cases using a morphometric grid as described for the mice. Immunopositive cells were counted in regions where subpial cortical demyelination was present as well as in normal appearing cortical regions (NAGM) when available. At least five separate visual fields were quantified for each cortical region within each sample, and densities were reported as cells/mm^2.

2.4.12 qRT-PCR analysis

To evaluate if the expression of genes related to inflammatory monocytes were differentially regulated between intracortically injected Th/+ $CCR2^+$ and Th/+ $CCR2^{-/-}$ mice, animals were perfused with PBS two days after injection, the ipsilateral cortex at the injection site was carefully separated from the WM and put in QIAzol Lysis Reagent. RNA was isolated using the RNeasy Micro Kit (Qiagen) and transcribed into complementary DNA (cDNA) using the High Capacity RNA-to-cDNA™ Kit (Life Technologies). From the cDNA obtained, 12.5 ng/PCR reaction were used and quantitative PCR (qPCR) was run on the *1Q5*™ Real Time PCR Detection System (BIO-Rad) using a standard qPCR Core Kit. The following FAM labeled primers/probes were selected for intron-spanning: Glyceraldehyde 3-phosphate dehydrogenase (GAPDH) (Mm99999915_g1), TNF-α (Mm00443258_m1), NOS2/iNOS (Mm00440502_m1) and CCL2 (Mm00441242_m1) (see Table 14). The expression levels of TNF-α, Nitric oxide synthase 2 (NOS2)/ Inducible-nitric oxide synthase (iNOS) and Chemokine (CC motif) ligand 2 (CCL2) were indicated as percent of the expression

of GAPDH (housekeeping gene). The qRT-PCR analysis was done in cooperation with Dr. Franziska Paap (Institute of Neuropathology, University Medical Center Göttingen).

2.4.13 Data analysis and statistics

Normality tests were applied to all data sets (D´Agostino and Pearson omnibus normality test) using GraphPad Prism 5.01 software. If samples followed a normal distribution, an unpaired t-test was used to compare two groups. In the absence of normality, a non-parametric test (Mann-Whitney U test) was applied. For comparisons between three or more groups one-way analysis of variance (ANOVA) followed by a post-hoc test: Dunn´s Multiple Comparison test (when all groups were compared to each other) or Dunnett's Multiple Comparison test (when groups were compared against a control) was selected. A $p<0.05$ was considered to be significant. Unless otherwise specified, all results are shown as mean ± s.e.m.

3 RESULTS

3.1 Analysis of inflammatory infiltrates in cortical demyelinated MS lesions

To address a possible contribution of adaptive and innate immune cells to cortical lesion pathogenesis in MS, brain biopsies from eight patients exhibiting inflammatory demyelination compatible with MS and featuring cortical demyelination were analyzed (see Table 18, Material and Methods section).

Cortical demyelinated areas in MPB-immunostained sections showed inflammatory hallmarks identified by the presence of few perivascular and parenchymal CD3+ T cells and KiM1P+ macrophages/activated microglia (Figure 7A). Cell densities were significantly higher in subpial cortical demyelinated areas when compared to cortical NAGM, especially for KiM1P+ phagocytes. Inflammatory monocytes, co-expressing CD14 and CCR2 were also observed by immunofluorescence IHC in the demyelinated cortex (Figure 7B). Additionally, a fraction of GrB+ CD3- cells which were mainly located around vessels and most likely represent NK cells were observed in sections double-labeled for these markers (Figure 7C).

3.2 Assessment of cortical demyelination in Th/+, 2D2 and C57BL/6J mice

To address whether pathogenic antibodies are required for the generation of cortical demyelinated lesions, mice received a stereotactic injection of pro-inflammatory cytokines (IFNγ and TNFα) into the motor cortex on day 2 after EAE onset. Three mouse lines were used: Th/+ mice ($rMOG_{1-125}$ -immunized) in which demyelinating anti-MOG antibodies can be found in the serum, 2D2 T cell receptor transgenic mice (MOG_{35-55}-immunized) which have a high frequency of MOG-specific T cells but no demyelinating antibodies and C57BL/6J mice ($rMOG_{1-125}$-immunized), which develop non-demyelinating antibodies to MOG peptides in response to immunization.

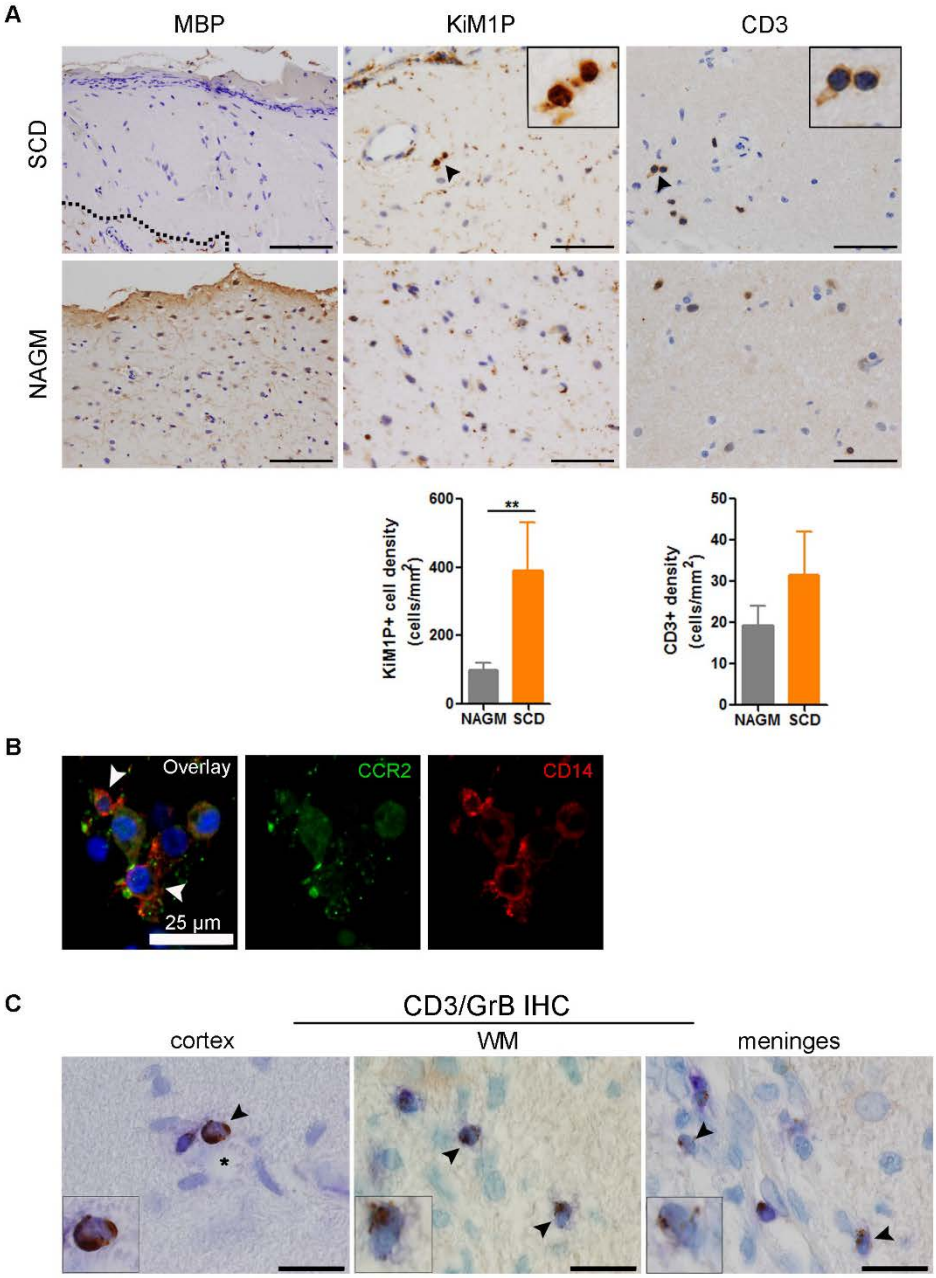

Figure 7: Adaptive and innate immune cells in cortical demyelinated MS lesions

(A) Early MS biopsies showed an extensive loss of MBP in subpial cortical demyelinated (SCD) regions as well as increased numbers of KiM1P+ phagocytes and CD3+ T cells in comparison to cortical normal appearing grey matter (NAGM). Exemplary KiM1P+ cells and CD3+ T cells are marked by arrowheads and amplified in the corresponding insets. The dotted line in the MBP SCD image demarcates a cortical area of preserved myelin Data represent mean ± s.e.m. (SCD n=8, NAGM n=5, **p<0.01, Mann Whitney U test). **(B)** MS biopsy stained for CCR2 (green) and CD14 (red) showed the presence of perivascular CCR2+CD14+ inflammatory monocytes (white arrowheads) in recently demyelinated cortical lesions. **(C)** GrB+CD3- NK cells (arrowheads) are part of the perivascular inflammatory infiltrates in recently demyelinated cortical MS lesions. The asterisk points to the lumen of a cortical vessel. CD3 (blue), GrB (brown). Scale bars, 100 µm (MBP), 50 µm (KiM1P and CD3) and 20 µm (CD3/GrB).

3.2.1 Cortical demyelination was only observed in Th/+ mice

Cortical demyelinated areas (subpially and around intracortical inflamed vessels) were only observed in Th/+ mice and peaked on day 5 after stereotactic injection (Figure 8). Demyelinated lesions were not confined to the ipsilateral cortex, but extended to the contralateral, non-injected hemispheres. This observation differs from the findings in the Lewis rat model (Merkler et al., 2006b), where the contralateral hemisphere remained unaffected.

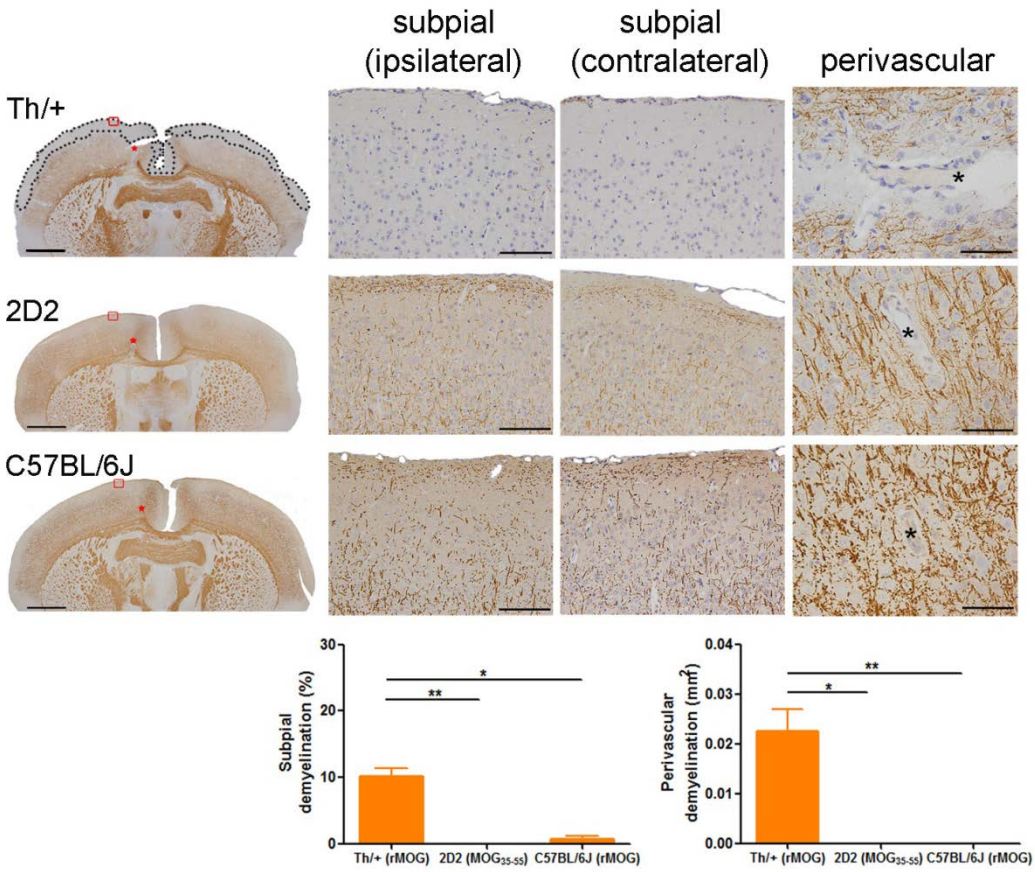

Figure 8: Cortical demyelination requires a pathogenic antibody response against MOG

MBP IHC (brown color) on day 5 after injection illustrates cortical demyelination in Th/+ mice (top), but not in 2D2 (middle) or C57BL6/J mice (bottom). The dotted line in the overview of the Th/+ mouse brain delineates the subpial cortical demyelinated areas in both, the ipsi- and contralateral hemispheres. Subpial demyelination is quantified in the left bar graph. Perivascular cortical demyelination is depicted in the panels on the right, (black asterisks mark the lumen of the vessel) and quantified in the right bar graph. Red squares in the brain overviews mark the areas enlarged in the subpial ipsilateral photographs. Red stars identify the injection site. Scale bars, 1 mm (brain overviews), 100 µm (subpial ipsilateral and contralateral) and 50 µm (perivascular). Data of three independent experiments are presented as mean ± s.e.m. (2D2 n=3, C57BL/6J n=5, Th/+ n=13, *p<0.05, **p<0.01, one-way ANOVA followed by Dunn's Multiple Comparison *post hoc* analysis).

3.2.2 Loss of oligodendrocytes and axonal damage in cortical demyelinated lesions of Th/+ mice

Cortical demyelination on day 5 after stereotactic injection was accompanied by a significant reduction of Olig2+ oligodendroglial cells and specially of p25+ mature oligodendrocytes in Th/+ mice (Figure 9). In addition, APP+ axons were observed almost exclusively in Th/+ mice around perivascularly demyelinated vessels. Neuronal densities (NeuN IHC) were not reduced.

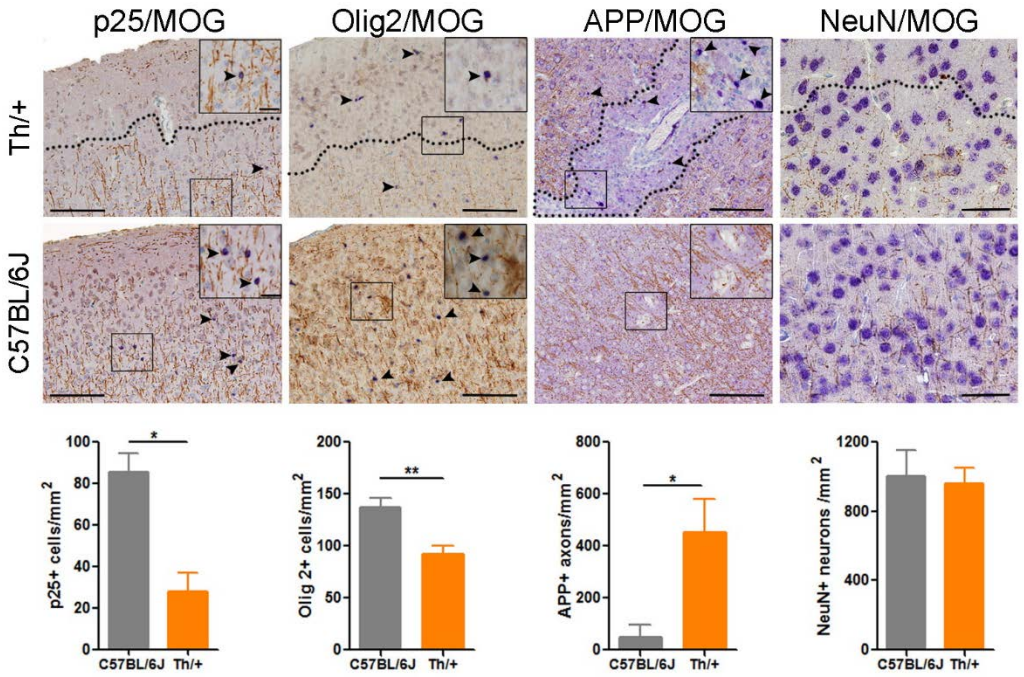

Figure 9: Oligodendrocyte loss and axonal damage occur in cortical demyelination in the mouse

Assessment of mature oligodendrocytes (p25+), oligodendroglial cells including OPC (Olig2+), axonal damage (APP+ axons) and neurons (NeuN+) in cortical demyelinated areas of Th/+ (top) and C57BL/6J mice (bottom). Cell markers (blue), MOG (brown). Cells were quantified in subpial demyelinated areas for Th/+ mice and normally myelinated layers I and II/III for C57BL/6J mice. A significant reduction in the densities of p25+ and Olig2+ cells was observed in subpial demyelinated areas of Th/+ mice. Increased axonal damage (APP+ axons) was found around perivascularly demyelinated vessels. Neuronal densities were similar in both groups. Arrowheads indicate exemplary APP+ axons, p25+ and Olig2+ cells, shown in detail in insets. Scale bars, 100 µm (representative for p25/MOG, Olig2/MOG and APP/MOG images), 20 µm (corresponding insets) and 50 µm (NeuN/MOG). Dotted lines in the images mark the border between demyelinated and normally myelinated areas in the cortex. Graphs show data from two independent experiments presented as mean ± s.e.m. (Th/+ n=7, C57BL/6J n=5, *p<0.05, **p<0.01, Mann Whitney U test).

3.2.3 Time course of cortical demyelination and inflammation in Th/+ mice

Time course experiments in Th/+ mice were performed to address the question whether cortical demyelination resolves rapidly, as previously shown in the cortical lesion model in Lewis rats (Merkler et al., 2006b). Compared to Lewis rats which showed significant remyelination already on day 14 after lesion induction, Th/+ mice remyelinated somewhat slowlier (Merkler et al., 2006b). Significant remyelination was observed on day 20 after injection for perivascular areas and on day 40 for subpial regions (Figure 10A). A reduction of macrophages and T cell infiltration was observed over time, paralleling remyelination. Already on day 10, the amount of Mac-3+ perivascular cuffings decreased, reaching significance from day 20 on. The T cell density was significantly decreased on day 40 after injection (Figure 10B).

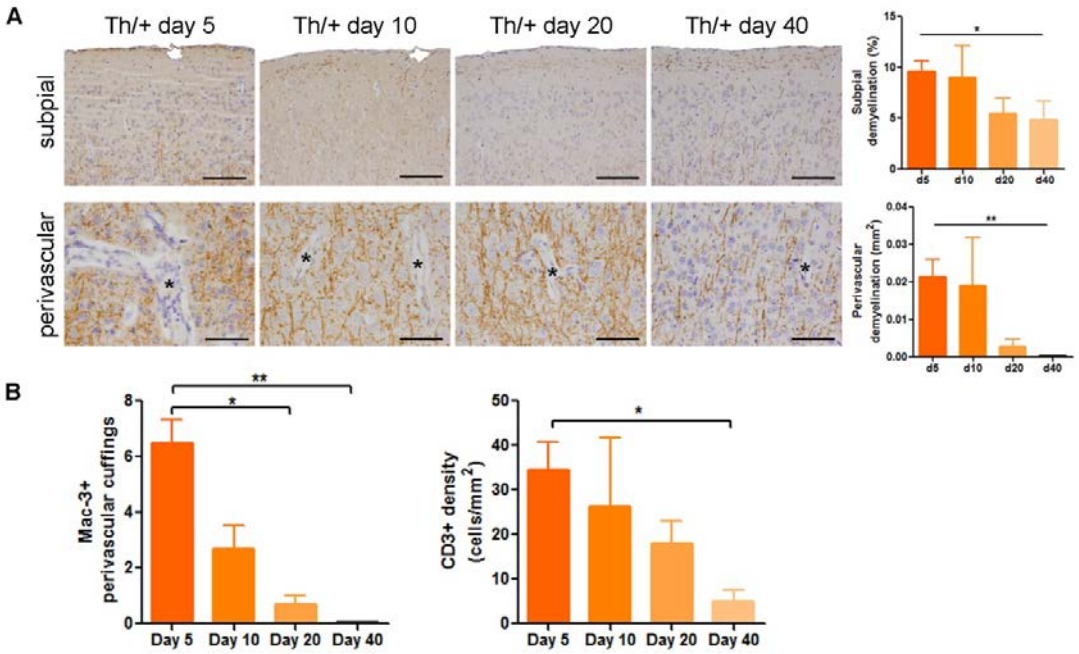

Figure 10: Time course of inflammation and demyelination in cortical demyelination in Th/+ mice

(A) Time course of cortical demyelination. MBP IHC assessment of the extent of subpial (upper panels, scale bar 100 µm) and perivascular demyelinated lesions (lower panels, scale bar 50 µm) on days 5, 10, 20 and 40 post-injection. Significant perivascular remyelination was observed on day 20, significant subpial remyelination on day 40 (bar graphs on the right). Asterisks mark parenchymal vessels. Data of two independent experiments are presented as mean ± s.e.m. (day 5 n=13, n=6 day 10, 20, 40, *p<0.05, **p<0.01, one-way ANOVA followed by Dunn´s Multiple Comparison *post hoc* analysis). **(B)** Time course of perivascular macrophage (Mac-3+) cuffings (left graph) and T cells (CD3+) (right graph), on day 5, 10, 20 and 40 after stereotactic injection. Data of two independent experiments shown as mean ± s.e.m. (Mac-3: day 5-40 n=6 each, CD3: day 5, 20 n=6, day 10, 40 n=5). One-way ANOVA followed by Dunn´s Multiple Comparison *post hoc* analysis,*p<0.05, **p<0.01 (statistical significance depicted in the graphs refers to the *post hoc* analysis).

3.2.4 Motor skill sequence (MOSS) test

To assess whether cortical demyelinated lesions lead to subtle motor dysfunctions or impair the adaptation to complex motor tasks, Th/+ and C57BL/6J mice were subjected to the MOSS test (see 2.4.6, Figure 11A) (Liebetanz and Merkler, 2006).

Animals were first trained on a regular wheel and later Th/+ and C57BL/6J mice were each randomized into two comparable groups which received PBS or cytokines stereotactically into the motor cortex (Figure 11B). While non-demyelinated cytokine- or PBS-injected C57BL/6J mice adapted to complex wheels comparably, the adaptation of cytokine- injected Th/+ mice was transiently impaired compared to PBS-injected Th/+ mice between day 4-6 post injection. Interestingly, running speed as well as running distance of cytokine-injected Th/+ mice significantly dropped at the time when inflammatory demyelination was most extensive. Of note, cytokine injections alone were not sufficient to impair the adaptation of C57BL/6J mice to complex wheels as shown in Figure 11B.

3.3 Assessment of early cortical inflammatory infiltrates in Th/+ mice

Leukocytes from the cortex of injected Th/+ mice were isolated on day 2 after stereotactic injection and characterized by flow cytometry. Cortical inflammatory infiltrates were predominantly composed of T cells, inflammatory monocytes, microglia cells, granulocytes, NK cells and few B cells (Figure 12).

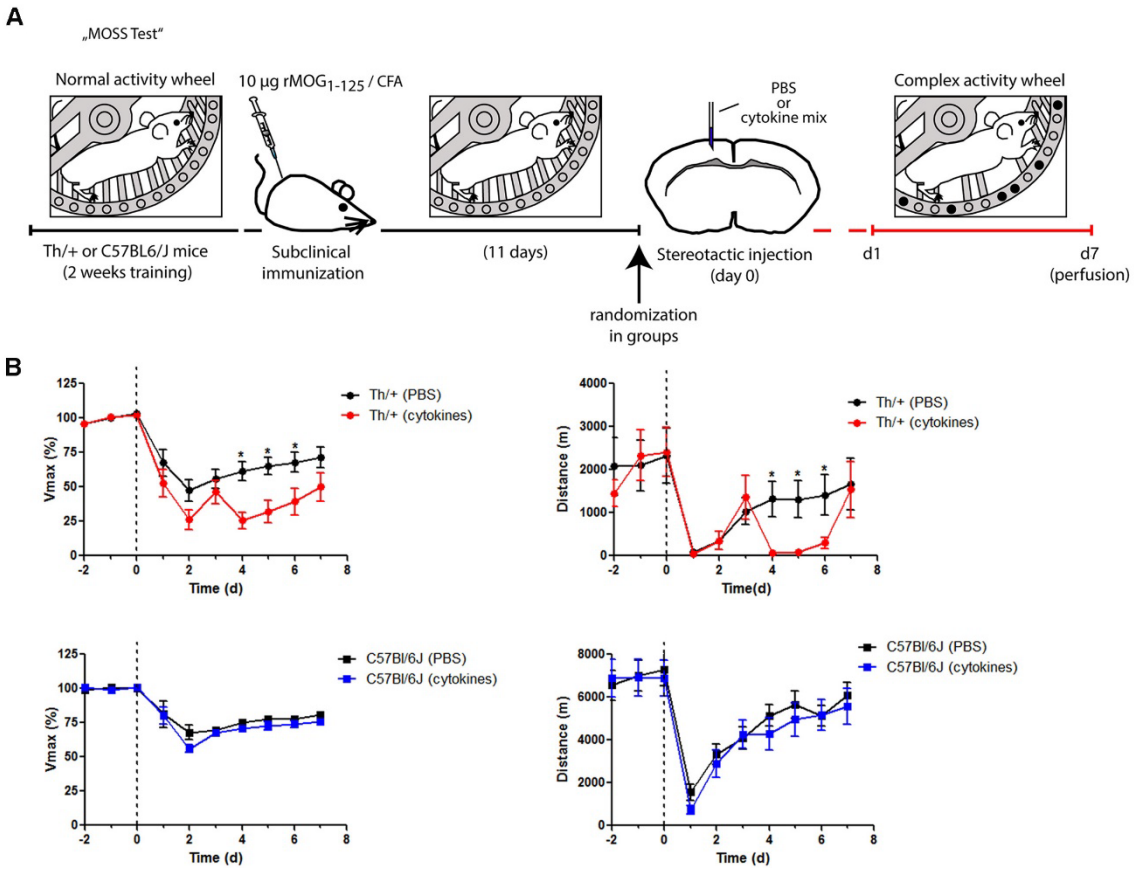

Figure 11: Adaptation to complex motor tasks is transiently impaired in cytokine injected Th/+ mice

(A) Schematic representation of the motor skill sequence (MOSS) test. **(B)** Th/+ mice (top graphs) injected with cytokines (red circles) or PBS (black circles) as well as C57BL/6J mice (bottom graphs), cytokine-(blue squares) or PBS-injected (black squares) were put into complex wheels after receiving stereotactic cortical injections. The relative maximal velocity (Vmax) and the running distance were recorded. The dotted vertical line in the graphs represents the day of the stereotactic injection. Representative data of one out of two independent experiments is presented as mean ± s.d. (n=10 mice/group, *p<0.05, **p<0.01, one-way ANOVA followed by Dunn´s Multiple Comparison *post hoc* analysis).

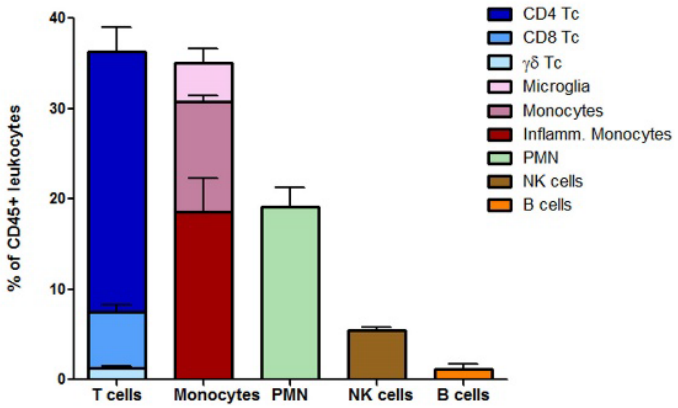

Figure 12: Composition of the early inflammatory infiltrates in the cortex of Th/+ mice

Cortical leukocytes from Th/+ mice (n=3) were analyzed by flow cytometry on day 2 post injection. The amount of the different immune cells identified is represented as percentage of the total numbers of $CD45^{+}$-leukocytes. Data are presented as mean ± s.e.m.

3.4 Characterization of the immune cell players required for cortical demyelination

NK cells, granulocytes and macrophages can exert antibody dependent cell cytotoxicity (ADCC) and, therefore, might contribute to the pathogenesis of cortical demyelinated lesions in Th/+ mice. To address the relevance of each cell type, mice deficient for inflammatory monocytes (Th/+ $CCR2^{-/-}$) were generated and PMN and NK cells were depleted by specific antibodies. To study the role of complement-dependent cytotoxicity (CDC) in the formation of cortical demyelination, Th/+ mice deficient for CD59a were generated and the complement cascade was blocked in Th/+ mice, using a C5 blocking antibody. These experiments aimed at defining the immunological requirements for the development of cortical demyelinated lesions.

3.4.1 Role of inflammatory monocytes in cortical demyelination

To assess if inflammatory monocytes are required for cortical inflammatory demyelination in our model, Th/+ $CCR2^{+/+}$ and Th/+ $CCR2^{-/-}$ mice were immunized with $rMOG_{1-125}$ and stereotactically injected on day 2 after EAE onset. Disease severity was similar in both groups; however, in line with previous reports CCR2-deficient animals developed EAE (Gaupp et al., 2003) at a later time point (Table 23).

Table 23: Clinical EAE data of Th/+ $CCR2^{+/+}$ and Th/+ $CCR2^{-/-}$ mice

Genotype	Sample size	Day of EAE onset (mean± SD)	Maximum EAE severity (mean± SD)
Th/+ $CCR2^{+/+}$	n=13	11.2 ± 1.1	3.3 ± 0.5
Th/+ $CCR2^{-/-}$	n=5	15 ± 1	3.2 ± 0.3

Statistical analysis: EAE onset: ***p<0.001 (Unpaired T test). Disease severity: p=0.46 (Mann Whitney U test)

In Th/+ $CCR2^{-/-}$ mice, the recruitment of inflammatory monocytes to the cortex was significantly impaired, as reflected in the FACS analysis performed on day 2 after the stereotactic injection (Figure 13A). In contrast, in Th/+ $CCR2^{+/+}$ mice $CCR2^{+}Ly6C^{hi}$-inflammatory monocytes represented more than 50 % of all $CD45^{+}CD11b^{+}Ly6G^{-}$ monocytes isolated from cortical tissue. In line with these findings, a significant reduction of

monocytes/macrophages was observed in the cortex of Th/+ CCR2$^{-/-}$ mice when assessing the number of Mac-3+ perivascular cuffings on day 5 after injection (Figure 13B).

Furthermore, mRNA levels of monocyte-related genes, like TNFα and iNOS revealed a significant reduction in Th/+CCR2$^{-/-}$ deficient mice when compared to the Th/+ CCR2$^{+/+}$ group (Figure 13C). Additionally, a trend towards a reduction in the gene expression of the CCL2 ligand was observed in Th/+ CCR2$^{-/-}$ animals (p=0.0782).

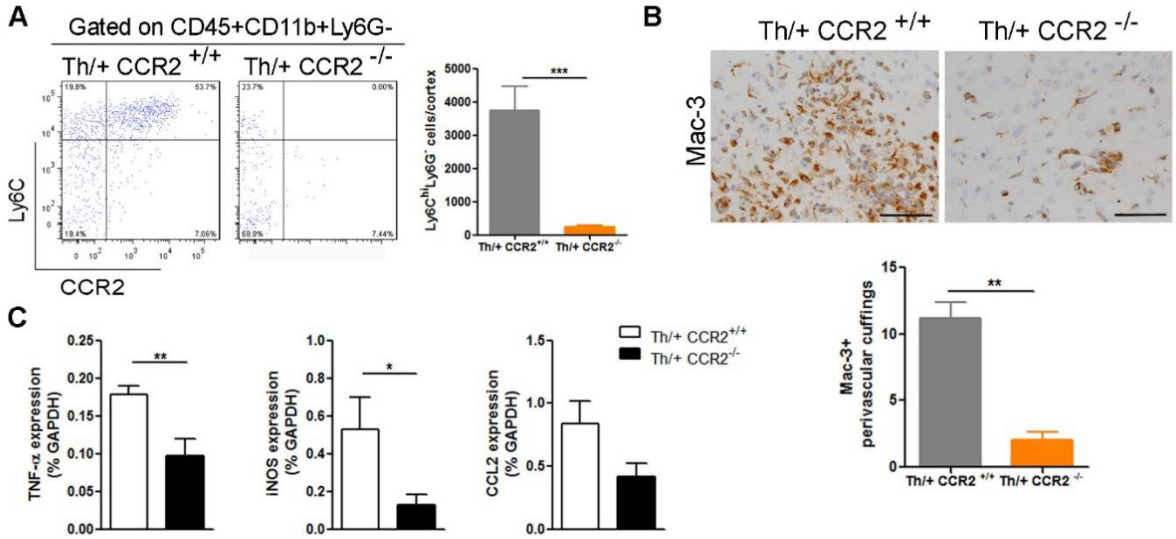

Figure 13: Impaired recruitment of inflammatory monocytes into the cortex of Th/+ CCR2$^{-/-}$ mice

(A) Inflammatory monocytes in the cortex of Th/+ CCR2$^{+/+}$ and Th/+ CCR2$^{-/-}$ mice were examined by flow cytometry on day 2 after injection and quantified (bar graph on the right). Ly6C^{high} Ly6G^{-} cells were significantly reduced in Th/+ CCR2$^{-/-}$ mice (n=7 mice/group). **(B)** Mac-3+ intracortical perivascular cuffings were significantly reduced in Th/+ CCR2$^{-/-}$ compared to Th/+ CCR2$^{+/+}$ mice on day 5 post stereotactic injection (n=6 mice/group). Scale bar 50 µm. **(C)** Gene expression analysis of monocyte-related cytokines and chemokines in the cortex of Th/+ CCR2$^{+/+}$ and Th/+ CCR2$^{-/-}$ mice on day 2 after stereotactic injection. The expression of TNF-α and iNOS was significantly reduced in Th/+ CCR2$^{-/-}$ mice. Results were normalized against GAPDH expression (n=5 animals/group). All quantitative data are expressed as mean ± s.e.m. and were analyzed by Mann Whitney U test (*p<0.05, **p<0.01, ***p<0.001).

Cortical demyelination was also evaluated in Th/+ CCR2$^{+/+}$ and Th/+ CCR2$^{-/-}$ mice by MBP IHC. Subpial and perivascular intracortical demyelination were substantially reduced in CCR2$^{-/-}$ deficient animals while Th/+ CCR2$^{+/+}$ developed extensive demyelinated lesions (Figure 14A). In contrast to cortical demyelination, the extent of spinal cord demyelination was comparable between Th/+ CCR2$^{-/-}$and Th/+ CCR2$^{+/+}$ mice (Figure 14B).

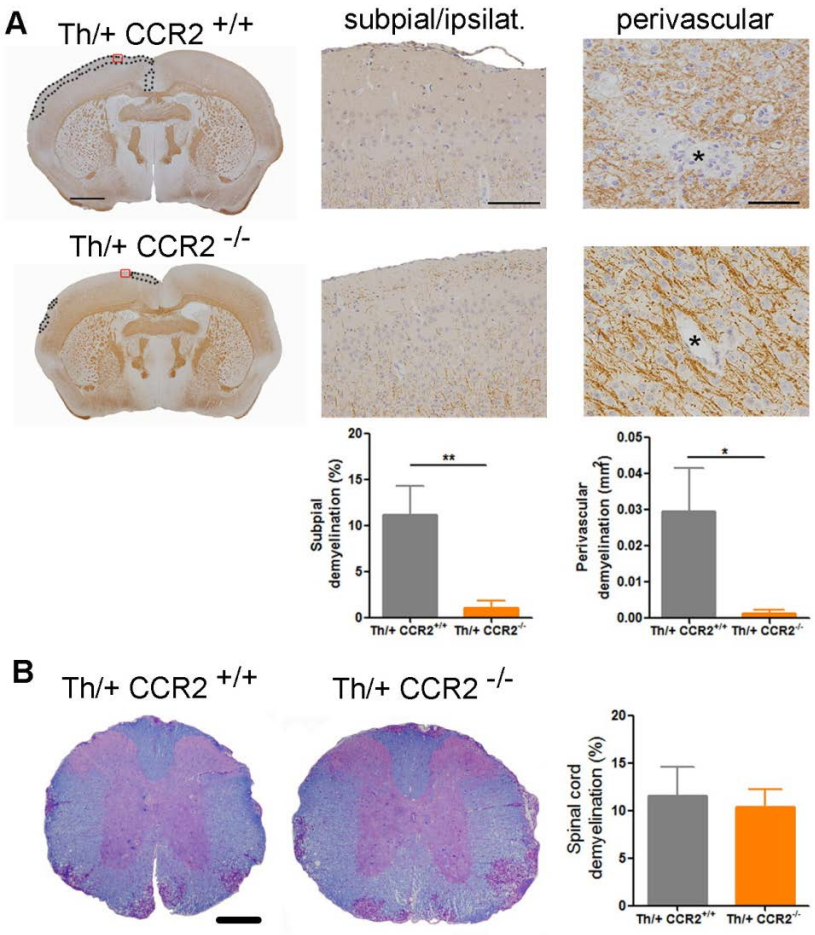

Figure 14: Inflammatory monocytes are required for cortical demyelination

(A) MBP IHC reflects a significant reduction in cortical demyelinated lesions (subpial, perivascular) in Th/+ CCR2 $^{-/-}$ (bottom) when compared to Th/+ CCR2$^{+/+}$ mice (top). Red squares in brain overviews refer to the magnified area in subpial ipsilateral photographs. Dotted lines define subpial-demyelinated areas. Scale bars, 1 mm (brain overviews), 100 µm (subpial ipsilateral) and 50 µm (perivascular). Data from three independent experiments are shown for Th/+ CCR2$^{+/+}$ mice (n=13) and from two independent experiments for Th/+ CCR2$^{-/-}$ mice (n=5). **(B)** Representative histochemical staining of myelin (LFB/PAS) in transversal spinal cord sections of Th/+ CCR2$^{+/+}$ (n=7) and Th/+ CCR2$^{-/-}$ mice (n=6) on day 5 after stereotactic injection. Both groups developed spinal cord demyelination to a similar extent. Scale bar, 200 µm. Data from two independent experiments. Quantitative data are expressed as mean ± s.e.m. (*p<0.05, **p<0.01, Mann Whitney U test).

Next, the effect of CCR2 inhibition on lesions was investigated in Th/+ mice using the specific antagonist RS 504393 for CCR2 (see 2.4.4.1). While subpial cortical demyelination did not differ between Th/+ mice treated with vehicle or the CCR2 inhibitor, perivascular cortical demyelination was significantly reduced in the latter group (Figure 15).

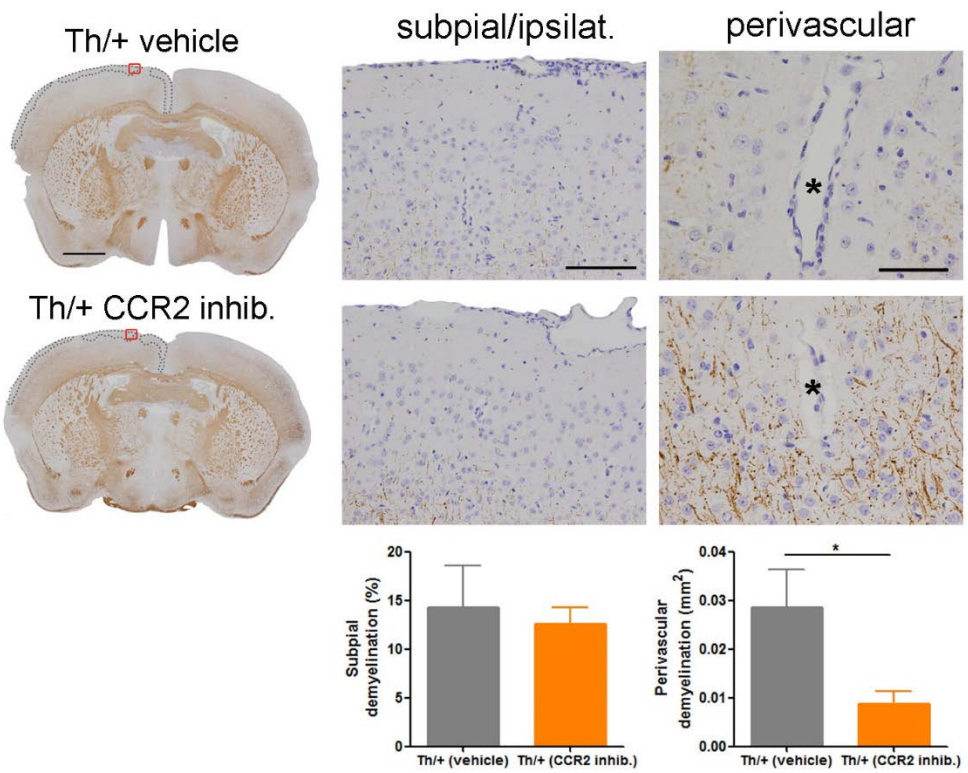

Figure 15: CCR2-inhibition in Th/+ mice reduces perivascular demyelination

Perivascular cortical demyelination in Th/+ mice was significantly reduced by the inhibition of CCR2 with 4 mg/kg RS 504393 daily starting at disease onset, when compared to vehicle treated animals while subpial cortical demyelination remained unaltered. Red squares in brain overviews immunostained for MBP refer to the magnified area in subpial ipsilateral photographs. Dotted lines define subpial-demyelinated areas. Scale bars, 1 mm (brain overviews), 100 µm (subpial ipsilateral) and 50 µm (perivascular). Data are expressed as mean ± s.e.m. (Th/+ vehicle n=4, Th/+ CCR2 inhibitor n=6, *p<0.05, Mann Whitney U test).

3.4.1.1 Cortical demyelination in marmosets is reduced by depletion of inflammatory monocytes

To translate our results in the mouse model into a potential treatment option for cortical demyelination in MS, we treated marmosets with EAE a humanized monoclonal antibody against CCR2 (DOC-2 Fr-2). Depleting inflammatory monocytes in marmosets starting 2 weeks after immunization led to a moderate reduction of subpial and a significant reduction of perivascular cortical demyelination (Figure 16A). Interestingly, the extent of demyelination in the spinal cord did not differ between the two groups (Figure 16B).

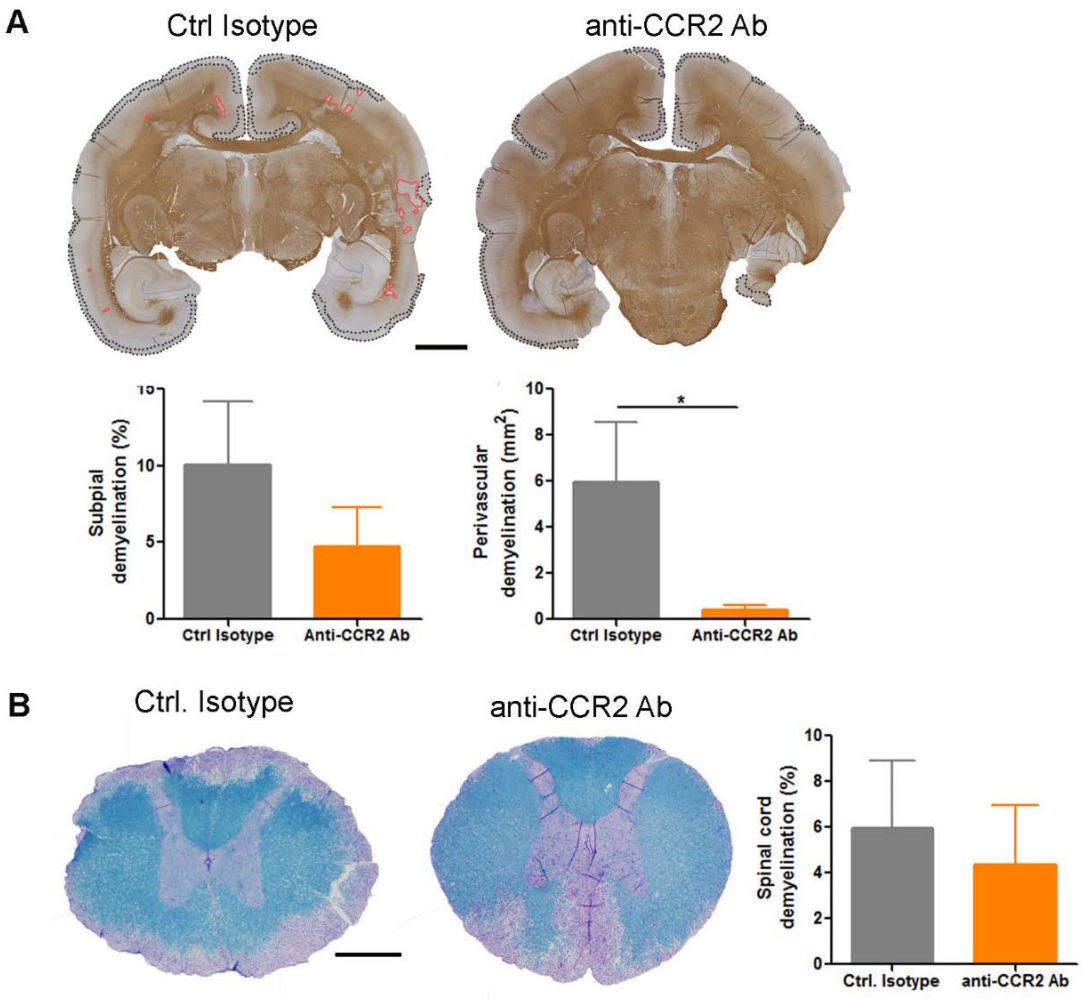

Figure 16: Reduction of cortical demyelination in marmosets depleted of inflammatory monocytes by a novel, humanized anti-CCR2 antibody

(A) Coronal brain sections immunostained for MBP (brown). Subpial cortical demyelinated regions (black dotted lines) and perivascular intracortical demyelinated areas (red lines) are delineated. Graphs show a moderate reduction of subpial cortical demyelination in marmosets depleted of inflammatory monocytes accompanied by a significant reduction of perivascular intracortical demyelination. **(B)** Representative images of transversal spinal cord sections stained with LFB/PAS show similar extents of demyelination in both groups. Scale bars, 1 cm (brain overviews), 500 µm (spinal cord sections). Data are expressed as mean ± s.e.m. (n=5 animals/group, *p<0.05, Mann Whitney U test).

3.4.2 Role of granulocytes in cortical demyelination

To define whether PMN are relevant for cortical demyelination, Th/+ mice were injected with a selective granulocyte-depleting antibody directed against Ly6G (Clone 1A8) (Daley et al., 2008) (see 2.4.4.3).

Depletion efficiency was assessed by flow cytometry in the blood (before stereotactic injection) and in cortical tissue (24 h after stereotactic injection, when PMN numbers where highest in untreated mice) (Figure 17A). FACS plots for 1A8 antibody-treated animals show a significant reduction in granulocyte numbers at the time point assessed when compared to Th/+ mice treated with the control isotype antibody 2A3. Additionally, CAE histochemistry was performed in brain tissue 24 h after the stereotactic injection and granulocytes were quantified in the cortical parenchyma and meninges (Figure 17B). A significant reduction of meningeal granulocytes was observed in Th/+ mice treated with the anti-Ly6G antibody and almost no positive cells were detected in the cortical parenchyma.

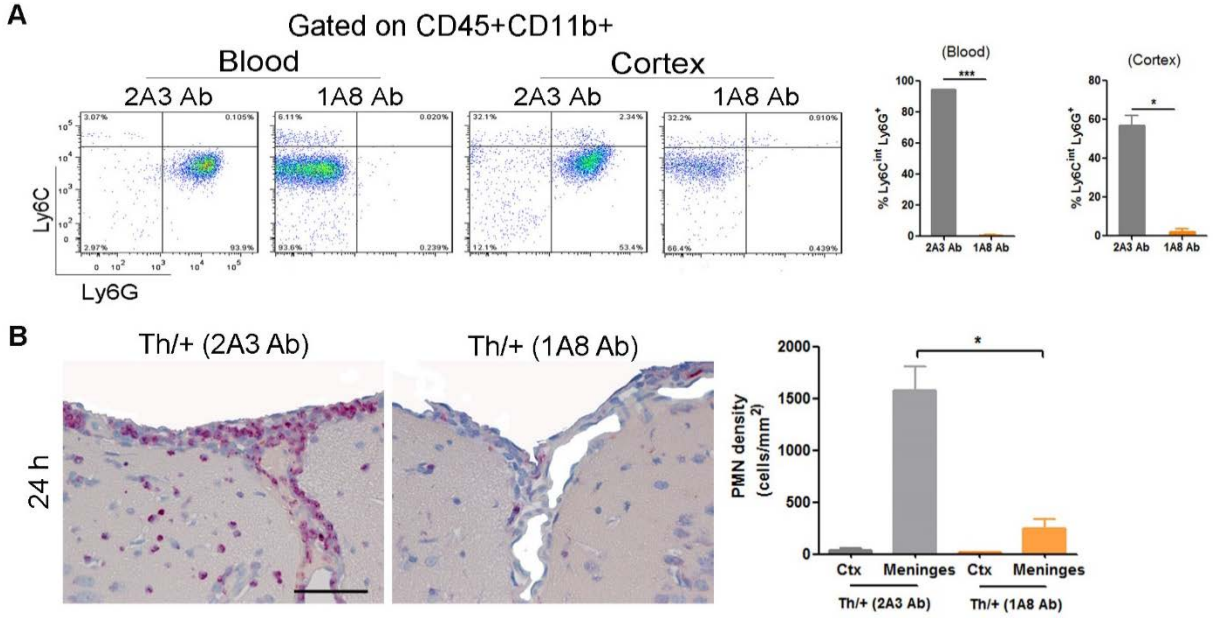

Figure 17: Granulocyte depletion in Th/+ mice

(A) The efficiency of PMN depletion was determined by flow cytometry in the blood (left dot plot, before stereotactic injection) and cortex (right dot plot, 24 h after stereotactic injection). Granulocytes were significantly reduced in the compartments analyzed in the depleted animals (Th/+ 1A8). Data represent two independent experiments (Blood: Th/+ 2A3 Ab, n= 8; Th/+ 1A8 Ab, n=7; Cortex: Th/+ 2A3 Ab, n= 4; Th/+ 1A8 Ab, n=5). **(B)** Representative brain sections of Th/+ mice stained with CAE histochemistry 24 h after stereotactic injection. A significant reduction in granulocyte numbers (dark pink cells) along the meninges was observed in granulocyte-depleted Th/+ mice (1A8 Ab). Granulocyte numbers in the cortical parenchyma did not differ between the groups. Scale bar, 50 µm (n=4 animals/group). Quantitative data are expressed as mean ± s.e.m. (*p<0.05, ***p<0.001, Mann Whitney U test).

Nevertheless, the extent of cortical demyelination on day 5 after intracerebral cytokine injection was similar in both groups as observed in MBP immunostained sections (Figure 18),

arguing against a relevant contribution of granulocytes to the generation of cortical demyelinated lesions.

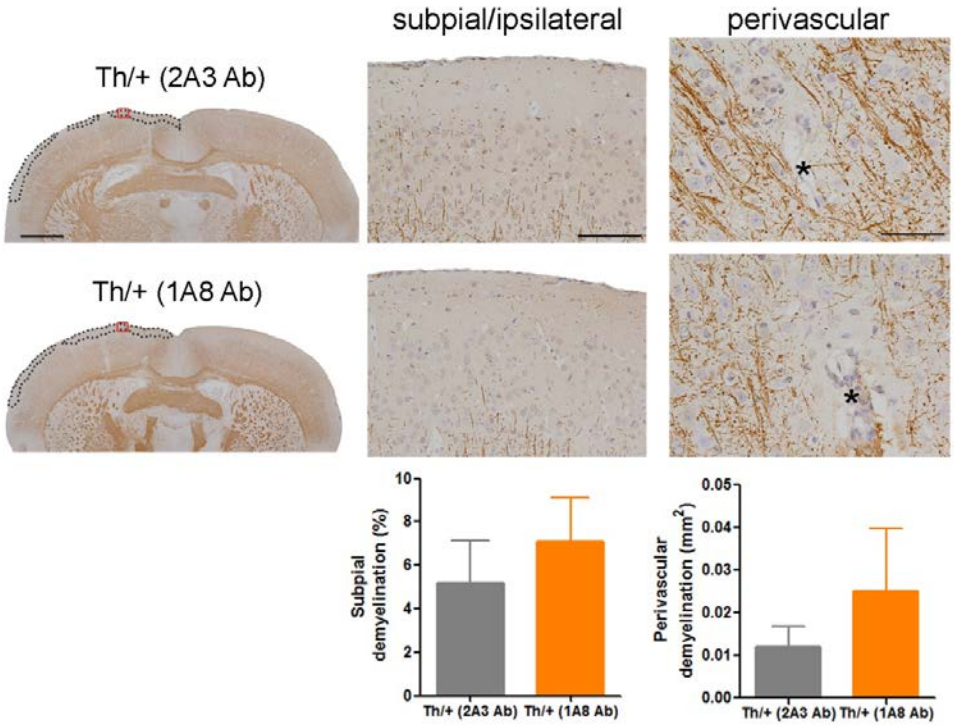

Figure 18: Granulocyte depletion does not affect the extent of cortical demyelination

Representative MBP immunostained sections of Th/+ mice treated with the 1A8 granulocyte depleting antibody or control isotype on day 5 post stereotactic injection. The extent or cortical demyelination was not affected by the depletion of granulocytes. Red squares in brain overviews mark the magnified areas in the subpial ipsilateral photographs; black dotted lines define subpial demyelinated areas; asterisks mark the lumen of parenchymal vessels. Scale bars represent 1 mm (brain overviews), 100 µm (subpial/ipsilateral panels), and 50 µm (perivascular panels). Graphs show data of two independent experiments (Th/+ 2A3 Ab, n=6, Th/+ 1A8 Ab, n=8). All quantitative data are expressed as mean ± s.e.m. (*p<0.05, ***p<0.001, Mann Whitney U test).

3.4.3 NK cells contribute to perivascular cortical demyelination

To assess the role of NK cells in cortical demyelination, Th/+ mice were depleted of NK cells before stereotactic injection. Therefore, the antibody PK136 targeting the NK1.1 receptor on the surface of NK cells was used (see 2.4.4.4).FACS analysis of blood (before stereotactic injection) and cortical tissue (24 h after stereotactic injection) showed that NK cell numbers were significantly reduced in Th/+ mice treated with the NK-depleting antibody PK136, when compared to the control isotype group (Figure 19A). While the extent of subpial demyelinated lesions was similar between both experimental groups, there was a

significant reduction in perivascular cortical demyelinated areas in NK-depleted animals (Figure 19B). Additional immunohistochemical stainings in non-depleted mice confirmed a predominant perivascular localization of NK cells in the inflamed cortex (Figure 19C, D).

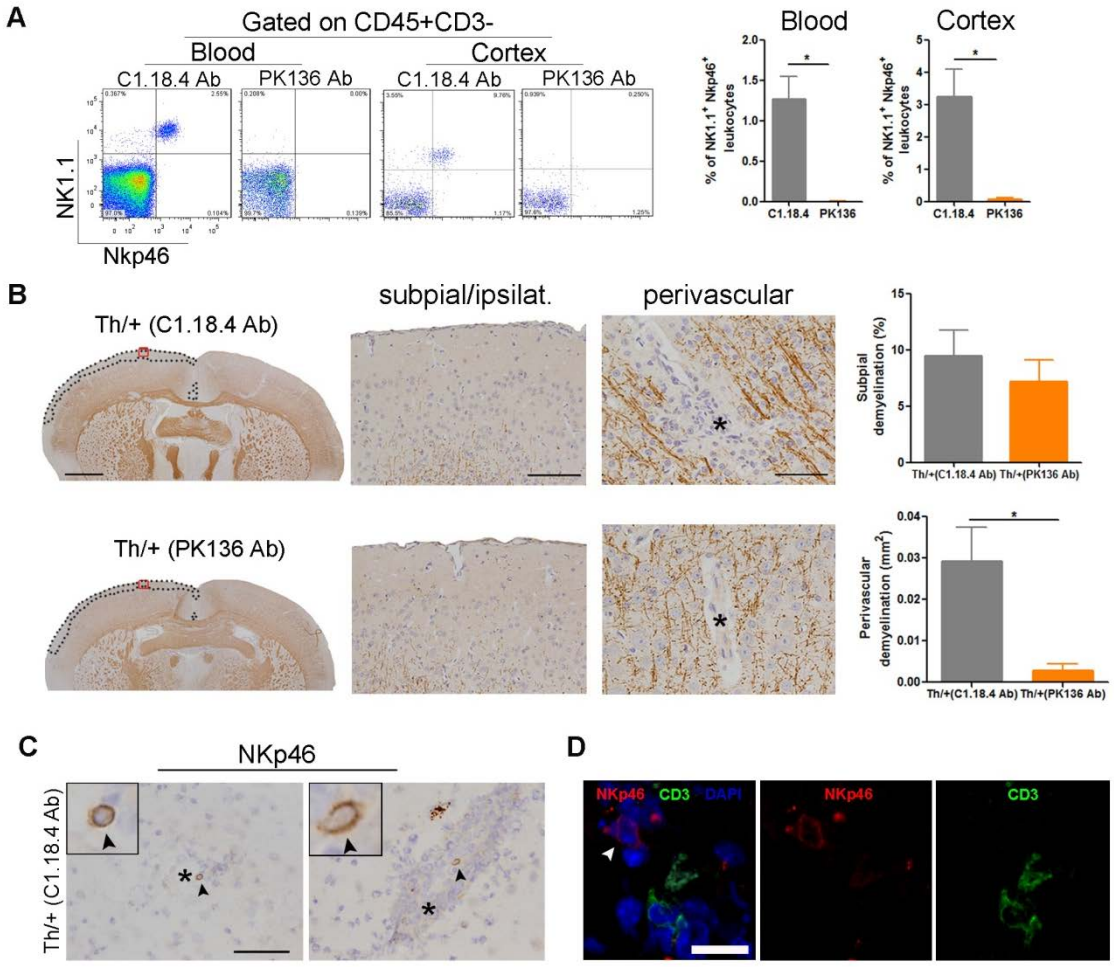

Figure 19: Role of NK cells in cortical demyelination

(A) NK depletion efficiency in Th/+ mice analyzed in the blood (before stereotactic injection) and cortical tissue (24 h after stereotactic injection) by FACS analysis. Data of two independent experiments are shown (Th/+ C1.18.4 Ab n=3, Th/+ PK136 Ab n=4; unpaired T test, Welch´s correction). **(B)** Perivascular cortical demyelination was significantly reduced in Th/+ mice depleted of NK cells (PK136 Ab) on day 5 post stereotactic injection. (n=7 animals/group, Mann Whitney U test). Scale bars, 1 mm (brain overviews), 100 µm (subpial/ipsilateral) and 50 µm (perivascular). Red squares in brain overviews mark the magnified areas in the subpial ipsilateral photographs; dotted lines delineate subpial cortical demyelinated areas. **(C)** Representative IHC of perivascularly located NK cells (NKp46, arrowheads) in the cortex of non NK cell-depleted Th/+ mice. Scale bar, 50 µm. Asterisks mark the lumen of the vessels. **(D)** Representative immunofluorescence staining of perivascularly located NK cells (NKp46, red channel; white arrowhead) showed no co-localization with CD3 (green channel), confirming them being NK, but not NKT cells. Nuclei were counterstained with DAPI (blue channel). Scale bar, 10 µm. All quantitative data are expressed as mean ± s.e.m. (*p<0.05).

3.4.3.1 NK cells participate in perivascular cortical demyelination, if the MOG-specific antibodies are of the IgG2a subclass

To support further the relevance of NK cells for cortical demyelination, EAE was induced in Rag1$^{-/-}$ mice and Rag1$^{-/-}$ γc$^{-/-}$ mice by the adoptive transfer of activated MOG-specific 2D2 T cells (see 2.4.5). One day after disease onset mice received 1.5 mg of the demyelinating anti-MOG antibody Z2 (IgG2a subclass) i.v. and were stereotactically injected with cytokines. Animals were perfused 5 days later, and the cortical demyelinated lesions were quantified (Figure 20A). Subpial cortical demyelination did not differ between Rag1$^{-/-}$ and Rag1$^{-/-}$γc$^{-/-}$ mice, but perivascular cortical demyelination was significantly reduced in the latter group (Figure 20B).

If the demyelinating anti-MOG antibody 8-18C5 (IgG1 subclass) was injected instead of the Z2 antibody, perivascular demyelination did not differ between the groups, and the demyelinated areas were smaller than those generated by using the Z2 antibody (Figure 20C).

3.4.4 Influence of the complement system on cortical demyelination

To address whether the complement system contributes to cortical demyelination, the generation of the MAC in Th/+ mice was blocked. To this end, the BB5.1 antibody against the mouse convertase C5, or a control isotype were injected intracerebrally together with the standard mixture of inflammatory cytokines in diseased Th/+ mice which had been immunized previously (Figure 6). This antibody inhibits the activity of the C5 convertase and consequently the cleavage of C5 into C5a and C5b fragments.

Additionally, Th/+ mice deficient for CD59a, the main inhibitor of the MAC on oligodendrocytes, were generated. We hypothesized that the extent of demyelination might increase in response to a less controlled classical complement pathway.

In the presence of the BB5.1 antibody, subpial demyelination was significantly reduced in Th/+ mice when compared to the group which received the control isotype (Figure 21A). Perivascular cortical demyelination, in contrast, was similar in both groups. CD59a-deficiency in Th/+ mice did not modulate the extent of cortical demyelination (Figure 21B).

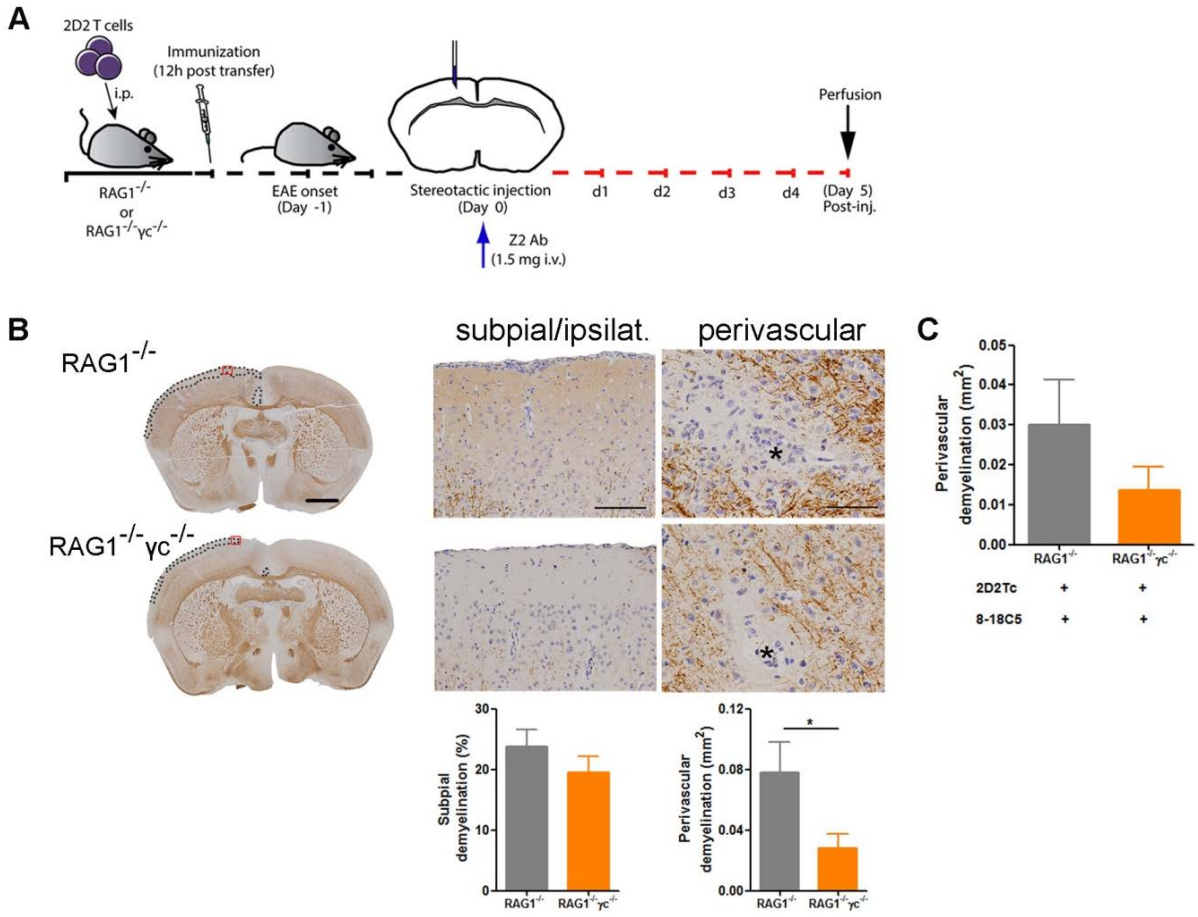

Figure 20: The contribution of NK cells to perivascular demyelination depends on the subclass of the pathogenic antibody

(A) Schematic representation of adoptive transfer experiments in Rag1$^{-/-}$ and Rag1$^{-/-}$γc$^{-/-}$ mice. **(B)** Representative MBP IHC of Rag1$^{-/-}$ (top) and Rag$^{-/-}$ γc$^{-/-}$ mice (bottom) adoptively transferred with 2D2 T cells and stereotactically injected with the pathogenic demyelinating anti-MOG antibody Z2. Quantifications revealed a significant reduction of perivascular cortical demyelination in NK cell-deficient mice while subpial cortical demyelination was similar in both groups (Rag1$^{-/-}$ n=5, Rag1$^{-/-}$ γc$^{-/-}$ n=4). Scale bars, 1 mm (brain overviews), 100 µm (subpial/ipsilateral) and 50 µm (perivascular). Red squares in the brain overviews mark the magnified areas in the subpial ipsilateral photographs; dotted lines delineate subpial demyelinated areas. **(C)** Quantification of perivascular cortical demyelination on MBP-immunostained sections of Rag1$^{-/-}$ and Rag1$^{-/-}$ γc$^{-/-}$ mice injected with the demyelinating anti-MOG antibody 8-18C5 (IgG1 subclass) did not show any differences between the groups (Rag1$^{-/-}$ n=5, Rag1$^{-/-}$ γc$^{-/-}$ n=4). All data are expressed as mean ± s.e.m. (*p<0.05, Mann Whitney U test).

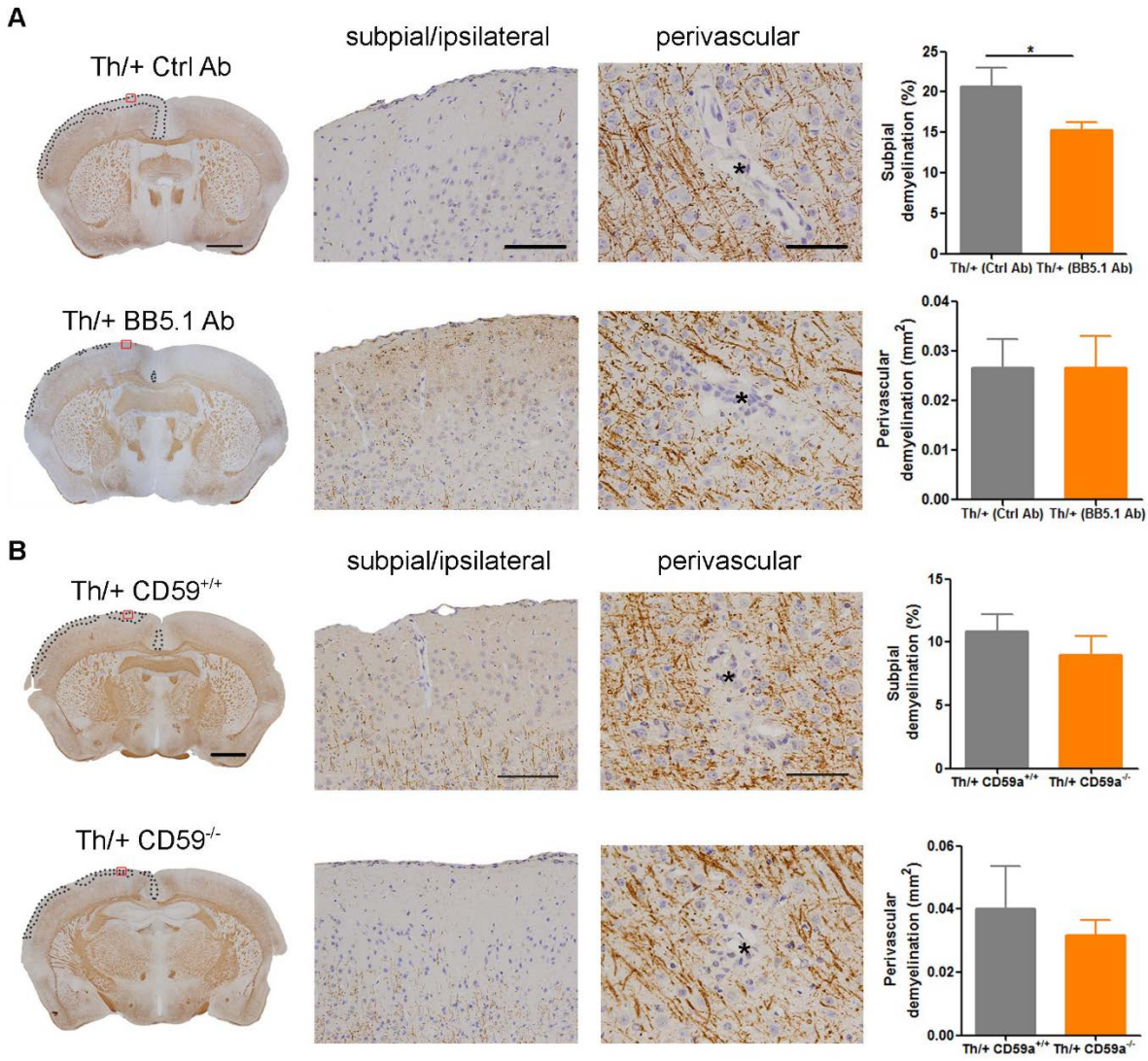

Figure 21: Complement dependent cytotoxicity contributes to subpial cortical demyelination

(A) Representative MBP IHC of stereotactically injected Th/+ mice which additionally received an intracerebral injection of the BB5.1 antibody, inhibiting C5 (top) or an isotype control (bottom) antibody. Quantification of demyelinated areas showed a significant reduction of subpial cortical demyelination in the group treated with the BB5.1 antibody. Data represent two independent experiments (9 mice/group, *p<0.05, unpaired T-test). **(B)** MBP IHC of Th/+ CD59a$^{+/+}$ and Th/+ CD59a$^{-/-}$mice intracerebrally injected with inflammatory cytokines showed that CD59a deficiency did not modulate the extent of cortical lesions in the model (n=6 mice/group, Mann Whitney U test). Red squares in the brain overviews mark the magnified areas in the subpial ipsilateral photographs and dotted lines define the respective subpial demyelinated areas. Asterisks point to the lumen of parenchymal vessels. Scale bars 1 mm (brain overview panels), 100 µm (subpial/ipsilateral panels) and 50 µm (perivascular panels). All quantitative data are presented as mean ± s.e.m.

3.4.5 Role of T and B cells in cortical demyelination

To determine whether T and B cells are required to induce cortical inflammatory demyelination, several experiments were designed in Rag1$^{-/-}$ and OSE mice. First, the demyelinating anti-MOG antibody 8-18C5 or a control isotype antibody were injected into Rag1$^{-/-}$ healthy mice (Figure 22A) and cortical demyelination was assessed 5 days after stereotactic injection.

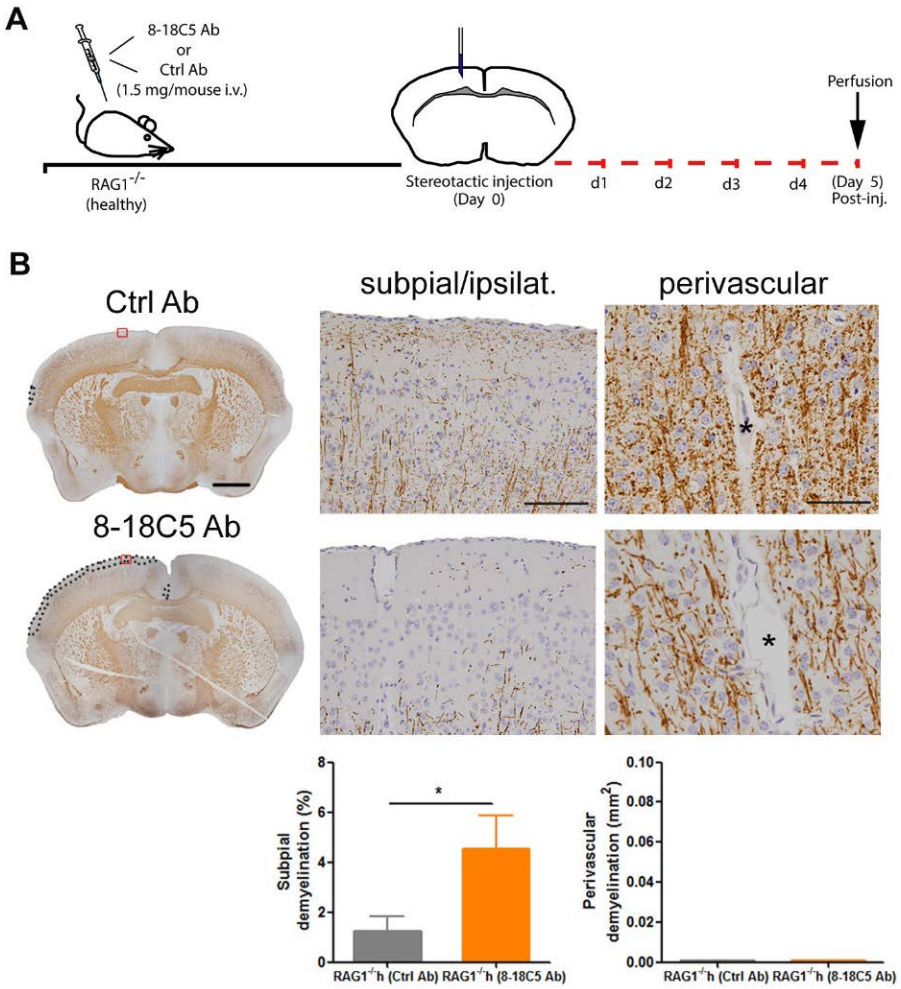

Figure 22: T cells are dispensable for subpial but not for perivascular demyelination

(A) Schematic representation of the experimental setup. **(B)** IHC for MBP on day 5 after stereotactic injection of 8-18C5 or control antibody transferred Rag1$^{-/-}$ mice. Healthy Rag1$^{-/-}$ mice, which received 8-18C5 Ab developed subpial but not perivascular demyelinated lesions. Red squares in brain overviews mark the magnified areas in the subpial ipsilateral photographs and dotted lines define the respective subpial demyelinated areas. Asterisks point out the lumen of parenchymal vessels. Scale bars 1 mm (brain overview panels), 100 µm (subpial/ipsilateral panels) and 50 µm (perivascular panels). Data are expressed as mean ± s.e.m. and represent two independent experiments for Rag1$^{-/-}$ mice (Ctrl. Ab, n=9) and Rag1$^{-/-}$ (8-18C5 Ab, n=8), *p<0.05, unpaired T-test.

A significant extent of subpial lesions was observed only in mice that had received the 8-18C5 antibody, implying that T cells and antigen presenting function of B cells are dispensable for the generation of subpial demyelinated lesions. Perivascular cortical demyelination was completely absent in Rag1$^{-/-}$ mice (Figure 22B). The same was true if the 8-18C5 antibody (IgG1 isotype) was replaced by the Z2 antibody (IgG2a subclass) (data not shown), which demonstrates that NK cells fail to induce perivascular cortical demyelination in the absence of activated T cells.

3.4.5.1 T cells are required for perivascular cortical demyelination

To address whether T-cell specificity as well as their activation state influence perivascular cortical demyelination, the extent of cortical lesions was compared between healthy Th/+ and OSE mice. It is worth noting that OSE healthy mice harbor non-activated MOG-specific T cells, in addition to the MOG-specific antibodies also present in Th/+ mice.

The assessment of lesions 5 days after stereotactic injection showed that subpial demyelination was present to a comparable extent in healthy Th/+ and OSE mice, whereas perivascular cortical demyelination was barely observed (Figure 23).

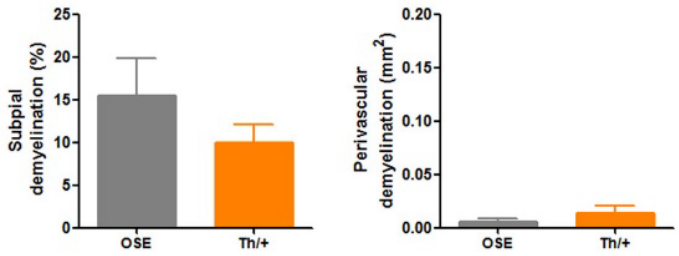

Figure 23: Assessment of cortical demyelination in healthy OSE and Th/+ mice

Quantitative assessment of subpial and perivascular cortical lesions in Th/+ healthy (n=5) and OSE healthy mice (n=6), did not reveal any differences between the groups. Data are expressed as mean ± s.e.m. and were analyzed by Mann Whitney U test.

If, however, healthy and diseased-OSE mice, immunized with $rMOG_{1-125}$, were compared, perivascular but not subpial demyelination was significantly increased in sick animals where MOG-specific T cells were activated (Figure 24A).

To exclude a potential bias due to different antibody titers or antibody isotypes in diseased versus healthy OSE mice, cortical demyelination was assessed in diseased and healthy $Rag1^{-/-}$mice, adoptively transferred with 2D2 or OT-II T cells respectively (see 2.4.5). Both experimental groups received 1.5 mg of the demyelinating anti-MOG antibody 8-18C5 i.v. before stereotactic injection (see schematic representation in Figure 24B).

As expected, subpial demyelination was similar in both 2D2 and OT-II transferred animals, but perivascular cortical demyelinated lesions were significantly larger in mice transferred with 2D2 T cells (Figure 24B). These findings indicate that encephalitogenic T cells are required for perivascular cortical demyelination in the presence of a pathogenic antibody, but are dispensable for subpial cortical demyelination.

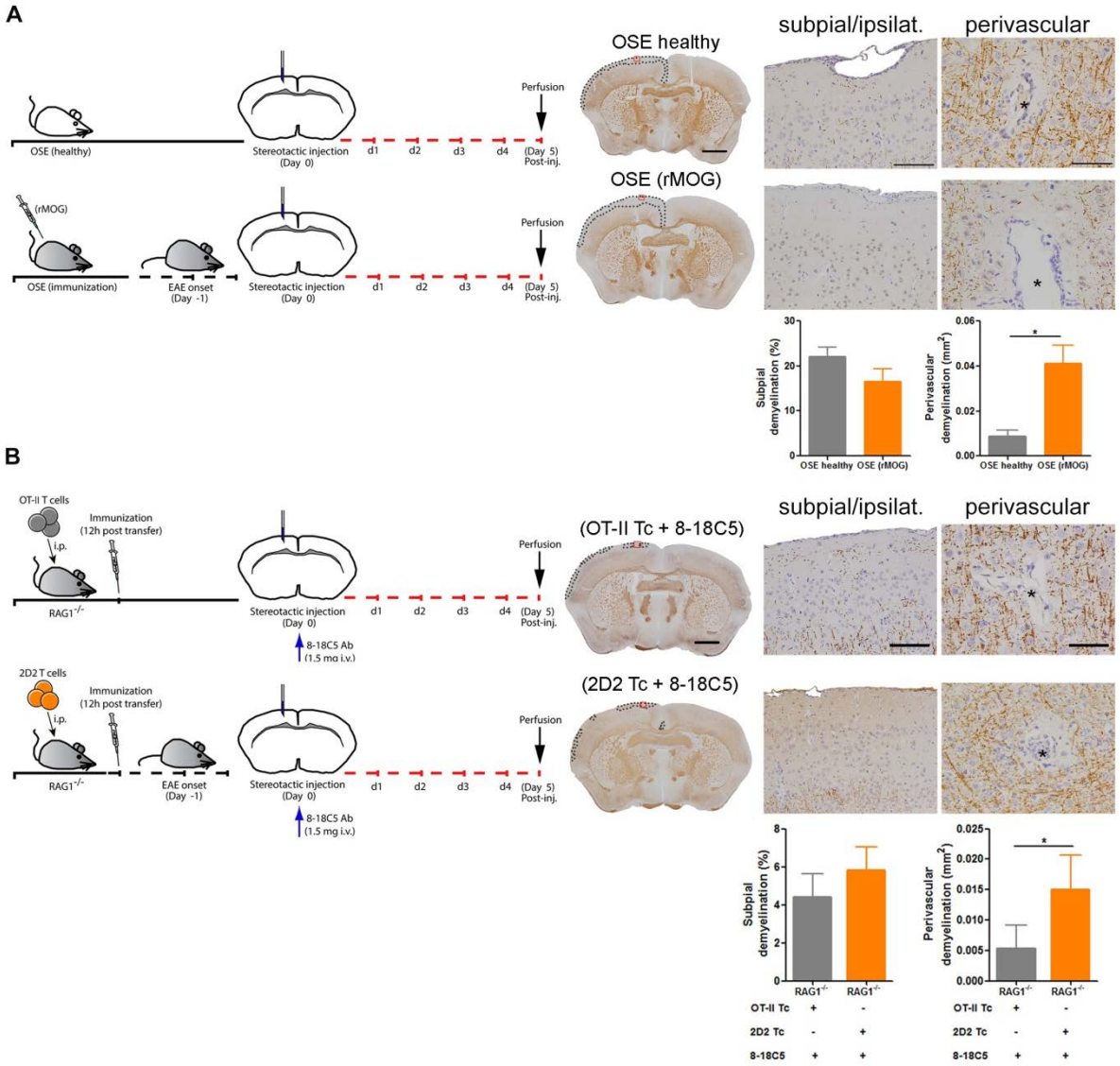

Figure 24: Influence of T cell activation and specificity on perivascular cortical demyelination

(A) Schematic representation of the experimental setup in OSE healthy vs OSE immunized mice (left). MBP IHC (right) demonstrates a significant increase in perivascular cortical demyelination in OSE immunized mice (n= 8) when compared to OSE healthy mice (n=4). Subpial demyelination did not differ between the groups. **(B)** Schematic representation of the experimental setup in adoptively transferred Rag1$^{-/-}$ mice. 2D2 or OT-II T-cells were transferred into Rag1$^{-/-}$ mice, and animals received 1.5 mg of the 8-18C5 antibody i.v. before intracortical cytokine injection. Quantification of cortical demyelination on MBP-immunostained brain sections showed barely any perivascular cortical demyelination in mice which received OT-II T-cells (grey bars) instead of MOG-specific 2D2 T-cells (orange bars). Subpial demyelination was comparable in both groups. Data of two independent experiments are shown, n=6 (Rag1$^{-/-}$, 2D2 Tc + 8-18C5) and n=12 (Rag1$^{-/-}$, OT-II Tc + 8-18C5). Red squares in brain overviews mark the magnified areas in the subpial ipsilateral photographs; dotted lines define the respective subpial demyelinated areas. Asterisks point to the lumen of parenchymal vessels. Scale bars represent 1 mm (brain overview panels), 100 µm (subpial/ipsilateral panels), and 50 µm (perivascular panels). All quantitative data are expressed as mean ± s.e.m. and analyzed by Mann Whitney U test, *p<0.05.

3.4.6 Encephalitogenic T cells increase the permeability of intracortical vessels to FITC-albumin

To assess BBB permeability and thus the influx, e.g. of pathogenic serum antibodies, in the present model, the cortical extravasation of FITC-albumin was measured in Th/+ mice (healthy or immunized) at 6 h and 24 h after stereotactic injection (see 2.4.8).

FITC-albumin extravasation was detected in subpial cortical areas already 6 h after intracortical cytokine injection, being more significant in immunized Th/+ mice (Figure 25). At this early time point, no signs of albumin extravasation from intracortical vessels were detected in any of the groups. 24 h after lesion induction, subpial FITC-albumin extravasation was comparable in both groups, whereas extravasation from intracortical vessels was much more pronounced in diseased Th/+ mice, harboring activated, encephalitogenic T cells.

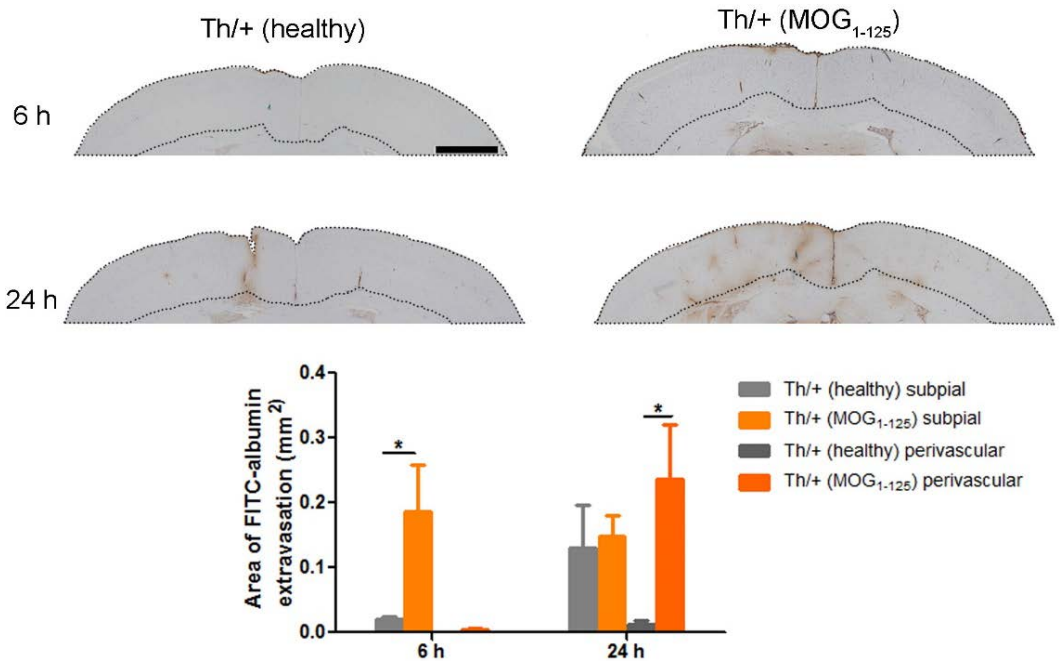

Figure 25: Extravasation of FITC-albumin from intracortical vessels requires activated, encephalitogenic T cells

Representative brain sections from Th/+ mice (healthy or immunized) FITC-immunostained 6 h and 24 h after stereotactic injection. Dotted lines define the areas analyzed for cortical FITC-albumin extravasation (brown signal). Subpial FITC extravasation was significantly increased in diseased Th/+ mice 6 h after injection, reaching comparable levels in both groups at 24 h. FITC-albumin extravasation from intracortical vessels was first observable 24 h after lesion induction, and was significantly increased in diseased Th/+ animals. Data are expressed as mean ± s.e.m. (Th/+ mice healthy, n=4; Th/+ mice diseased, n=5; *p<0.05, Mann Whitney U test). Scale bar, 500 µm.

3.4.7 VLA-4 blockade does not decrease cortical demyelination

To assess the effect of blocking leukocyte entrance into the CNS on the extent of cortical demyelination, the Natalizumab mouse analogue antibody PS/2 was used (see 2.4.4.6). This antibody recognizes the α4-integrin chain (CD49d) of VLA-4 on the surface of leukocytes, impeding the interaction with the corresponding ligand (VCAM-1) on the surface of endothelial cells.

Interestingly, no reduction of cortical demyelination was observed in animals treated with the PS/2 antibody when compared to the control isotype group (Figure 26).

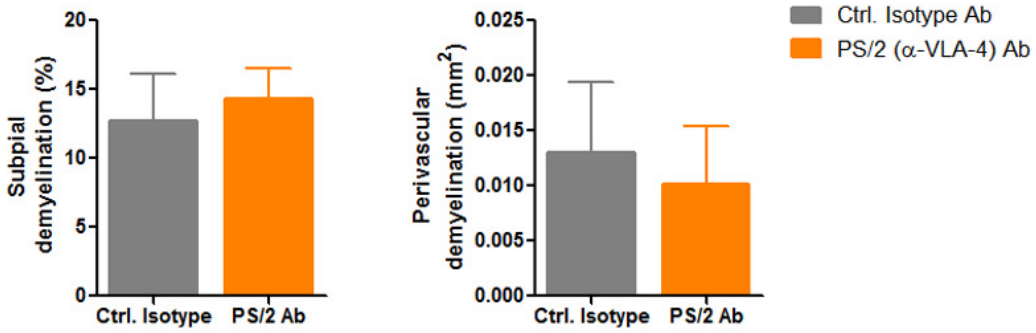

Figure 26: Influence of VLA-4 blockade on cortical demyelination

Quantification of subpial (left) and perivascular (right) cortical demyelination on MBP-immunostained sections from stereotactically injected Th/+ mice in which VLA-4 was blocked. No significant differences were found regarding the extent of subpial or perivascular cortical demyelination in Th/+ mice systemically treated with the PS/2 antibody (n=6) when compared to mice treated with control isotype antibody (n=5). Data are expressed as mean ± s.e.m. (One-way ANOVA, Dunnett's Multiple Comparison Test).

4 DISCUSSION

4.1 The inflammatory component present in cortical demyelinated MS lesions may contribute to cortical pathology

Cortical demyelination is a prominent feature in chronic progressive MS (Peterson et al., 2001, Bo et al., 2003a, Bo et al., 2003b, Kutzelnigg et al., 2005) that has been associated with disease progression and cognitive impairment in the patients (Calabrese et al., 2012). In post-mortem tissue from MS patients, cortical demyelinated areas can even exceed those of WM demyelination (Bo et al., 2003b). Furthermore, cortical demyelination has been also found in 38 % of biopsied patients in early stages of the disease (Filippi et al., 2010, Lucchinetti et al., 2011), and the majority of the lesions depicted are inflammatory at this time point (Lucchinetti et al., 2011, Popescu et al., 2011).

In the present study, the analysis of MS biopsy tissue featuring subpial cortical demyelinated areas revealed the presence of inflammatory infiltrates (T cells and macrophages/microglia) in line with previous reports (Lucchinetti et al., 2011, Popescu et al., 2011, Rodriguez et al., 2014). Moreover, the significant increase of microglia and macrophage activation in subpial cortical demyelinated areas confirmed the recent evolution of the lesions and their inflammatory signature (Rodriguez et al., 2014). The inflammatory phenotype reported in early cortical lesions was further reinforced by the presence of inflammatory monocytes co-expressing CD14 and CCR2 in two of the biopsies assessed in our study (MS cases 3 and 6, see Table 18). CCR2 is expressed in human “classical monocytes” ($CD14^{++}CD16^{-}$, phagocytic function) and in “intermediate monocytes” ($CD14^{++}CD16^{+}$, inflammatory function) (Ancuta et al., 2003). Interestingly, CCR2+ intermediate monocytes have been proposed as pathogenic cellular players in inflammatory disorders like Crohn’s disease (Grip et al., 2007) and cardiovascular diseases (Shantsila et al., 2011).

NK cells and cytotoxic T lymphocytes use the perforin/granzyme pathway as a main mechanism to kill pathogen-infected cells and tumor cells (Russell and Ley, 2002, Lieberman, 2003). The expression or the absence of CD3 in cells positive for GrB was used to differentiate cytotoxic T cells (CD3+ GrB+) from NK cells (CD3- GrB+) in the present study

(Inverardi et al., 1991). In the biopsies analyzed for this work, CD3- GrB+ NK cells were identified in the meninges, in demyelinated WM regions and cortical demyelinated tissue, frequently in close proximity to cortical vessels. This is in line with recent findings in post-mortem tissue of SPMS patients presenting more active than chronic lesions (2 cases out of 12), where few NK cells were identified in demyelinated cortex and WM lesions, often located near blood vessels (Durrenberger et al., 2012).

In summary, the findings in MS biopsies confirm that cells from both the adaptive and innate immune response are present in early cortical demyelination and may contribute to cortical lesion pathogenesis at this early stage.

4.2 Cortical demyelination in Th/+ mice reflects the different cortical demyelinated lesions found in MS

The mouse model of cortical demyelination developed in this thesis is based on a demyelinating anti-MOG antibody response in 8-18C5 knock-in (Th/+) mice (Litzenburger et al., 1998). In Th/+ mice, around 30 % of the transgenic B cells can bind MOG and high titers of MOG-specific antibodies are found in the serum of naïve animals. Naïve Th/+ mice do not develop neither spontaneous neurological disease, nor demyelination. Upon immunization with rMOG, the mature transgenic B cells differentiate to plasma cells that secrete MOG-specific IgG antibodies, of both IgG1 and IgG2a subclasses indicative of isotype switching (Litzenburger et al., 1998). Furthermore, Th/+ mice and 2D2 mice form the basis for the generation of the OSE mouse, which characteristically develops spontaneous autoimmune demyelination (Bettelli et al., 2006, Krishnamoorthy et al., 2006).

In the present study, Th/+ mice exhibited well-demarcated areas of confluent cortical demyelination, not only restricted to the injected brain hemisphere, but also extending to the contralateral (non-injected) side. Cortical demyelinated lesions were triggered by the focal injection of IFNγ and TNFα (targeted lesion approach). Reproducible demyelinated lesions were obtained affecting subpial as well as intracortical perivascular areas of the brain, reflecting the cortical lesion types observed in MS (Peterson et al., 2001, Bo et al., 2003b). In this model, subpial demyelinated lesions extended from the pia mater into superficial cortical layers (mostly until layer II/III).

Additionally, leukocortical lesions were observed in some of the mice, but they did not constitute the prime interest of the present work.

Up to now, inflammatory cortical demyelination has been experimentally observed in marmoset monkeys (Pomeroy et al., 2005, Merkler et al., 2006a, Pomeroy et al., 2008, Kramann et al., 2015) and MHC congenic rats (Storch et al., 2006) immunized with rMOG. In rats, cortical demyelination depended on particular combinations of MHC class I and II alleles (Storch et al., 2006). Furthermore, Lewis rats immunized with subclinical doses of rMOG have been shown to develop demyelinating cortical lesions after receiving an intracortical injection of pro-inflammatory cytokines (Merkler et al., 2006b, Rodriguez et al., 2014). Our model was developed in some analogy – however with important modifications – to the rat model.

In addition, cortical demyelination in the cerebral and cerebellar cortex has been reported in mice subjected to the cuprizone diet (Skripuletz et al., 2008, Skripuletz et al., 2010). Though the cuprizone model is useful for studying the dynamics of de- and remyelination, this toxic demyelination model is independent of adaptive immune cells (McMahon et al., 2001, Praet et al., 2014, Salinas Tejedor et al., 2015), which are part of the inflammatory response seen in cortical demyelination in MS.

4.3 Remyelination of cortical demyelination in Th/+ mice

In the present model, a relatively rapid resolution of demyelination, paralleled by a reduction of inflammatory infiltrates in the tissue (T cells and microglia/macrophages) was observed, evidencing a successful reparative process as reported previously (Franklin et al., 1997, Merkler et al., 2006b). Although in the present study remyelination was not assessed by electron microscopy, the lack of a detectable lesion in MBP IHC 40 days after lesion induction suggests efficient remyelination. Starting around day 10 after stereotactic injection, regions of thin myelin characteristically observed during remyelination increased with time, most obvious in subpial areas. Similar indications of effective cortical remyelination have been reported in MOG-immunized rats receiving an intracortical injection of pro-inflammatory cytokines (Merkler et al., 2006b), or in the subarachnoid space (Gardner et al., 2013), as well as in MS studies, where GM lesions remyelinated more efficiently than those in the WM (Albert et al., 2007, Chang et al., 2012).

A recent study comparing contiguous WM and GM in leukocortical lesions has revealed a significant preservation/generation of OPCs in the GM demyelinated areas. In addition, WM demyelinated areas, but not the cortical ones, exhibited a significant increase in reactive astrocytes and associated extracellular molecules that may inhibit oligodendrocyte production and myelination (Chang et al., 2012), providing an explanation for the higher remyelinating capacity observed in cortical areas.

4.4 Myelin and oligodendrocyte pathology in cortical lesions in Th/+ mice

Oligodendrocyte pathology in MS is variable, with studies reporting oligodendrocyte preservation in acute lesions (Raine et al., 1981, Lassmann, 1983, Lucchinetti et al., 1999, Rodriguez et al., 2014) or oligodendrocyte loss in newly forming lesions (Prineas et al., 1984, Barnett and Prineas, 2004). In the cortical demyelination model in Th/+ mice, a significant reduction of Olig2+ oligodendrocytes was observed in subpial demyelinated areas on day 5 after stereotactic injection. Olig2 constitutes a transcription factor necessary for oligodendroglial development, expressed during the entire maturation process of oligodendrocytes (Mei et al., 2013). Additionally, mature oligodendrocytes (p25+) were significantly reduced in the same areas, probably accounting for the decrease in the total number of oligodendrocytes at this early time point. Nevertheless, remyelination was not compromised in the long term. It is possible that OPCs readily repopulated the lesions and differentiated into myelinating oligodendrocytes; alternatively, OPCs may have been spared from the pathological process, as suggested above. Further studies are required to delineate the time course of oligodendrocyte damage, proliferation, migration, and differentiation in this model.

4.5 Axonal damage is present in cortical lesions in Th/+ mice

Acutely damaged axons, immunopositive for APP, were observed in cortical demyelinated lesions in Th/+ mice on day 5 after stereotactic injection. APP is synthesized in the neuronal cell body and transported to the synapses via fast anterograde axonal transport (Koo et al., 1990). In acutely injured axons, axonal transport is disrupted, resulting in the accumulation of axonally transported proteins like APP (Ferguson et al., 1997).

In early MS, acute axonal damage has been associated with inflammation and macrophage infiltration (Kuhlmann et al., 2002). Part of the damaged axons may then transect and degenerate, thus leading to axonal reduction (Trapp et al., 1998). However, a proportion of APP+ axons will survive the insult and resume full functionality (Nikic et al., 2011).

The significant increase in APP+ axons observed in cortical demyelination in Th/+ mice is in line with studies in MS patients reporting the presence of axonal damage in cortical demyelinated lesions (Peterson et al., 2001, Kutzelnigg et al., 2005).

4.6 Cortical demyelination in Th/+ mice exhibits neuronal preservation

On day 5 after stereotactic injection, neuronal density in subpial demyelinated areas in Th/+ mice was not reduced. Regarding neuronal injury in MS, reports differ, ranging from substantial to little if any neuronal loss in cortical demyelination (Peterson et al., 2001, Wegner et al., 2006, Lassmann, 2010, Magliozzi et al., 2010, Lucchinetti et al., 2011). These differences may in part be due to different sensitivities of the methods applied, or result from the intrinsic heterogeneity of the lesions. The cortical demyelination model presented in this study, like several others (Merkler et al., 2006b, Gardner et al., 2013, Rodriguez et al., 2014), reflects an acute inflammatory episode, in contrast to the chronic inflammatory process present in MS patients, which likely explains why a reduction in neuronal numbers is not observed in our model.

4.7 Cortical demyelination transiently impairs the performance of Th/+ mice in the complex running wheel

The motor skill sequence (MOSS) test was developed in 2006 (Liebetanz and Merkler, 2006) and its use in different animals models allowed, e.g., the detection of functional impairments associated with demyelination of the corpus callosum in the cuprizone model (Liebetanz and Merkler, 2006), and with developmental disruptions in the internal granule layer of the cerebellum (Maloney et al., 2011).

In the present study, a transient behavioral impairment of Th/+ mice between days 4 and 6 after cytokine injection into the motor cortex could be observed. The mice ran slowlier and covered less distance in the complex wheel than the control animals. The impairment in the cytokine-, but no PBS-injected Th/+ mice coincides with the time when the maximum amount of inflammatory cortical demyelination was observed in the model. C57BL/6J mice injected with cytokines or PBS performed similarly in the complex wheel, indicating that the injection of inflammatory cytokines alone is not sufficient to impair the adaptation to complex wheel running.

4.8 The generation of subpial and perivascular cortical lesions is controlled by different immunological mechanisms

Cortical demyelination requires a pathogenic antibody response against MOG

Confluent demyelination is a pathological hallmark of MS. In most EAE models, the formation of substantial areas of demyelination relates to a pathogenic antibody response against extracellular epitopes of myelin proteins (Linington and Lassmann, 1987, Piddlesden et al., 1993, Adelmann et al., 1995, Brehm et al., 1999, Genain et al., 1999, von Budingen et al., 2002, Bourquin et al., 2003, Storch et al., 2006). In line with this, in our model, cortical demyelination could be induced by intracortical stereotactic injection of pro-inflammatory cytokines in Th/+ but not in 2D2 or C57BL/6J mice. Th/+ mice are heavy chain knock-in mice for 8-18C5, a well-known demyelinating MOG-specific antibody (Linington et al., 1988, Kerlero de Rosbo et al., 1990, Linington et al., 1993, Litzenburger et al., 1998). While immunization of Lewis rats with $rMOG_{1-125}$, which includes the extracellular part of MOG, induces demyelinating MOG-specific conformational antibodies (Adelmann et al., 1995), the antibody response of C57BL/6J mice to rat $rMOG_{1-125}$ immunization is largely confined to linear peptides (Bourquin et al., 2003, Marta et al., 2005). A contribution of antibodies to demyelination in MS has been postulated by studies demonstrating myelin-specific antibodies in patient sera (Gaertner et al., 2004, Zhou et al., 2006, Brilot et al., 2009) as well as by Ig depositions and complement products in MS tissue (Diaz-Villoslada et al., 1999, Genain et al., 1999, Lucchinetti et al., 2000, Lassmann et al., 2001).

However, antibodies against MOG are only inconsistently found in MS patients, suggesting that the targets of pathogenic antibodies in MS still have to be identified.

The pathogenic potential of demyelinating antibodies has been previously attributed to their ability to fix complement (CDC) (Piddlesden et al., 1993, Storch and Lassmann, 1997, Storch et al., 1998, Urich et al., 2006, Breij et al., 2008) or to induce ADCC (Desjarlais and Lazar, 2011). Both CDC and ADCC depend on the Ig subclass of the antibody in question. IgG2a and 2b constitute the most potent subclasses for activating effector functions of antibodies in mice following a hierarchical order: IgG2a ≥ IgG2b > IgG1 » IgG3 (Fossati-Jimack et al., 2000, Nimmerjahn and Ravetch, 2005, Aschermann et al., 2010). Since plasma cells in Th/+ mice immunized with rMOG synthesize MOG-specific antibodies of the IgG1 and IgG2 isotypes (Litzenburger et al., 1998), both mechanisms (ADCC and CDC) may be operative in the animal model developed in this work. In addition, antibody-dependent cellular phagocytosis (ADCP) could also play a role. In ADCP, accessory cells with phagocytic function like macrophages and neutrophils, phagocytose antibody-coated bacteria through engagement of their Fc receptors (Janeway CA Jr, 2001). In this regard, a study reported the presence of phagocytic cells containing immune complexes formed by Ig and myelin proteins in MS lesions and EAE brain tissue (Genain et al., 1999). Considering the high specificity of the anti-MOG antibodies produced in Th/+ mice (Litzenburger et al., 1998) as well as the important role of monocytes in EAE (Yamasaki et al., 2014) and MS (Bruck et al., 1995), this mechanism could be operative as well in the cortical demyelination model presented here.

Inflammatory monocytes are required for cortical demyelination

Since inflammatory monocytes are present in the cortical biopsies analyzed and constitute a major cell population infiltrating the cortex of Th/+ mice, several experiments were performed to elucidate their role in cortical demyelination. The experiments presented here suggest that inflammatory monocytes are required for the generation of cortical lesions. First, Th/+ CCR2$^{-/-}$ mice developed significantly less subpial and perivascular intracortical demyelinated lesions upon stereotactic cytokine injection. Additionally, the specific blockade of CCR2 with the antagonist RS-504393 reduced perivascular demyelination in CCR2-competent animals.

Finally, the depletion of CCR2+ inflammatory monocytes in marmoset monkeys using a humanized antibody against CCR2 revealed a moderate decline in subpial demyelination, and a significant reduction of perivascular cortical demyelinated lesions.

Interestingly, the blockade or depletion of CCR2+ monocytes was more efficient in reducing perivascular than subpial cortical demyelination, suggesting that subpial demyelination depends less on inflammatory cells than perivascular cortical demyelination. As such, any interference with pathogenic cell populations impairs perivascular cortical demyelination measurably while subpial demyelination remains unaffected.

Spinal cord pathology is not modulated by CCR2 deficiency or inhibition in mice and marmosets

Recently it has been demonstrated that CCR2+ monocyte-derived macrophages initiate spinal cord demyelination at EAE onset, often at the nodes of Ranvier (Yamasaki et al., 2014). However, PMNs, which have been accused of taking over CCR2+ monocyte functions in the absence of CCR2, did not efficiently replace CCR2+ monocytes with respect to inflammatory demyelination (Yamasaki et al., 2014). Interestingly, spinal cord demyelination was comparable between Th/+ $CCR2^{-/-}$and Th/+ $CCR2^{+/+}$ mice, and depletion of CCR2+ monocytes did not significantly reduce spinal cord demyelination in marmosets immunized with MOG_{1-125}. Both models differ from Yamasaka et al. by the presence of demyelinating serum antibodies, which might get sufficient access to the spinal cord by a T cell and PMN induced breakage of the spinal cord BBB.

Neutrophils are not instrumental for cortical demyelination

Granulocytes contribute to astrocyte loss in anti-aquaporin-4 (AQP4) antibody-mediated animal models of neuromyelitis optica (NMO) (Saadoun et al., 2012) and to ADCC in tumor models (Stockmeyer et al., 2003, Challacombe et al., 2006). In EAE, evidence has been provided that neutrophils constitute a significant proportion of the circulating and CNS-infiltrating cells during the pre-clinical phase of the disease indicative of their involvement in the early stage of BBB breakdown (Mantovani et al., 2011, Christy et al., 2013, Aube et al., 2014, Rumble et al., 2015). While many neutrophils can be detected in early stages of spinal cord EAE, a remarkable resistance of the brain to neutrophil entry has been documented in

acute inflammation (Andersson et al., 1992b, a, Enzmann et al., 2013). PMNs are not generally part of the inflammatory infiltrates of early MS lesions. However, plasma levels of neutrophil-related factors like CXCL5 were upregulated in RRMS patients during acute lesion formation and the additional expression of CXCL1 and neutrophil elastase correlated with clinical disability in these patients (Rumble et al., 2015).

In the present study, the contribution of granulocytes to cortical demyelination was investigated by depleting neutrophils in Th/+ mice using the anti-Ly6G antibody 1A8. FACS analysis performed 24 hours after stereotactic intracerebral injection revealed an efficient depletion of circulating neutrophils in the blood and in the cerebral cortex of Th/+ mice treated with the anti-Ly6G antibody. However, the extent of cortical demyelination did not differ between depleted or non-depleted Th/+ mice, arguing against a relevant contribution of granulocytes to cortical demyelination in our model.

Natural killer cells contribute to perivascular cortical demyelination

It is widely accepted that NK cells have two main effector functions: the direct killing of target cells (cytotoxicity) and the secretion of cytokines and chemokines. For a long time, NK cells were viewed only as “killers” but increasing attention has been given to their immunoregulatory function shaping adaptive immune responses (Fu et al., 2014). In EAE, NK cell-depletion has resulted in either an increased disease severity, related to an absence of NK cell-mediated killing of encephalitogenic T cells (Zhang et al., 1997, Xu et al., 2005), or an improvement in the clinical course of EAE (Winkler-Pickett et al., 2008). In addition, the expansion of CD56+ NK cells in a human-mouse chimera model of EAE improved the clinical disease and reduced the amount of Th17 cells in the CNS (Hao et al., 2011).

In the present model, the depletion of NK cells in Th/+ mice resulted in a significant reduction of perivascular but not subpial demyelinated lesions, consistent with a predominant perivascular localization of NK cells in the inflamed cortex of mice and in MS biopsies. Furthermore, it was demonstrated that the contribution of NK cells to perivascular demyelination depends on a pathogenic antibody response, since perivascular demyelinated lesions were not observed in C57BL/6J or 2D2 mice (which also have NK cells), and on the IgG subclass of the antibody present.

Additionally, NK cells contributed to perivascular cortical demyelination only in the presence of encephalitogenic T cells, since healthy $Rag1^{-/-}$ mice injected with the Z2 antibody did not develop perivascular intracortical lesions.

These findings suggest that ADCC is the mechanism by which NK cells participate in perivascular cortical demyelination and that the recruitment of NK cells to the cortex is dependent on encephalitogenic T cells. In this regard, it has been shown that activated CD4+T cells boost NK cell activation via IL-2 secretion (Horowitz et al., 2010).

Furthermore, NK cells can be recruited to the CNS by the secretion of chemokines, e.g. CX_3CL1 (produced by neurons), and CCL2 and CXCL10 produced by microglia, astrocytes and infiltrating inflammatory cells (Shi et al., 2011).

Evidence of NK cell-mediated ADCC has been provided in animal models of NMO involving the pathogenic antibody AQP4 (Ratelade et al., 2012). Further studies reported that NK cells could kill oligodendrocytes in vitro independently of pathogenic antibodies, using, among others, the activating receptor NKG2D (Morse et al., 2001, Saikali et al., 2007).

In humans, NK cells are commonly divided into two functional subsets based on the cell-surface density of CD56 and CD16: $CD56^{dim}$ CD16+ NK cells (cytotoxic functions) and $CD56^{bright}$ CD16- NK cells (immunoregulatory functions) (Cooper et al., 2001). In MS, RRMS patients were shown to harbor reduced numbers of IFNγ-producing $CD56^{bright}$ NK cells in the blood (Lunemann et al., 2011), while PPMS and SPMS patients exhibited high percentages of circulating $CD56^{dim}$ NK cells with increased cytotoxic properties (Plantone et al., 2013). Interestingly, NK cells can exert regulatory functions in an inflammatory context by being cytotoxic against T cells (Bielekova et al., 2004, Bielekova et al., 2006, Hu et al., 2009, Bielekova et al., 2011). This hypothesis is supported further by studies in RRMS that associate periods of reduced NK cell killing activity with susceptibility to the development of clinical attacks and active lesions on MRI (Kastrukoff et al., 2003).

Taken together, in our model, NK cells, in cooperation with an encephalitogenic T cell response, contribute to perivascular cortical demyelination in the presence of a pathogenic antibody response, which includes potent Ig isotypes for ADCC.

Complement - dependent cytotoxicity contributes to subpial demyelination

The relevance of the complement system in EAE models remains controversial. Nataf and colleagues reported a reduction in EAE severity in mice deficient for C3 (Nataf et al., 2000) while another group, using a higher dose of MOG, reported similar EAE severity in knockout and control mice (Calida et al., 2001). Moreover, the expression of the complement inhibitor sCrry prevented EAE (Davoust et al., 1999), and a complement-mediated exacerbation of the disease could be induced by transferring the pathogenic 8-18C5 antibody into FcRγ-deficient mice, but not in C1q-deficient animals (Urich et al., 2006).

In the present study, blocking the formation of the MAC using a C5 convertase blocking antibody, BB5.1, significantly reduced the extent of subpial demyelination, although perivascular demyelination was not decreased. Given that murine and human NK cells locate specifically around intracortical vessels, this may indicate that in the absence of CDC, ADCC can still induce substantial perivascular cortical demyelination. However, considering that the intracortically injected BB5.1 antibody is much larger in size than the injected cytokines, the BB5.1 antibody may diffuse less well in the tissue and thus, the contribution of the complement system to perivascular demyelination might be underestimated under these experimental conditions.

It was surprising that cortical demyelination was not increased in Th/+ CD59a$^{-/-}$ mice. CD59, is an important regulator of complement activation and represents the only membrane bound inhibitor of C5b-9 formation (Nangaku, 2003). CD59 deficiency, in combination with a lack of the decay accelerating factor (DAF), a membrane bound complement inhibitor at the C3/C5 convertase step on erythrocytes, results in paroxysmal nocturnal hemoglobinuria (PNH) in humans (Risitano, 2012).

In mice, CD59 deficiency causes spontaneous intravascular hemolysis and hemoglobinuria (Holt et al., 2001). However, experiments in mice and rats where CD59 expression has been blocked, suggested that any interpretation of the results could be confounded by the presence of the protein Crry, an inhibitor of early complement activation. Crry is the rodent analogue of the human DAF and membrane cofactor protein (MCP), both regulators of the complement cascade. Several studies in models of glomerular endothelial injury in rats (Nangaku et al., 1998) or nephropathy models (Cunningham et al., 2001)

suggest an essential role for CD59 only when upstream inhibitors of the complement cascade are exhausted by excessive activation or loss of inhibitory functions. Thus, the presence of Crry, mediating upstream regulation of the complement cascade might explain the results obtained in Th/+ CD59a$^{-/-}$ mice in the present work.

Encephalitogenic T cells are dispensable for subpial but not for perivascular cortical demyelination

Myelin reactive T cells are instrumental for EAE induction (Furtado et al., 2008, O'Connor et al., 2008). The present study demonstrates that encephalitogenic T cells are dispensable for subpial but not for perivascular demyelination, since Rag1$^{-/-}$ healthy mice i.v. injected with the pathogenic antibody 8-18C5 and stereotactically injected with the pro-inflammatory cytokine mixture, developed subpial but not perivascular lesions. Furthermore, it was demonstrated that only myelin-specific, activated T cells were able to trigger the formation of perivascular cortical demyelination.

The conclusion that encephalitogenic T cells are required for perivascular but not for subpial cortical demyelination was supported by experiments assessing intracortical extravasation of FITC-albumin in healthy versus diseased Th/+ mice stereotactically injected with pro-inflammatory cytokines. Extravasation of FITC-albumin from intracortical vessels was significantly more pronounced in diseased animals and first observable 24 h after injection. In contrast, subpial albumin-FITC extravasation was already observed at 6 h, becoming substantial in both experimental paradigms 24 h after lesion induction, indicating that intracortically injected cytokines are sufficient to open meningeal or subpial cortical vessels effectively. In contrast, intracortical vessels might require a stronger stimulus, like the interaction with encephalitogenic T cells or other inflammatory cells to become permeable to FITC-albumin.

Several experimental models and studies in MS tissue support the role of inflammatory cytokines for demyelination and thus highlight the significance of the results obtained here. For example, TNFα, lL-1β and IL-17A have been reported to increase BBB permeability and activate parenchymal vessels (Brown and Sawchenko, 2007, Steinman, 2013). Moreover, the stereotactic injection of IFNγ and TNFα in MOG-immunized rats induced meningeal and

intracortical inflammation accompanied by extensive subpial and intracortical demyelination (Merkler et al., 2006b, Gardner et al., 2013). Also, high levels of these two cytokines have been detected in the CSF of MS patients during acute relapses (Maimone et al., 1991), and it has been proposed that the diffusion of pro-inflammatory cytokines from inflamed meninges could support the cortical pathology observed in the upper demyelinated layers of the brain (Magliozzi et al., 2010). In line, recent findings report IFNγ and TNFα expression in T cells and monocytes/macrophages respectively, accumulated in the inflamed meninges of SPMS brains (Gardner et al., 2013).

Reiteratively, the results obtained in this study denote the existence of distinct barrier properties within the cortical vasculature that might differentially influence tissue vulnerability to demyelination. In this respect, slight differences between meningeal and parenchymal vessels have been reported. Meningeal vessels lack astrocytic ensheathment (Allt and Lawrenson, 1997), which may make them more permeable to immune cells and soluble factors, whereas parenchymal microvessels lack the expression of P-selectin (Barkalow et al., 1996, Yong et al., 1997, Kivisakk et al., 2003). It has been shown that P-selectin expression in meningeal vessels and in the choroid plexus stromal vessels promotes lymphocyte trafficking into the SAS and the CSF respectively (Carrithers et al., 2000, Kivisakk et al., 2003, Ransohoff and Engelhardt, 2012). In this regard, imaging studies in EAE confirmed that the SAS is the first place where encephalitogenic T cells are reactivated by APC, resulting in proliferation and parenchymal infiltration. Subsequently, the parenchymal vasculature becomes activated as part of a two-step process orchestrated by immune cells to invade the CNS (Lassmann and Wisniewski, 1978, Bartholomaus et al., 2009, Kivisakk et al., 2009, Reboldi et al., 2009), which might also explain the delayed perivascular extravasation of FITC-albumin observed between the 6 h and 24 h time points.

The blockade of VLA-4 with the antibody PS/2 does not modulate cortical demyelination in Th/+ mice

The specific α4-integrin chain (CD49d) and the common β1-integrin chain (CD29) form the integrin VLA-4 (Schwab et al., 2015). Once VLA-4 is activated by chemokines (Campbell et al., 1998), it binds to VCAM-1 on endothelial cells of the BBB and mediates firm adhesion of immune cells, as a pre-requisite for transmigration (Engelhardt and Ransohoff, 2012).

The rationale behind blocking the expression of VLA-4 in stereotactically injected Th/+ mice using the PS/2 antibody was based on previous studies where blocking α4-integrin has been shown to be protective in both EAE and MS (Yednock et al., 1992, Engelhardt et al., 1998, Polman et al., 2006, Stuve et al., 2006, Hausler et al., 2015). Indeed, the blockade of VLA-4 with the monoclonal antibody Natalizumab has become the most effective therapy for RRMS patients (Schwab et al., 2015). In the present study, treatment with the Natalizumab mouse analogue PS/2 did not protect Th/+ mice against subpial cortical demyelination, in line with the notion that subpial demyelination is less dependent on the infiltration of inflammatory cells.

5 SUMMARY AND CONCLUSIONS

Inflammatory demyelination is the histopathological hallmark of MS and does not only affect the white matter but also the cortex. Imaging and histopathological studies suggest that cortical pathology is a correlate of cognitive dysfunction and disease progression, and driven by an inflammatory process in early stages of the disease. Cortical demyelinated lesions have been classified into subpial, perivascular (intracortical) and leukocortical lesions according to lesion localization. Subpial demyelinated plaques are by far, the most frequent and extensive cortical lesion type. First, the cortical immune cell infiltration was characterized in more detail in a cohort of eight MS biopsies. T cells, CCR2+ monocytes and microglia activation were observed in cortical demyelinated areas. Interestingly, NK cells were present as well, mainly localized around inflamed cortical vessels.

To elucidate the contribution of immune cell subpopulations to cortical demyelination, a novel cortical demyelination model in the mouse was established. The model combined the heavy chain knock-in mouse for 8-18C5, a well-known demyelinating antibody, (Th/+ mouse) with a stereotactic targeting approach to induce cortical demyelination. Th/+ mice developed MS-like subpial and perivascular cortical demyelinated lesions in response to intracortical cytokine injections also in the non-injected hemisphere, which translated clinically into a transient deficit to adapt to complex wheel running. Time course experiments demonstrated that cortical inflammation resolved rapidly and that the demyelinated lesions remyelinated efficiently. Axonal damage, as evidenced by APP+ axons was present around demyelinated cortical vessels but neuronal numbers were not reduced.

CCR2+ monocytes were found to be instrumental for cortical demyelination, since Th/+ $CCR2^{-/-}$ had significantly less subpial and perivascular cortical demyelination than Th/+ $CCR2^{+/+}$ mice. In order to translate our results into a preclinical treatment approach, we evaluated a novel humanized antibody against CCR2, which efficiently depletes CCR2+ monocytes in the marmoset EAE model. A moderate reduction of subpial and a significant reduction of perivascular cortical demyelination in response to CCR2+ monocyte depletion were observed, further substantiating their importance for cortical demyelination. Depleting marmosets of CCR2+ monocytes was well tolerated, and this targeted therapy might be a future treatment option for MS.

NK cells were found to augment perivascular but not subpial cortical demyelination, which was in line with a preferential perivascular localization of NK cells in human cortical lesions as well as in the mouse demyelinated cortex. The contribution of NK cells to perivascular cortical demyelination depended on encephalitogenic T cells and the IgG2a isotype of the demyelinating antibody. This suggests that T cells are required for the recruitment of NK cells to the inflamed cortex and that NK cells contribute to cortical demyelination through ADCC.

Next, the contribution of adaptive immune cells for cortical demyelination was dissected. Antigen presenting functions of B cells were neither required for subpial nor for perivascular cortical demyelination in the presence of a demyelinating antibody. In contrast, activated and myelin-specific T cells were absolutely required for perivascular cortical demyelination but also dispensable for subpial cortical demyelination, suggesting that subpial cortical demyelination is largely independent of adaptive immunity. In this line, blockade of α4-integrin with PS/2, the mouse analogue of Natalizumab, did not reduce subpial demyelination. However, subpial demyelination was reduced in the presence of an antibody blocking the generation of the membrane attack complex, highlighting the classical complement pathway as an effector mechanism for subpial demyelination.

In order to better understand why subpial demyelination is generated much easier than perivascular cortical demyelination, FITC-albumin was injected in healthy versus diseased Th/+ mice. A comparable extent of subpial extravasation of FITC-albumin was observed in both healthy and diseased Th/+ mice, in response to intracortical cytokine injections, while perivascular FITC-albumin extravasation was restricted to diseased animals. This suggests that meningeal and intracortical vessels differ with respect to their barrier functions.

In summary, we have developed a novel animal model for cortical demyelination in the mouse, which has proven to be predictive for a novel targeted therapy evaluated in marmosets. It also demonstrates the exquisite vulnerability of the subpial cortex for demyelination and offers a rational explanation why treatments targeting the adaptive immune response might fail in preventing subpial demyelination, the most extensive cortical lesion type seen in progressive MS.

6 BIBLIOGRAPHY

Adelmann M, Wood J, Benzel I, Fiori P, Lassmann H, Matthieu JM, Gardinier MV, Dornmair K, Linington C (1995) The N-terminal domain of the myelin oligodendrocyte glycoprotein (MOG) induces acute demyelinating experimental autoimmune encephalomyelitis in the Lewis rat. Journal of neuroimmunology 63:17-27.

Albert M, Antel J, Bruck W, Stadelmann C (2007) Extensive cortical remyelination in patients with chronic multiple sclerosis. Brain pathology 17:129-138.

Allen AC, Kelly S, Basdeo SA, Kinsella K, Mulready KJ, Mills KH, Tubridy N, Walsh C, Brady JJ, Hutchinson M, Fletcher JM (2012) A pilot study of the immunological effects of high-dose vitamin D in healthy volunteers. Multiple sclerosis 18:1797-1800.

Allt G, Lawrenson JG (1997) Is the pial microvessel a good model for blood-brain barrier studies? Brain research Brain research reviews 24:67-76.

Almohmeed YH, Avenell A, Aucott L, Vickers MA (2013) Systematic review and meta-analysis of the sero-epidemiological association between Epstein Barr virus and multiple sclerosis. PloS one 8:e61110.

Ancuta P, Rao R, Moses A, Mehle A, Shaw SK, Luscinskas FW, Gabuzda D (2003) Fractalkine preferentially mediates arrest and migration of CD16+ monocytes. The Journal of experimental medicine 197:1701-1707.

Andersson PB, Perry VH, Gordon S (1992a) The acute inflammatory response to lipopolysaccharide in CNS parenchyma differs from that in other body tissues. Neuroscience 48:169-186.

Andersson PB, Perry VH, Gordon S (1992b) Intracerebral injection of proinflammatory cytokines or leukocyte chemotaxins induces minimal myelomonocytic cell recruitment to the parenchyma of the central nervous system. The Journal of experimental medicine 176:255-259.

Ascherio A, Munger KL (2007) Environmental risk factors for multiple sclerosis. Part I: the role of infection. Ann Neurol 61:288-299.

Aschermann S, Lux A, Baerenwaldt A, Biburger M, Nimmerjahn F (2010) The other side of immunoglobulin G: suppressor of inflammation. Clinical and experimental immunology 160:161-167.

Aube B, Levesque SA, Pare A, Chamma E, Kebir H, Gorina R, Lecuyer MA, Alvarez JI, De Koninck Y, Engelhardt B, Prat A, Cote D, Lacroix S (2014) Neutrophils mediate blood-spinal cord barrier disruption in demyelinating neuroinflammatory diseases. Journal of immunology 193:2438-2454.

Axtell RC, de Jong BA, Boniface K, van der Voort LF, Bhat R, De Sarno P, Naves R, Han M, Zhong F, Castellanos JG, Mair R, Christakos A, Kolkowitz I, Katz L, Killestein J, Polman CH, de Waal Malefyt R, Steinman L, Raman C (2010) T helper type 1 and 17 cells determine efficacy of interferon-beta in multiple sclerosis and experimental encephalomyelitis. Nature medicine 16:406-412.

Babbe H, Roers A, Waisman A, Lassmann H, Goebels N, Hohlfeld R, Friese M, Schroder R, Deckert M, Schmidt S, Ravid R, Rajewsky K (2000) Clonal expansions of CD8(+) T cells dominate the T cell infiltrate in active multiple sclerosis lesions as shown by micromanipulation and single cell polymerase chain reaction. The Journal of experimental medicine 192:393-404.

Barkalow FJ, Goodman MJ, Gerritsen ME, Mayadas TN (1996) Brain endothelium lack one of two pathways of P-selectin-mediated neutrophil adhesion. Blood 88:4585-4593.

Barkhof F, Bruck W, De Groot CJ, Bergers E, Hulshof S, Geurts J, Polman CH, van der Valk P (2003) Remyelinated lesions in multiple sclerosis: magnetic resonance image appearance. Archives of neurology 60:1073-1081.

Barnden MJ, Allison J, Heath WR, Carbone FR (1998) Defective TCR expression in transgenic mice constructed using cDNA-based alpha- and beta-chain genes under the control of heterologous regulatory elements. Immunology and cell biology 76:34-40.

Barnett MH, Prineas JW (2004) Relapsing and remitting multiple sclerosis: pathology of the newly forming lesion. Ann Neurol 55:458-468.

Baron JL, Madri JA, Ruddle NH, Hashim G, Janeway CA, Jr. (1993) Surface expression of alpha 4 integrin by CD4 T cells is required for their entry into brain parenchyma. The Journal of experimental medicine 177:57-68.

Bartholomaus I, Kawakami N, Odoardi F, Schlager C, Miljkovic D, Ellwart JW, Klinkert WE, Flugel-Koch C, Issekutz TB, Wekerle H, Flugel A (2009) Effector T cell interactions with meningeal vascular structures in nascent autoimmune CNS lesions. Nature 462:94-98.

Baxter AG (2007) The origin and application of experimental autoimmune encephalomyelitis. Nature reviews Immunology 7:904-912.

Beecham AH, Patsopoulos NA, Xifara DK, Davis MF, Kemppinen A, Cotsapas C, Shah TS, Spencer C, Booth D, Goris A (2013) Analysis of immune-related loci identifies 48 new susceptibility variants for multiple sclerosis. Nature genetics 45:1353-1360.

Ben-Nun A, Wekerle H, Cohen IR (1981) The rapid isolation of clonable antigen-specific T lymphocyte lines capable of mediating autoimmune encephalomyelitis. European journal of immunology 11:195-199.

Bettelli E, Baeten D, Jager A, Sobel RA, Kuchroo VK (2006) Myelin oligodendrocyte glycoprotein-specific T and B cells cooperate to induce a Devic-like disease in mice. The Journal of clinical investigation 116:2393-2402.

Bettelli E, Pagany M, Weiner HL, Linington C, Sobel RA, Kuchroo VK (2003) Myelin oligodendrocyte glycoprotein-specific T cell receptor transgenic mice develop spontaneous autoimmune optic neuritis. The Journal of experimental medicine 197:1073-1081.

Bielekova B, Catalfamo M, Reichert-Scrivner S, Packer A, Cerna M, Waldmann TA, McFarland H, Henkart PA, Martin R (2006) Regulatory CD56(bright) natural killer cells mediate immunomodulatory effects of IL-2Ralpha-targeted therapy (daclizumab) in multiple sclerosis. Proceedings of the National Academy of Sciences of the United States of America 103:5941-5946.

Bielekova B, Richert N, Herman ML, Ohayon J, Waldmann TA, McFarland H, Martin R, Blevins G (2011) Intrathecal effects of daclizumab treatment of multiple sclerosis. Neurology 77:1877-1886.

Bielekova B, Richert N, Howard T, Blevins G, Markovic-Plese S, McCartin J, Frank JA, Wurfel J, Ohayon J, Waldmann TA, McFarland HF, Martin R (2004) Humanized anti-CD25 (daclizumab) inhibits disease activity in multiple sclerosis patients failing to respond to interferon beta. Proceedings of the National Academy of Sciences of the United States of America 101:8705-8708.

Bitsch A, Schuchardt J, Bunkowski S, Kuhlmann T, Bruck W (2000) Acute axonal injury in multiple sclerosis. Correlation with demyelination and inflammation. Brain : a journal of neurology 123 (Pt 6):1174-1183.

Bjartmar C, Wujek JR, Trapp BD (2003) Axonal loss in the pathology of MS: consequences for understanding the progressive phase of the disease. Journal of the neurological sciences 206:165-171.

Bo L, Geurts JJ, van der Valk P, Polman C, Barkhof F (2007) Lack of correlation between cortical demyelination and white matter pathologic changes in multiple sclerosis. Archives of neurology 64:76-80.

Bo L, Vedeler CA, Nyland H, Trapp BD, Mork SJ (2003a) Intracortical multiple sclerosis lesions are not associated with increased lymphocyte infiltration. Multiple sclerosis 9:323-331.

Bo L, Vedeler CA, Nyland HI, Trapp BD, Mork SJ (2003b) Subpial demyelination in the cerebral cortex of multiple sclerosis patients. Journal of neuropathology and experimental neurology 62:723-732.

Boggild MD, Williams R, Haq N, Hawkins CP (1996) Cortical plaques visualised by fluid-attenuated inversion recovery imaging in relapsing multiple sclerosis. Neuroradiology 38 Suppl 1:S10-13.

Boorsma DM (1984) Direct immunoenzyme double staining applicable for monoclonal antibodies. Histochemistry 80:103-106.

Boretius S, Escher A, Dallenga T, Wrzos C, Tammer R, Bruck W, Nessler S, Frahm J, Stadelmann C (2012) Assessment of lesion pathology in a new animal model of MS by multiparametric MRI and DTI. NeuroImage 59:2678-2688.

Boretius S, Schmelting B, Watanabe T, Merkler D, Tammer R, Czeh B, Michaelis T, Frahm J, Fuchs E (2006) Monitoring of EAE onset and progression in the common marmoset monkey by sequential high-resolution 3D MRI. NMR in biomedicine 19:41-49.

Bourquin C, Schubart A, Tobollik S, Mather I, Ogg S, Liblau R, Linington C (2003) Selective unresponsiveness to conformational B cell epitopes of the myelin oligodendrocyte glycoprotein in H-2b mice. Journal of immunology 171:455-461.

Brehm U, Piddlesden SJ, Gardinier MV, Linington C (1999) Epitope specificity of demyelinating monoclonal autoantibodies directed against the human myelin oligodendrocyte glycoprotein (MOG). Journal of neuroimmunology 97:9-15.

Breij EC, Brink BP, Veerhuis R, van den Berg C, Vloet R, Yan R, Dijkstra CD, van der Valk P, Bo L (2008) Homogeneity of active demyelinating lesions in established multiple sclerosis. Ann Neurol 63:16-25.

Brilot F, Dale RC, Selter RC, Grummel V, Kalluri SR, Aslam M, Busch V, Zhou D, Cepok S, Hemmer B (2009) Antibodies to native myelin oligodendrocyte glycoprotein in children with inflammatory demyelinating central nervous system disease. Ann Neurol 66:833-842.

Brown DA, Sawchenko PE (2007) Time course and distribution of inflammatory and neurodegenerative events suggest structural bases for the pathogenesis of experimental autoimmune encephalomyelitis. The Journal of comparative neurology 502:236-260.

Brownell B, Hughes JT (1962) The distribution of plaques in the cerebrum in multiple sclerosis. Journal of neurology, neurosurgery, and psychiatry 25:315-320.

Browning V, Joseph M, Sedrak M (2012) Multiple sclerosis: a comprehensive review for the physician assistant. JAAPA : official journal of the American Academy of Physician Assistants 25:24-29.

Bruck W, Porada P, Poser S, Rieckmann P, Hanefeld F, Kretzschmar HA, Lassmann H (1995) Monocyte/macrophage differentiation in early multiple sclerosis lesions. Ann Neurol 38:788-796.

Bruck W, Stadelmann C (2005) The spectrum of multiple sclerosis: new lessons from pathology. Current opinion in neurology 18:221-224.

Buc M (2013) Role of regulatory T cells in pathogenesis and biological therapy of multiple sclerosis. Mediators of inflammation 2013:963748.

Calabrese M, De Stefano N, Atzori M, Bernardi V, Mattisi I, Barachino L, Morra A, Rinaldi L, Romualdi C, Perini P, Battistin L, Gallo P (2007) Detection of cortical inflammatory lesions by double inversion recovery magnetic resonance imaging in patients with multiple sclerosis. Archives of neurology 64:1416-1422.

Calabrese M, De Stefano N, Atzori M, Bernardi V, Mattisi I, Barachino L, Rinaldi L, Morra A, McAuliffe MM, Perini P, Battistin L, Gallo P (2008) Extensive cortical inflammation is associated with epilepsy in multiple sclerosis. Journal of neurology 255:581-586.

Calabrese M, Filippi M, Gallo P (2010) Cortical lesions in multiple sclerosis. Nature reviews Neurology 6:438-444.

Calabrese M, Filippi M, Rovaris M, Bernardi V, Atzori M, Mattisi I, Favaretto A, Grossi P, Barachino L, Rinaldi L, Romualdi C, Perini P, Gallo P (2009) Evidence for relative cortical sparing in benign multiple sclerosis: a longitudinal magnetic resonance imaging study. Multiple sclerosis 15:36-41.

Calabrese M, Magliozzi R, Ciccarelli O, Geurts JJ, Reynolds R, Martin R (2015) Exploring the origins of grey matter damage in multiple sclerosis. Nature reviews Neuroscience 16:147-158.

Calabrese M, Poretto V, Favaretto A, Alessio S, Bernardi V, Romualdi C, Rinaldi F, Perini P, Gallo P (2012) Cortical lesion load associates with progression of disability in multiple sclerosis. Brain : a journal of neurology 135:2952-2961.

Calida DM, Constantinescu C, Purev E, Zhang GX, Ventura ES, Lavi E, Rostami A (2001) Cutting edge: C3, a key component of complement activation, is not required for the development of myelin oligodendrocyte glycoprotein peptide-induced experimental autoimmune encephalomyelitis in mice. Journal of immunology 166:723-726.

Campbell JJ, Hedrick J, Zlotnik A, Siani MA, Thompson DA, Butcher EC (1998) Chemokines and the arrest of lymphocytes rolling under flow conditions. Science 279:381-384.

Cao X, Shores EW, Hu-Li J, Anver MR, Kelsall BL, Russell SM, Drago J, Noguchi M, Grinberg A, Bloom ET, et al. (1995) Defective lymphoid development in mice lacking expression of the common cytokine receptor gamma chain. Immunity 2:223-238.

Carrithers MD, Visintin I, Kang SJ, Janeway CA, Jr. (2000) Differential adhesion molecule requirements for immune surveillance and inflammatory recruitment. Brain : a journal of neurology 123 (Pt 6):1092-1101.

Challacombe JM, Suhrbier A, Parsons PG, Jones B, Hampson P, Kavanagh D, Rainger GE, Morris M, Lord JM, Le TT, Hoang-Le D, Ogbourne SM (2006) Neutrophils are a key component of the antitumor efficacy of topical chemotherapy with ingenol-3-angelate. Journal of immunology 177:8123-8132.

Chang A, Staugaitis SM, Dutta R, Batt CE, Easley KE, Chomyk AM, Yong VW, Fox RJ, Kidd GJ, Trapp BD (2012) Cortical remyelination: a new target for repair therapies in multiple sclerosis. Ann Neurol 72:918-926.

Choi SR, Howell OW, Carassiti D, Magliozzi R, Gveric D, Muraro PA, Nicholas R, Roncaroli F, Reynolds R (2012) Meningeal inflammation plays a role in the pathology of primary progressive multiple sclerosis. Brain : a journal of neurology 135:2925-2937.

Christy AL, Walker ME, Hessner MJ, Brown MA (2013) Mast cell activation and neutrophil recruitment promotes early and robust inflammation in the meninges in EAE. Journal of autoimmunity 42:50-61.

Compston A, Coles A (2002) Multiple sclerosis. Lancet 359:1221-1231.

Compston A, Coles A (2008) Multiple sclerosis. Lancet 372:1502-1517.

Constantinescu CS, Farooqi N, O'Brien K, Gran B (2011) Experimental autoimmune encephalomyelitis (EAE) as a model for multiple sclerosis (MS). British journal of pharmacology 164:1079-1106.

Cooper MA, Fehniger TA, Caligiuri MA (2001) The biology of human natural killer-cell subsets. Trends in immunology 22:633-640.

Cortese I, Chaudhry V, So YT, Cantor F, Cornblath DR, Rae-Grant A (2011) Evidence-based guideline update: Plasmapheresis in neurologic disorders: report of the Therapeutics and Technology Assessment Subcommittee of the American Academy of Neurology. Neurology 76:294-300.

Cunningham PN, Hack BK, Ren G, Minto AW, Morgan BP, Quigg RJ (2001) Glomerular complement regulation is overwhelmed in passive Heymann nephritis. Kidney international 60:900-909.

Daley JM, Thomay AA, Connolly MD, Reichner JS, Albina JE (2008) Use of Ly6G-specific monoclonal antibody to deplete neutrophils in mice. Journal of leukocyte biology 83:64-70.

Dalla Libera D, Di Mitri D, Bergami A, Centonze D, Gasperini C, Grasso MG, Galgani S, Martinelli V, Comi G, Avolio C, Martino G, Borsellino G, Sallusto F, Battistini L, Furlan R (2011) T regulatory cells are markers of disease activity in multiple sclerosis patients. PloS one 6:e21386.

Davis SL, Frohman TC, Crandall CG, Brown MJ, Mills DA, Kramer PD, Stuve O, Frohman EM (2008) Modeling Uhthoff's phenomenon in MS patients with internuclear ophthalmoparesis. Neurology 70:1098-1106.

Davoust N, Nataf S, Reiman R, Holers MV, Campbell IL, Barnum SR (1999) Central nervous system-targeted expression of the complement inhibitor sCrry prevents experimental allergic encephalomyelitis. Journal of immunology 163:6551-6556.

Dawson JD (1916) The histology of disseminated sclerosis. Transactions of the Royal Society of Edinburgh 50:517-740.

De Stefano N, Narayanan S, Francis GS, Arnaoutelis R, Tartaglia MC, Antel JP, Matthews PM, Arnold DL (2001) Evidence of axonal damage in the early stages of multiple sclerosis and its relevance to disability. Archives of neurology 58:65-70.

Desjarlais JR, Lazar GA (2011) Modulation of antibody effector function. Experimental cell research 317:1278-1285.

Diaz-Villoslada P, Shih A, Shao L, Genain CP, Hauser SL (1999) Autoreactivity to myelin antigens: myelin/oligodendrocyte glycoprotein is a prevalent autoantigen. Journal of neuroimmunology 99:36-43.

Duffy SS, Lees JG, Moalem-Taylor G (2014) The contribution of immune and glial cell types in experimental autoimmune encephalomyelitis and multiple sclerosis. Multiple sclerosis international 2014:285245.

Durrenberger PF, Ettorre A, Kamel F, Webb LV, Sim M, Nicholas RS, Malik O, Reynolds R, Boyton RJ, Altmann DM (2012) Innate immunity in multiple sclerosis white matter lesions: expression of natural cytotoxicity triggering receptor 1 (NCR1). Journal of neuroinflammation 9:1.

Dutta R, Trapp BD (2007) Pathogenesis of axonal and neuronal damage in multiple sclerosis. Neurology 68:S22-31; discussion S43-54.

Dutta R, Trapp BD (2011) Mechanisms of neuronal dysfunction and degeneration in multiple sclerosis. Progress in neurobiology 93:1-12.

Eichler F, Van Haren K (2007) Immune response in leukodystrophies. Pediatric neurology 37:235-244.

Engelhardt B (2006) Molecular mechanisms involved in T cell migration across the blood-brain barrier. Journal of neural transmission 113:477-485.

Engelhardt B, Laschinger M, Schulz M, Samulowitz U, Vestweber D, Hoch G (1998) The development of experimental autoimmune encephalomyelitis in the mouse requires alpha4-integrin but not alpha4beta7-integrin. The Journal of clinical investigation 102:2096-2105.

Engelhardt B, Ransohoff RM (2012) Capture, crawl, cross: the T cell code to breach the blood-brain barriers. Trends in immunology 33:579-589.

Enzmann G, Mysiorek C, Gorina R, Cheng YJ, Ghavampour S, Hannocks MJ, Prinz V, Dirnagl U, Endres M, Prinz M, Beschorner R, Harter PN, Mittelbronn M, Engelhardt B, Sorokin L (2013) The neurovascular unit as a selective barrier to polymorphonuclear granulocyte (PMN) infiltration into the brain after ischemic injury. Acta Neuropathol 125:395-412.

Farh KK, Marson A, Zhu J, Kleinewietfeld M, Housley WJ, Beik S, Shoresh N, Whitton H, Ryan RJ, Shishkin AA, Hatan M, Carrasco-Alfonso MJ, Mayer D, Luckey CJ, Patsopoulos NA, De Jager PL, Kuchroo VK, Epstein CB, Daly MJ, Hafler DA, Bernstein BE (2015) Genetic and epigenetic fine mapping of causal autoimmune disease variants. Nature 518:337-343.

Ferguson B, Matyszak MK, Esiri MM, Perry VH (1997) Axonal damage in acute multiple sclerosis lesions. Brain : a journal of neurology 120 (Pt 3):393-399.

Filippi M, Dousset V, McFarland HF, Miller DH, Grossman RI (2002) Role of magnetic resonance imaging in the diagnosis and monitoring of multiple sclerosis: consensus report of the White Matter Study Group. Journal of magnetic resonance imaging : JMRI 15:499-504.

Filippi M, Rocca MA, Barkhof F, Bruck W, Chen JT, Comi G, DeLuca G, De Stefano N, Erickson BJ, Evangelou N, Fazekas F, Geurts JJ, Lucchinetti C, Miller DH, Pelletier D, Popescu BF, Lassmann H, Attendees of the Correlation between Pathological MRIfiMSw (2012) Association between pathological and MRI findings in multiple sclerosis. The Lancet Neurology 11:349-360.

Filippi M, Rocca MA, Calabrese M, Sormani MP, Rinaldi F, Perini P, Comi G, Gallo P (2010) Intracortical lesions: relevance for new MRI diagnostic criteria for multiple sclerosis. Neurology 75:1988-1994.

Filippi M, Yousry T, Baratti C, Horsfield MA, Mammi S, Becker C, Voltz R, Spuler S, Campi A, Reiser MF, Comi G (1996) Quantitative assessment of MRI lesion load in multiple sclerosis. A comparison of conventional spin-echo with fast fluid-attenuated inversion recovery. Brain : a journal of neurology 119 (Pt 4):1349-1355.

Fischer MT, Sharma R, Lim JL, Haider L, Frischer JM, Drexhage J, Mahad D, Bradl M, van Horssen J, Lassmann H (2012) NADPH oxidase expression in active multiple sclerosis lesions in relation to oxidative tissue damage and mitochondrial injury. Brain : a journal of neurology 135:886-899.

Fischer MT, Wimmer I, Hoftberger R, Gerlach S, Haider L, Zrzavy T, Hametner S, Mahad D, Binder CJ, Krumbholz M, Bauer J, Bradl M, Lassmann H (2013) Disease-specific molecular events in cortical multiple sclerosis lesions. Brain : a journal of neurology 136:1799-1815.

Fossati-Jimack L, Ioan-Facsinay A, Reininger L, Chicheportiche Y, Watanabe N, Saito T, Hofhuis FMA, Gessner JE, Schiller C, Schmidt RE, Honjo T, Verbeek JS, Izui S (2000) Markedly different pathogenicity of four immunoglobulin G isotype-switch variants of an antierythrocyte autoantibody is based on their capacity to interact in vivo with the low-affinity Fc gamma receptor III. Journal of Experimental Medicine 191:1293-1302.

Franklin RJ, Gilson JM, Blakemore WF (1997) Local recruitment of remyelinating cells in the repair of demyelination in the central nervous system. Journal of neuroscience research 50:337-344.

Frei Y, Lambris JD, Stockinger B (1987) Generation of a monoclonal antibody to mouse C5 application in an ELISA assay for detection of anti-C5 antibodies. Molecular and cellular probes 1:141-149.

Frischer JM, Bramow S, Dal-Bianco A, Lucchinetti CF, Rauschka H, Schmidbauer M, Laursen H, Sorensen PS, Lassmann H (2009) The relation between inflammation and neurodegeneration in multiple sclerosis brains. Brain : a journal of neurology 132:1175-1189.

Fritzsching B, Haas J, Konig F, Kunz P, Fritzsching E, Poschl J, Krammer PH, Bruck W, Suri-Payer E, Wildemann B (2011) Intracerebral human regulatory T cells: analysis of CD4+ CD25+ FOXP3+ T cells in brain lesions and cerebrospinal fluid of multiple sclerosis patients. PloS one 6:e17988.

Fu BQ, Tian ZG, Wei HM (2014) Subsets of human natural killer cells and their regulatory effects. Immunology 141:483-489.

Furtado GC, Marcondes MC, Latkowski JA, Tsai J, Wensky A, Lafaille JJ (2008) Swift entry of myelin-specific T lymphocytes into the central nervous system in spontaneous autoimmune encephalomyelitis. Journal of immunology 181:4648-4655.

Gaertner S, de Graaf KL, Greve B, Weissert R (2004) Antibodies against glycosylated native MOG are elevated in patients with multiple sclerosis. Neurology 63:2381-2383.

Gajofatto A, Benedetti MD (2015) Treatment strategies for multiple sclerosis: When to start, when to change, when to stop? World journal of clinical cases 3:545-555.

Galea I, Bechmann I, Perry VH (2007) What is immune privilege (not)? Trends in immunology 28:12-18.

Gardner C, Magliozzi R, Durrenberger PF, Howell OW, Rundle J, Reynolds R (2013) Cortical grey matter demyelination can be induced by elevated pro-inflammatory cytokines in the subarachnoid space of MOG-immunized rats. Brain : a journal of neurology 136:3596-3608.

Gaupp S, Pitt D, Kuziel WA, Cannella B, Raine CS (2003) Experimental autoimmune encephalomyelitis (EAE) in CCR2(-/-) mice: susceptibility in multiple strains. The American journal of pathology 162:139-150.

Genain CP, Cannella B, Hauser SL, Raine CS (1999) Identification of autoantibodies associated with myelin damage in multiple sclerosis. Nature medicine 5:170-175.

Geurts JJ, Barkhof F (2008) Grey matter pathology in multiple sclerosis. The Lancet Neurology 7:841-851.

Geurts JJ, Bo L, Pouwels PJ, Castelijns JA, Polman CH, Barkhof F (2005a) Cortical lesions in multiple sclerosis: combined postmortem MR imaging and histopathology. AJNR American journal of neuroradiology 26:572-577.

Geurts JJ, Bo L, Roosendaal SD, Hazes T, Daniels R, Barkhof F, Witter MP, Huitinga I, van der Valk P (2007) Extensive hippocampal demyelination in multiple sclerosis. Journal of neuropathology and experimental neurology 66:819-827.

Geurts JJ, Pouwels PJ, Uitdehaag BM, Polman CH, Barkhof F, Castelijns JA (2005b) Intracortical lesions in multiple sclerosis: improved detection with 3D double inversion-recovery MR imaging. Radiology 236:254-260.

Gilmore CP, Donaldson I, Bo L, Owens T, Lowe J, Evangelou N (2009) Regional variations in the extent and pattern of grey matter demyelination in multiple sclerosis: a comparison between the cerebral cortex, cerebellar cortex, deep grey matter nuclei and the spinal cord. Journal of neurology, neurosurgery, and psychiatry 80:182-187.

Girolamo F, Ferrara G, Strippoli M, Rizzi M, Errede M, Trojano M, Perris R, Roncali L, Svelto M, Mennini T, Virgintino D (2011) Cerebral cortex demyelination and oligodendrocyte precursor response to experimental autoimmune encephalomyelitis. Neurobiology of disease 43:678-689.

Gold R, Linington C, Lassmann H (2006) Understanding pathogenesis and therapy of multiple sclerosis via animal models: 70 years of merits and culprits in experimental autoimmune encephalomyelitis research. Brain : a journal of neurology 129:1953-1971.

Goldschmidt T, Antel J, Konig FB, Bruck W, Kuhlmann T (2009) Remyelination capacity of the MS brain decreases with disease chronicity. Neurology 72:1914-1921.

Graber JJ, Dhib-Jalbut S (2011) Biomarkers of disease activity in multiple sclerosis. Journal of the neurological sciences 305:1-10.

Gran B, Hemmer B, Vergelli M, McFarland HF, Martin R (1999) Molecular mimicry and multiple sclerosis: Degenerate T-Cell recognition and the induction of autoimmunity. Ann Neurol 45:559-567.

Grip O, Bredberg A, Lindgren S, Henriksson G (2007) Increased subpopulations of CD16(+) and CD56(+) blood monocytes in patients with active Crohn's disease. Inflammatory bowel diseases 13:566-572.

Haahr S, Hollsberg P (2006) Multiple sclerosis is linked to Epstein-Barr virus infection. Reviews in medical virology 16:297-310.

Haas J, Hug A, Viehover A, Fritzsching B, Falk CS, Filser A, Vetter T, Milkova L, Korporal M, Fritz B, Storch-Hagenlocher B, Krammer PH, Suri-Payer E, Wildemann B (2005) Reduced suppressive effect of CD4+CD25high regulatory T cells on the T cell immune response against myelin oligodendrocyte glycoprotein in patients with multiple sclerosis. European journal of immunology 35:3343-3352.

Hansen T, Skytthe A, Stenager E, Petersen HC, Bronnum-Hansen H, Kyvik KO (2005) Concordance for multiple sclerosis in Danish twins: an update of a nationwide study. Multiple sclerosis 11:504-510.

Hao J, Campagnolo D, Liu R, Piao W, Shi S, Hu B, Xiang R, Zhou Q, Vollmer T, Van Kaer L, La Cava A, Shi FD (2011) Interleukin-2/interleukin-2 antibody therapy induces target organ natural killer cells that inhibit central nervous system inflammation. Ann Neurol 69:721-734.

Hatterer E, Davoust N, Didier-Bazes M, Vuaillat C, Malcus C, Belin MF, Nataf S (2006) How to drain without lymphatics? Dendritic cells migrate from the cerebrospinal fluid to the B-cell follicles of cervical lymph nodes. Blood 107:806-812.

Hauser SL, Goodwin DS (2008) Multiple sclerosis and other demyelinating diseases. In: Harrison´s Principles of Internal Medicine, vol. II (Fauci, A. S. et al., eds), pp 2611-2621 New York: McGraw-Hill Medical.

Hauser SL, Waubant E, Arnold DL, Vollmer T, Antel J, Fox RJ, Bar-Or A, Panzara M, Sarkar N, Agarwal S, Langer-Gould A, Smith CH, Group HT (2008) B-cell depletion with rituximab in relapsing-remitting multiple sclerosis. The New England journal of medicine 358:676-688.

Hausler D, Nessler S, Kruse N, Bruck W, Metz I (2015) Natalizumab analogon therapy is effective in a B cell-dependent multiple sclerosis model. Neuropathology and applied neurobiology.

Healthline (2015) Countries with the highest prevalence rates of multiple sclerosis as of 2015 (per 100,000 people). In Statista - The Statistics Portal, from http://www.statista.com/statistics/372361/prevalence-rate-of-ms-in-select-countries/. p

Healy BC, Ali EN, Guttmann CR, Chitnis T, Glanz BI, Buckle G, Houtchens M, Stazzone L, Moodie J, Berger AM, Duan Y, Bakshi R, Khoury S, Weiner H, Ascherio A (2009) Smoking and disease progression in multiple sclerosis. Archives of neurology 66:858-864.

Hemmer B, Kerschensteiner M, Korn T (2015) Role of the innate and adaptive immune responses in the course of multiple sclerosis. The Lancet Neurology 14:406-419.

Henderson AP, Barnett MH, Parratt JD, Prineas JW (2009) Multiple sclerosis: distribution of inflammatory cells in newly forming lesions. Ann Neurol 66:739-753.

Hermesh T, Moran TM, Jain D, Lopez CB (2012) Granulocyte colony-stimulating factor protects mice during respiratory virus infections. PloS one 7:e37334.

Hernan MA, Olek MJ, Ascherio A (2001) Cigarette smoking and incidence of multiple sclerosis. American journal of epidemiology 154:69-74.

Holland NJ, Schneider DM, Rapp R, Kalb RC (2011) Meeting the needs of people with primary progressive multiple sclerosis, their families, and the health-care community. International journal of MS care 13:65-74.

Holt DS, Botto M, Bygrave AE, Hanna SM, Walport MJ, Morgan BP (2001) Targeted deletion of the CD59 gene causes spontaneous intravascular hemolysis and hemoglobinuria. Blood 98:442-449.

Horowitz A, Behrens RH, Okell L, Fooks AR, Riley EM (2010) NK cells as effectors of acquired immune responses: effector CD4+ T cell-dependent activation of NK cells following vaccination. Journal of immunology 185:2808-2818.

Howell OW, Reeves CA, Nicholas R, Carassiti D, Radotra B, Gentleman SM, Serafini B, Aloisi F, Roncaroli F, Magliozzi R, Reynolds R (2011) Meningeal inflammation is widespread and linked to cortical pathology in multiple sclerosis. Brain : a journal of neurology 134:2755-2771.

Hu Y, Turner MJ, Shields J, Gale MS, Hutto E, Roberts BL, Siders WM, Kaplan JM (2009) Investigation of the mechanism of action of alemtuzumab in a human CD52 transgenic mouse model. Immunology 128:260-270.

Huugen D, van Esch A, Xiao H, Peutz-Kootstra CJ, Buurman WA, Tervaert JW, Jennette JC, Heeringa P (2007) Inhibition of complement factor C5 protects against anti-myeloperoxidase antibody-mediated glomerulonephritis in mice. Kidney international 71:646-654.

Inverardi L, Witson JC, Fuad SA, Winkler-Pickett RT, Ortaldo JR, Bach FH (1991) CD3 negative "small agranular lymphocytes" are natural killer cells. Journal of immunology 146:4048-4052.

Janeway CA Jr TP, Walport M, et al. (2001) The destruction of antibody-coated pathogens via Fc receptors. In: Immunobiology: The Immune System in Health and Disease: New York: Garland Science.

Jersild C, Fog T, Hansen GS, Thomsen M, Svejgaard A, Dupont B (1973) Histocompatibility determinants in multiple sclerosis, with special reference to clinical course. Lancet 2:1221-1225.

Kastrukoff LF, Lau A, Wee R, Zecchini D, White R, Paty DW (2003) Clinical relapses of multiple sclerosis are associated with 'novel' valleys in natural killer cell functional activity. Journal of neuroimmunology 145:103-114.

Kerlero de Rosbo N, Honegger P, Lassmann H, Matthieu JM (1990) Demyelination induced in aggregating brain cell cultures by a monoclonal antibody against myelin/oligodendrocyte glycoprotein. Journal of neurochemistry 55:583-587.

Kidd D, Barkhof F, McConnell R, Algra PR, Allen IV, Revesz T (1999) Cortical lesions in multiple sclerosis. Brain : a journal of neurology 122 (Pt 1):17-26.

Kivisakk P, Imitola J, Rasmussen S, Elyaman W, Zhu B, Ransohoff RM, Khoury SJ (2009) Localizing central nervous system immune surveillance: meningeal antigen-presenting cells activate T cells during experimental autoimmune encephalomyelitis. Ann Neurol 65:457-469.

Kivisakk P, Mahad DJ, Callahan MK, Trebst C, Tucky B, Wei T, Wu L, Baekkevold ES, Lassmann H, Staugaitis SM, Campbell JJ, Ransohoff RM (2003) Human cerebrospinal fluid central memory CD4+

T cells: evidence for trafficking through choroid plexus and meninges via P-selectin. Proceedings of the National Academy of Sciences of the United States of America 100:8389-8394.

Klaver R, Popescu V, Voorn P, Galis-de Graaf Y, van der Valk P, de Vries HE, Schenk GJ, Geurts JJ (2015) Neuronal and axonal loss in normal-appearing gray matter and subpial lesions in multiple sclerosis. Journal of neuropathology and experimental neurology 74:453-458.

Koch-Henriksen N, Sorensen PS (2010) The changing demographic pattern of multiple sclerosis epidemiology. The Lancet Neurology 9:520-532.

Koch M, Kingwell E, Rieckmann P, Tremlett H, Neurologists UMC (2010) The natural history of secondary progressive multiple sclerosis. Journal of neurology, neurosurgery, and psychiatry 81:1039-1043.

Koo EH, Sisodia SS, Archer DR, Martin LJ, Weidemann A, Beyreuther K, Fischer P, Masters CL, Price DL (1990) Precursor of amyloid protein in Alzheimer disease undergoes fast anterograde axonal transport. Proceedings of the National Academy of Sciences of the United States of America 87:1561-1565.

Kramann N, Neid K, Menken L, Schlumbohm C, Stadelmann C, Fuchs E, Bruck W, Wegner C (2015) Increased Meningeal T and Plasma Cell Infiltration is Associated with Early Subpial Cortical Demyelination in Common Marmosets with Experimental Autoimmune Encephalomyelitis. Brain pathology 25:276-286.

Krishnamoorthy G, Lassmann H, Wekerle H, Holz A (2006) Spontaneous opticospinal encephalomyelitis in a double-transgenic mouse model of autoimmune T cell/B cell cooperation. The Journal of clinical investigation 116:2385-2392.

Kuhlmann T, Lingfeld G, Bitsch A, Schuchardt J, Bruck W (2002) Acute axonal damage in multiple sclerosis is most extensive in early disease stages and decreases over time. Brain : a journal of neurology 125:2202-2212.

Kuhlmann T, Miron V, Cui Q, Wegner C, Antel J, Bruck W (2008) Differentiation block of oligodendroglial progenitor cells as a cause for remyelination failure in chronic multiple sclerosis. Brain : a journal of neurology 131:1749-1758.

Kurtzke JF (2000) Epidemiology of multiple sclerosis. Does this really point toward an etiology? Lectio Doctoralis. Neurological sciences : official journal of the Italian Neurological Society and of the Italian Society of Clinical Neurophysiology 21:383-403.

Kutzelnigg A, Lassmann H (2006) Cortical demyelination in multiple sclerosis: a substrate for cognitive deficits? Journal of the neurological sciences 245:123-126.

Kutzelnigg A, Lucchinetti CF, Stadelmann C, Bruck W, Rauschka H, Bergmann M, Schmidbauer M, Parisi JE, Lassmann H (2005) Cortical demyelination and diffuse white matter injury in multiple sclerosis. Brain : a journal of neurology 128:2705-2712.

Kuziel WA, Morgan SJ, Dawson TC, Griffin S, Smithies O, Ley K, Maeda N (1997) Severe reduction in leukocyte adhesion and monocyte extravasation in mice deficient in CC chemokine receptor 2. Proceedings of the National Academy of Sciences of the United States of America 94:12053-12058.

Lamere MW, Moquin A, Lee FE, Misra RS, Blair PJ, Haynes L, Randall TD, Lund FE, Kaminski DA (2011) Regulation of antinucleoprotein IgG by systemic vaccination and its effect on influenza virus clearance. Journal of virology 85:5027-5035.

Lang HL, Jacobsen H, Ikemizu S, Andersson C, Harlos K, Madsen L, Hjorth P, Sondergaard L, Svejgaard A, Wucherpfennig K, Stuart DI, Bell JI, Jones EY, Fugger L (2002) A functional and structural basis for TCR cross-reactivity in multiple sclerosis. Nature immunology 3:940-943.

Lassmann H (1983) Comparative neuropathology of chronic experimental allergic encephalomyelitis and multiple sclerosis. Schriftenreihe Neurologie 25:1-135.

Lassmann H (2010) Axonal and neuronal pathology in multiple sclerosis: what have we learnt from animal models. Experimental neurology 225:2-8.

Lassmann H, Bruck W, Lucchinetti C (2001) Heterogeneity of multiple sclerosis pathogenesis: implications for diagnosis and therapy. Trends in molecular medicine 7:115-121.

Lassmann H, Wisniewski HM (1978) Chronic relapsing EAE. Time course of neurological symptoms and pathology. Acta Neuropathol 43:35-42.

Lieberman J (2003) The ABCs of granule-mediated cytotoxicity: new weapons in the arsenal. Nature reviews Immunology 3:361-370.

Liebetanz D, Merkler D (2006) Effects of commissural de- and remyelination on motor skill behaviour in the cuprizone mouse model of multiple sclerosis. Experimental neurology 202:217-224.

Linington C, Berger T, Perry L, Weerth S, Hinze-Selch D, Zhang Y, Lu HC, Lassmann H, Wekerle H (1993) T cells specific for the myelin oligodendrocyte glycoprotein mediate an unusual autoimmune inflammatory response in the central nervous system. European journal of immunology 23:1364-1372.

Linington C, Bradl M, Lassmann H, Brunner C, Vass K (1988) Augmentation of demyelination in rat acute allergic encephalomyelitis by circulating mouse monoclonal antibodies directed against a myelin/oligodendrocyte glycoprotein. The American journal of pathology 130:443-454.

Linington C, Lassmann H (1987) Antibody responses in chronic relapsing experimental allergic encephalomyelitis: correlation of serum demyelinating activity with antibody titre to the myelin/oligodendrocyte glycoprotein (MOG). Journal of neuroimmunology 17:61-69.

Litzenburger T, Fassler R, Bauer J, Lassmann H, Linington C, Wekerle H, Iglesias A (1998) B lymphocytes producing demyelinating autoantibodies: development and function in gene-targeted transgenic mice. The Journal of experimental medicine 188:169-180.

Locatelli G, Wortge S, Buch T, Ingold B, Frommer F, Sobottka B, Kruger M, Karram K, Buhlmann C, Bechmann I, Heppner FL, Waisman A, Becher B (2012) Primary oligodendrocyte death does not elicit anti-CNS immunity. Nature neuroscience 15:543-550.

Lublin FD, Reingold SC (1996) Defining the clinical course of multiple sclerosis: results of an international survey. National Multiple Sclerosis Society (USA) Advisory Committee on Clinical Trials of New Agents in Multiple Sclerosis. Neurology 46:907-911.

Lublin FD, Reingold SC, Cohen JA, Cutter GR, Sorensen PS, Thompson AJ, Wolinsky JS, Balcer LJ, Banwell B, Barkhof F, Bebo B, Jr., Calabresi PA, Clanet M, Comi G, Fox RJ, Freedman MS, Goodman AD, Inglese M, Kappos L, Kieseier BC, Lincoln JA, Lubetzki C, Miller AE, Montalban X, O'Connor PW, Petkau J, Pozzilli C, Rudick RA, Sormani MP, Stuve O, Waubant E, Polman CH (2014) Defining the clinical course of multiple sclerosis: the 2013 revisions. Neurology 83:278-286.

Lucchinetti C, Bruck W, Parisi J, Scheithauer B, Rodriguez M, Lassmann H (1999) A quantitative analysis of oligodendrocytes in multiple sclerosis lesions. A study of 113 cases. Brain : a journal of neurology 122 (Pt 12):2279-2295.

Lucchinetti C, Bruck W, Parisi J, Scheithauer B, Rodriguez M, Lassmann H (2000) Heterogeneity of multiple sclerosis lesions: implications for the pathogenesis of demyelination. Ann Neurol 47:707-717.

Lucchinetti CF, Popescu BF, Bunyan RF, Moll NM, Roemer SF, Lassmann H, Bruck W, Parisi JE, Scheithauer BW, Giannini C, Weigand SD, Mandrekar J, Ransohoff RM (2011) Inflammatory cortical demyelination in early multiple sclerosis. The New England journal of medicine 365:2188-2197.

Lumsden CE (1970) The neuropathology of multiple sclerosis. In: Multiple Sclerosis and Other Demyelinating Diseases. p. 217-309.

Lunemann A, Tackenberg B, DeAngelis T, da Silva RB, Messmer B, Vanoaica LD, Miller A, Apatoff B, Lublin FD, Lunemann JD, Munz C (2011) Impaired IFN-gamma production and proliferation of NK cells in multiple sclerosis. International immunology 23:139-148.

Magliozzi R, Howell O, Vora A, Serafini B, Nicholas R, Puopolo M, Reynolds R, Aloisi F (2007) Meningeal B-cell follicles in secondary progressive multiple sclerosis associate with early onset of disease and severe cortical pathology. Brain : a journal of neurology 130:1089-1104.

Magliozzi R, Howell OW, Reeves C, Roncaroli F, Nicholas R, Serafini B, Aloisi F, Reynolds R (2010) A Gradient of neuronal loss and meningeal inflammation in multiple sclerosis. Ann Neurol 68:477-493.

Maimone D, Gregory S, Arnason BG, Reder AT (1991) Cytokine levels in the cerebrospinal fluid and serum of patients with multiple sclerosis. Journal of neuroimmunology 32:67-74.

Maloney SE, Noguchi KK, Wozniak DF, Fowler SC, Farber NB (2011) Long-term Effects of Multiple Glucocorticoid Exposures in Neonatal Mice. Behavioral sciences 1:4-30.

Mantovani A, Cassatella MA, Costantini C, Jaillon S (2011) Neutrophils in the activation and regulation of innate and adaptive immunity. Nature reviews Immunology 11:519-531.

Marta CB, Oliver AR, Sweet RA, Pfeiffer SE, Ruddle NH (2005) Pathogenic myelin oligodendrocyte glycoprotein antibodies recognize glycosylated epitopes and perturb oligodendrocyte physiology. Proceedings of the National Academy of Sciences of the United States of America 102:13992-13997.

Matsushima GK, Morell P (2001) The neurotoxicant, cuprizone, as a model to study demyelination and remyelination in the central nervous system. Brain pathology 11:107-116.

McDonald WI, Compston A, Edan G, Goodkin D, Hartung HP, Lublin FD, McFarland HF, Paty DW, Polman CH, Reingold SC, Sandberg-Wollheim M, Sibley W, Thompson A, van den Noort S, Weinshenker BY, Wolinsky JS (2001) Recommended diagnostic criteria for multiple sclerosis: guidelines from the International Panel on the diagnosis of multiple sclerosis. Ann Neurol 50:121-127.

McMahon EJ, Cook DN, Suzuki K, Matsushima GK (2001) Absence of macrophage-inflammatory protein-1alpha delays central nervous system demyelination in the presence of an intact blood-brain barrier. Journal of immunology 167:2964-2971.

Mei F, Wang H, Liu S, Niu J, Wang L, He Y, Etxeberria A, Chan JR, Xiao L (2013) Stage-specific deletion of Olig2 conveys opposing functions on differentiation and maturation of oligodendrocytes. The Journal of neuroscience : the official journal of the Society for Neuroscience 33:8454-8462.

Merkler D, Boscke R, Schmelting B, Czeh B, Fuchs E, Bruck W, Stadelmann C (2006a) Differential macrophage/microglia activation in neocortical EAE lesions in the marmoset monkey. Brain pathology 16:117-123.

Merkler D, Ernsting T, Kerschensteiner M, Bruck W, Stadelmann C (2006b) A new focal EAE model of cortical demyelination: multiple sclerosis-like lesions with rapid resolution of inflammation and extensive remyelination. Brain : a journal of neurology 129:1972-1983.

Merkler D, Schmelting B, Czeh B, Fuchs E, Stadelmann C, Bruck W (2006c) Myelin oligodendrocyte glycoprotein-induced experimental autoimmune encephalomyelitis in the common marmoset reflects the immunopathology of pattern II multiple sclerosis lesions. Multiple sclerosis 12:369-374.

Metz I, Weigand SD, Popescu BF, Frischer JM, Parisi JE, Guo Y, Lassmann H, Bruck W, Lucchinetti CF (2014) Pathologic heterogeneity persists in early active multiple sclerosis lesions. Ann Neurol 75:728-738.

Miller D, Barkhof F, Montalban X, Thompson A, Filippi M (2005) Clinically isolated syndromes suggestive of multiple sclerosis, part I: natural history, pathogenesis, diagnosis, and prognosis. The Lancet Neurology 4:281-288.

Miller SD, Karpus WJ (2007) Experimental autoimmune encephalomyelitis in the mouse. Current protocols in immunology / edited by John E Coligan [et al] Chapter 15:Unit 15 11.

Milo R, Kahana E (2010) Multiple sclerosis: geoepidemiology, genetics and the environment. Autoimmunity reviews 9:A387-394.

Mohammad MG, Tsai VW, Ruitenberg MJ, Hassanpour M, Li H, Hart PH, Breit SN, Sawchenko PE, Brown DA (2014) Immune cell trafficking from the brain maintains CNS immune tolerance. The Journal of clinical investigation 124:1228-1241.

Mombaerts P, Iacomini J, Johnson RS, Herrup K, Tonegawa S, Papaioannou VE (1992) RAG-1-deficient mice have no mature B and T lymphocytes. Cell 68:869-877.

Morse RH, Seguin R, McCrea EL, Antel JP (2001) NK cell-mediated lysis of autologous human oligodendrocytes. Journal of neuroimmunology 116:107-115.

Mumford CJ, Wood NW, Kellar-Wood H, Thorpe JW, Miller DH, Compston DA (1994) The British Isles survey of multiple sclerosis in twins. Neurology 44:11-15.

Nangaku M (2003) Complement regulatory proteins: are they important in disease? Journal of the American Society of Nephrology : JASN 14:2411-2413.

Nangaku M, Alpers CE, Pippin J, Shankland SJ, Kurokawa K, Adler S, Morgan BP, Johnson RJ, Couser WG (1998) CD59 protects glomerular endothelial cells from immune-mediated thrombotic microangiopathy in rats. Journal of the American Society of Nephrology : JASN 9:590-597.

Nataf S, Carroll SL, Wetsel RA, Szalai AJ, Barnum SR (2000) Attenuation of experimental autoimmune demyelination in complement-deficient mice. Journal of immunology 165:5867-5873.

Nelson F, Datta S, Garcia N, Rozario NL, Perez F, Cutter G, Narayana PA, Wolinsky JS (2011) Intracortical lesions by 3T magnetic resonance imaging and correlation with cognitive impairment in multiple sclerosis. Multiple sclerosis 17:1122-1129.

Nierlich PN, Klaus C, Bigenzahn S, Pilat N, Koporc Z, Pree I, Baranyi U, Taniguchi M, Muehlbacher F, Wekerle T (2010) The role of natural killer T cells in costimulation blockade-based mixed chimerism. Transplant international : official journal of the European Society for Organ Transplantation 23:1179-1189.

Nikic I, Merkler D, Sorbara C, Brinkoetter M, Kreutzfeldt M, Bareyre FM, Bruck W, Bishop D, Misgeld T, Kerschensteiner M (2011) A reversible form of axon damage in experimental autoimmune encephalomyelitis and multiple sclerosis. Nature medicine 17:495-499.

Nimmerjahn F, Ravetch JV (2005) Divergent immunoglobulin g subclass activity through selective Fc receptor binding. Science 310:1510-1512.

Noseworthy JH, Lucchinetti C, Rodriguez M, Weinshenker BG (2000) Multiple sclerosis. The New England journal of medicine 343:938-952.

Noval Rivas M, Weatherly K, Hazzan M, Vokaer B, Dremier S, Gaudray F, Goldman M, Salmon I, Braun MY (2009) Reviving function in CD4+ T cells adapted to persistent systemic antigen. Journal of immunology 183:4284-4291.

O'Connor RA, Prendergast CT, Sabatos CA, Lau CW, Leech MD, Wraith DC, Anderton SM (2008) Cutting edge: Th1 cells facilitate the entry of Th17 cells to the central nervous system during experimental autoimmune encephalomyelitis. Journal of immunology 181:3750-3754.

Papadopoulos D, Dukes S, Patel R, Nicholas R, Vora A, Reynolds R (2009) Substantial archaeocortical atrophy and neuronal loss in multiple sclerosis. Brain pathology 19:238-253.

Patrikios P, Stadelmann C, Kutzelnigg A, Rauschka H, Schmidbauer M, Laursen H, Sorensen PS, Bruck W, Lucchinetti C, Lassmann H (2006) Remyelination is extensive in a subset of multiple sclerosis patients. Brain : a journal of neurology 129:3165-3172.

Peelen E, Damoiseaux J, Smolders J, Knippenberg S, Menheere P, Tervaert JW, Hupperts R, Thewissen M (2011) Th17 expansion in MS patients is counterbalanced by an expanded CD39+ regulatory T cell population during remission but not during relapse. Journal of neuroimmunology 240-241:97-103.

Peterson JW, Bo L, Mork S, Chang A, Trapp BD (2001) Transected neurites, apoptotic neurons, and reduced inflammation in cortical multiple sclerosis lesions. Ann Neurol 50:389-400.

Piddlesden SJ, Lassmann H, Zimprich F, Morgan BP, Linington C (1993) The demyelinating potential of antibodies to myelin oligodendrocyte glycoprotein is related to their ability to fix complement. The American journal of pathology 143:555-564.

Pirko I, Lucchinetti CF, Sriram S, Bakshi R (2007) Gray matter involvement in multiple sclerosis. Neurology 68:634-642.

Pitt D, Nagelmeier IE, Wilson HC, Raine CS (2003) Glutamate uptake by oligodendrocytes: Implications for excitotoxicity in multiple sclerosis. Neurology 61:1113-1120.

Plantone D, Marti A, Frisullo G, Iorio R, Damato V, Nociti V, Patanella AK, Bianco A, Mirabella M, Batocchi AP (2013) Circulating CD56dim NK cells expressing perforin are increased in progressive multiple sclerosis. Journal of neuroimmunology 265:124-127.

Pohar J, Pirher N, Bencina M, Mancek-Keber M, Jerala R (2013) The role of UNC93B1 protein in surface localization of TLR3 receptor and in cell priming to nucleic acid agonists. The Journal of biological chemistry 288:442-454.

Polman CH, O'Connor PW, Havrdova E, Hutchinson M, Kappos L, Miller DH, Phillips JT, Lublin FD, Giovannoni G, Wajgt A, Toal M, Lynn F, Panzara MA, Sandrock AW, Investigators A (2006) A randomized, placebo-controlled trial of natalizumab for relapsing multiple sclerosis. The New England journal of medicine 354:899-910.

Polman CH, Reingold SC, Banwell B, Clanet M, Cohen JA, Filippi M, Fujihara K, Havrdova E, Hutchinson M, Kappos L, Lublin FD, Montalban X, O'Connor P, Sandberg-Wollheim M, Thompson AJ, Waubant E, Weinshenker B, Wolinsky JS (2011) Diagnostic criteria for multiple sclerosis: 2010 revisions to the McDonald criteria. Ann Neurol 69:292-302.

Polman CH, Reingold SC, Edan G, Filippi M, Hartung HP, Kappos L, Lublin FD, Metz LM, McFarland HF, O'Connor PW, Sandberg-Wollheim M, Thompson AJ, Weinshenker BG, Wolinsky JS (2005)

Diagnostic criteria for multiple sclerosis: 2005 revisions to the "McDonald Criteria". Ann Neurol 58:840-846.

Pomeroy IM, Jordan EK, Frank JA, Matthews PM, Esiri MM (2008) Diffuse cortical atrophy in a marmoset model of multiple sclerosis. Neuroscience letters 437:121-124.

Pomeroy IM, Matthews PM, Frank JA, Jordan EK, Esiri MM (2005) Demyelinated neocortical lesions in marmoset autoimmune encephalomyelitis mimic those in multiple sclerosis. Brain : a journal of neurology 128:2713-2721.

Popescu BF, Bunyan RF, Parisi JE, Ransohoff RM, Lucchinetti CF (2011) A case of multiple sclerosis presenting with inflammatory cortical demyelination. Neurology 76:1705-1710.

Popescu BF, Lucchinetti CF (2012) Pathology of demyelinating diseases. Annual review of pathology 7:185-217.

Popescu BF, Pirko I, Lucchinetti CF (2013) Pathology of multiple sclerosis: where do we stand? Continuum 19:901-921.

Poser CM, Paty DW, Scheinberg L, McDonald WI, Davis FA, Ebers GC, Johnson KP, Sibley WA, Silberberg DH, Tourtellotte WW (1983) New diagnostic criteria for multiple sclerosis: guidelines for research protocols. Ann Neurol 13:227-231.

Pouwels PJ, Kuijer JP, Mugler JP, 3rd, Guttmann CR, Barkhof F (2006) Human gray matter: feasibility of single-slab 3D double inversion-recovery high-spatial-resolution MR imaging. Radiology 241:873-879.

Praet J, Guglielmetti C, Berneman Z, Van der Linden A, Ponsaerts P (2014) Cellular and molecular neuropathology of the cuprizone mouse model: clinical relevance for multiple sclerosis. Neurosci Biobehav Rev 47:485-505.

Prineas JW, Kwon EE, Cho ES, Sharer LR (1984) Continual breakdown and regeneration of myelin in progressive multiple sclerosis plaques. Annals of the New York Academy of Sciences 436:11-32.

Prineas JW, Kwon EE, Cho ES, Sharer LR, Barnett MH, Oleszak EL, Hoffman B, Morgan BP (2001) Immunopathology of secondary-progressive multiple sclerosis. Ann Neurol 50:646-657.

Prodinger C, Bunse J, Kruger M, Schiefenhovel F, Brandt C, Laman JD, Greter M, Immig K, Heppner F, Becher B, Bechmann I (2011) CD11c-expressing cells reside in the juxtavascular parenchyma and extend processes into the glia limitans of the mouse nervous system. Acta Neuropathol 121:445-458.

Raine CS, Scheinberg L, Waltz JM (1981) Multiple sclerosis. Oligodendrocyte survival and proliferation in an active established lesion. Laboratory investigation; a journal of technical methods and pathology 45:534-546.

Ramagopalan SV, Dyment DA, Ebers GC (2008) Genetic epidemiology: the use of old and new tools for multiple sclerosis. Trends in neurosciences 31:645-652.

Ransohoff RM, Engelhardt B (2012) The anatomical and cellular basis of immune surveillance in the central nervous system. Nature reviews Immunology 12:623-635.

Ratelade J, Zhang H, Saadoun S, Bennett JL, Papadopoulos MC, Verkman AS (2012) Neuromyelitis optica IgG and natural killer cells produce NMO lesions in mice without myelin loss. Acta Neuropathol 123:861-872.

Reboldi A, Coisne C, Baumjohann D, Benvenuto F, Bottinelli D, Lira S, Uccelli A, Lanzavecchia A, Engelhardt B, Sallusto F (2009) C-C chemokine receptor 6-regulated entry of TH-17 cells into the CNS through the choroid plexus is required for the initiation of EAE. Nature immunology 10:514-523.

Risitano AM (2012) Paroxysmal nocturnal hemoglobinuria and other complement-mediated hematological disorders. Immunobiology 217:1080-1087.

Rodriguez EG, Wegner C, Kreutzfeldt M, Neid K, Thal DR, Jurgens T, Bruck W, Stadelmann C, Merkler D (2014) Oligodendroglia in cortical multiple sclerosis lesions decrease with disease progression, but regenerate after repeated experimental demyelination. Acta Neuropathol 128:231-246.

Roosendaal SD, Moraal B, Pouwels PJ, Vrenken H, Castelijns JA, Barkhof F, Geurts JJ (2009) Accumulation of cortical lesions in MS: relation with cognitive impairment. Multiple sclerosis 15:708-714.

Ruifrok AC, Johnston DA (2001) Quantification of histochemical staining by color deconvolution. Anal Quant Cytol Histol 23:291-299.

Rumble JM, Huber AK, Krishnamoorthy G, Srinivasan A, Giles DA, Zhang X, Wang L, Segal BM (2015) Neutrophil-related factors as biomarkers in EAE and MS. The Journal of experimental medicine 212:23-35.

Russell JH, Ley TJ (2002) Lymphocyte-mediated cytotoxicity. Annual review of immunology 20:323-370.

Saadoun S, Waters P, MacDonald C, Bell BA, Vincent A, Verkman AS, Papadopoulos MC (2012) Neutrophil protease inhibition reduces neuromyelitis optica-immunoglobulin G-induced damage in mouse brain. Ann Neurol 71:323-333.

Sadaba MC, Tzartos J, Paino C, Garcia-Villanueva M, Alvarez-Cermeno JC, Villar LM, Esiri MM (2012) Axonal and oligodendrocyte-localized IgM and IgG deposits in MS lesions. Journal of neuroimmunology 247:86-94.

Saikali P, Antel JP, Newcombe J, Chen Z, Freedman M, Blain M, Cayrol R, Prat A, Hall JA, Arbour N (2007) NKG2D-mediated cytotoxicity toward oligodendrocytes suggests a mechanism for tissue injury in multiple sclerosis. The Journal of neuroscience : the official journal of the Society for Neuroscience 27:1220-1228.

Salinas Tejedor L, Berner G, Jacobsen K, Gudi V, Jungwirth N, Hansmann F, Gingele S, Prajeeth CK, Baumgartner W, Hoffmann A, Skripuletz T, Stangel M (2015) Mesenchymal stem cells do not exert direct beneficial effects on CNS remyelination in the absence of the peripheral immune system. Brain Behav Immun.

Sander M (1898) Hirnrindenbefunde bei multipler Sklerose. Monatschrift Psychiatrie Neurol IV:429–436.

Sawcer S, Hellenthal G, Pirinen M, Spencer CC, Patsopoulos NA, Moutsianas L, Dilthey A (2011) Genetic risk and a primary role for cell-mediated immune mechanisms in multiple sclerosis. Nature 476:214-219.

Scalfari A, Neuhaus A, Daumer M, Muraro PA, Ebers GC (2014) Onset of secondary progressive phase and long-term evolution of multiple sclerosis. Journal of neurology, neurosurgery, and psychiatry 85:67-75.

Schwab N, Schneider-Hohendorf T, Wiendl H (2015) Therapeutic uses of anti-alpha4-integrin (anti-VLA-4) antibodies in multiple sclerosis. International immunology 27:47-53.

Seewann A, Kooi EJ, Roosendaal SD, Pouwels PJ, Wattjes MP, van der Valk P, Barkhof F, Polman CH, Geurts JJ (2012) Postmortem verification of MS cortical lesion detection with 3D DIR. Neurology 78:302-308.

Seewann A, Vrenken H, Kooi EJ, van der Valk P, Knol DL, Polman CH, Pouwels PJ, Barkhof F, Geurts JJ (2011) Imaging the tip of the iceberg: visualization of cortical lesions in multiple sclerosis. Multiple sclerosis 17:1202-1210.

Shantsila E, Wrigley B, Tapp L, Apostolakis S, Montoro-Garcia S, Drayson MT, Lip GY (2011) Immunophenotypic characterization of human monocyte subsets: possible implications for cardiovascular disease pathophysiology. Journal of thrombosis and haemostasis : JTH 9:1056-1066.

Sharief MK, Thompson EJ (1991) Intrathecal immunoglobulin M synthesis in multiple sclerosis. Relationship with clinical and cerebrospinal fluid parameters. Brain : a journal of neurology 114 (Pt 1A):181-195.

Shi FD, Ljunggren HG, La Cava A, Van Kaer L (2011) Organ-specific features of natural killer cells. Nature reviews Immunology 11:658-671.

Shi SR, Cote RJ, Taylor CR (2001) Antigen retrieval techniques: current perspectives. J Histochem Cytochem 49:931-937.

Skripuletz T, Bussmann JH, Gudi V, Koutsoudaki PN, Pul R, Moharregh-Khiabani D, Lindner M, Stangel M (2010) Cerebellar cortical demyelination in the murine cuprizone model. Brain pathology 20:301-312.

Skripuletz T, Lindner M, Kotsiari A, Garde N, Fokuhl J, Linsmeier F, Trebst C, Stangel M (2008) Cortical demyelination is prominent in the murine cuprizone model and is strain-dependent. The American journal of pathology 172:1053-1061.

Skulina C, Schmidt S, Dornmair K, Babbe H, Roers A, Rajewsky K, Wekerle H, Hohlfeld R, Goebels N (2004) Multiple sclerosis: brain-infiltrating CD8+ T cells persist as clonal expansions in the cerebrospinal fluid and blood. Proceedings of the National Academy of Sciences of the United States of America 101:2428-2433.

Sospedra M, Martin R (2005) Immunology of multiple sclerosis. Annual review of immunology 23:683-747.

Srinivasan R, Sailasuta N, Hurd R, Nelson S, Pelletier D (2005) Evidence of elevated glutamate in multiple sclerosis using magnetic resonance spectroscopy at 3 T. Brain : a journal of neurology 128:1016-1025.

Stadelmann C, Albert M, Wegner C, Bruck W (2008) Cortical pathology in multiple sclerosis. Current opinion in neurology 21:229-234.

Stadelmann C, Wegner C, Bruck W (2011) Inflammation, demyelination, and degeneration - recent insights from MS pathology. Biochimica et biophysica acta 1812:275-282.

Steinman L (2013) Inflammatory cytokines at the summits of pathological signal cascades in brain diseases. Science signaling 6:pe3.

Stirling DP, Stys PK (2010) Mechanisms of axonal injury: internodal nanocomplexes and calcium deregulation. Trends in molecular medicine 16:160-170.

Stockmeyer B, Beyer T, Neuhuber W, Repp R, Kalden JR, Valerius T, Herrmann M (2003) Polymorphonuclear granulocytes induce antibody-dependent apoptosis in human breast cancer cells. Journal of immunology 171:5124-5129.

Storch M, Lassmann H (1997) Pathology and pathogenesis of demyelinating diseases. Current opinion in neurology 10:186-192.

Storch MK, Bauer J, Linington C, Olsson T, Weissert R, Lassmann H (2006) Cortical demyelination can be modeled in specific rat models of autoimmune encephalomyelitis and is major

histocompatibility complex (MHC) haplotype-related. Journal of neuropathology and experimental neurology 65:1137-1142.

Storch MK, Piddlesden S, Haltia M, Iivanainen M, Morgan P, Lassmann H (1998) Multiple sclerosis: in situ evidence for antibody- and complement-mediated demyelination. Ann Neurol 43:465-471.

Strober W (2001) Trypan blue exclusion test of cell viability. Current protocols in immunology / edited by John E Coligan [et al] Appendix 3:Appendix 3B.

Stromnes IM, Goverman JM (2006) Passive induction of experimental allergic encephalomyelitis. Nature protocols 1:1952-1960.

Stuve O, Marra CM, Bar-Or A, Niino M, Cravens PD, Cepok S, Frohman EM, Phillips JT, Arendt G, Jerome KR, Cook L, Grand'Maison F, Hemmer B, Monson NL, Racke MK (2006) Altered CD4+/CD8+ T-cell ratios in cerebrospinal fluid of natalizumab-treated patients with multiple sclerosis. Archives of neurology 63:1383-1387.

Theien BE, Vanderlugt CL, Eagar TN, Nickerson-Nutter C, Nazareno R, Kuchroo VK, Miller SD (2001) Discordant effects of anti-VLA-4 treatment before and after onset of relapsing experimental autoimmune encephalomyelitis. The Journal of clinical investigation 107:995-1006.

Torkildsen O, Brunborg LA, Myhr KM, Bo L (2008) The cuprizone model for demyelination. Acta neurologica Scandinavica Supplementum 188:72-76.

Trapp BD, Peterson J, Ransohoff RM, Rudick R, Mork S, Bo L (1998) Axonal transection in the lesions of multiple sclerosis. The New England journal of medicine 338:278-285.

Urich E, Gutcher I, Prinz M, Becher B (2006) Autoantibody-mediated demyelination depends on complement activation but not activatory Fc-receptors. Proceedings of the National Academy of Sciences of the United States of America 103:18697-18702.

Vercellino M, Plano F, Votta B, Mutani R, Giordana MT, Cavalla P (2005) Grey matter pathology in multiple sclerosis. Journal of neuropathology and experimental neurology 64:1101-1107.

Viglietta V, Baecher-Allan C, Weiner HL, Hafler DA (2004) Loss of functional suppression by CD4+CD25+ regulatory T cells in patients with multiple sclerosis. The Journal of experimental medicine 199:971-979.

Villoslada P, Hauser SL, Bartke I, Unger J, Heald N, Rosenberg D, Cheung SW, Mobley WC, Fisher S, Genain CP (2000) Human nerve growth factor protects common marmosets against autoimmune encephalomyelitis by switching the balance of T helper cell type 1 and 2 cytokines within the central nervous system. The Journal of experimental medicine 191:1799-1806.

Vogel DY, Vereyken EJ, Glim JE, Heijnen PD, Moeton M, van der Valk P, Amor S, Teunissen CE, van Horssen J, Dijkstra CD (2013) Macrophages in inflammatory multiple sclerosis lesions have an intermediate activation status. Journal of neuroinflammation 10:35.

von Budingen HC, Hauser SL, Fuhrmann A, Nabavi CB, Lee JI, Genain CP (2002) Molecular characterization of antibody specificities against myelin/oligodendrocyte glycoprotein in autoimmune demyelination. Proceedings of the National Academy of Sciences of the United States of America 99:8207-8212.

Wallin MT, Culpepper WJ, Coffman P, Pulaski S, Maloni H, Mahan CM, Haselkorn JK, Kurtzke JF, Veterans Affairs Multiple Sclerosis Centres of Excellence Epidemiology G (2012) The Gulf War era multiple sclerosis cohort: age and incidence rates by race, sex and service. Brain : a journal of neurology 135:1778-1785.

Wegner C, Esiri MM, Chance SA, Palace J, Matthews PM (2006) Neocortical neuronal, synaptic, and glial loss in multiple sclerosis. Neurology 67:960-967.

Wingerchuk DM, Carter JL (2014) Multiple sclerosis: current and emerging disease-modifying therapies and treatment strategies. Mayo Clinic proceedings 89:225-240.

Winkler-Pickett R, Young HA, Cherry JM, Diehl J, Wine J, Back T, Bere WE, Mason AT, Ortaldo JR (2008) In vivo regulation of experimental autoimmune encephalomyelitis by NK cells: alteration of primary adaptive responses. Journal of immunology 180:4495-4506.

Wucherpfennig KW, Strominger JL (1995) Molecular mimicry in T cell-mediated autoimmunity: viral peptides activate human T cell clones specific for myelin basic protein. Cell 80:695-705.

Xie L, Kang H, Xu Q, Chen MJ, Liao Y, Thiyagarajan M, O'Donnell J, Christensen DJ, Nicholson C, Iliff JJ, Takano T, Deane R, Nedergaard M (2013) Sleep drives metabolite clearance from the adult brain. Science 342:373-377.

Xu W, Fazekas G, Hara H, Tabira T (2005) Mechanism of natural killer (NK) cell regulatory role in experimental autoimmune encephalomyelitis. Journal of neuroimmunology 163:24-30.

Yamasaki R, Lu H, Butovsky O, Ohno N, Rietsch AM, Cialic R, Wu PM, Doykan CE, Lin J, Cotleur AC, Kidd G, Zorlu MM, Sun N, Hu W, Liu L, Lee JC, Taylor SE, Uehlein L, Dixon D, Gu J, Floruta CM, Zhu M, Charo IF, Weiner HL, Ransohoff RM (2014) Differential roles of microglia and monocytes in the inflamed central nervous system. The Journal of experimental medicine 211:1533-1549.

Yednock TA, Cannon C, Fritz LC, Sanchez-Madrid F, Steinman L, Karin N (1992) Prevention of experimental autoimmune encephalomyelitis by antibodies against alpha 4 beta 1 integrin. Nature 356:63-66.

Yong T, Zheng MQ, Linthicum DS (1997) Nicotine induces leukocyte rolling and adhesion in the cerebral microcirculation of the mouse. Journal of neuroimmunology 80:158-164.

Yuseff MI, Pierobon P, Reversat A, Lennon-Dumenil AM (2013) How B cells capture, process and present antigens: a crucial role for cell polarity. Nature reviews Immunology 13:475-486.

Zhang B, Yamamura T, Kondo T, Fujiwara M, Tabira T (1997) Regulation of experimental autoimmune encephalomyelitis by natural killer (NK) cells. The Journal of experimental medicine 186:1677-1687.

Zhou D, Srivastava R, Nessler S, Grummel V, Sommer N, Bruck W, Hartung HP, Stadelmann C, Hemmer B (2006) Identification of a pathogenic antibody response to native myelin oligodendrocyte glycoprotein in multiple sclerosis. Proceedings of the National Academy of Sciences of the United States of America 103:19057-19062.